2019

Shining light on the storm: Using high-frequency optical water quality sensors to characterize and interpret storm nutrient and carbon dynamics among contrasting land uses

Matthew CH Vaughan
University of Vermont

SHINING LIGHT ON THE STORM: USING HIGH-FREQUENCY OPTICAL WATER QUALITY SENSORS TO CHARACTERIZE AND INTERPRET STORM NUTRIENT AND CARBON DYNAMICS AMONG CONTRASTING LAND USES

A Dissertation Presented

by

Matthew C. H. Vaughan

to

The Faculty of the Graduate College

of

The University of Vermont

In Partial Fulfilment of the Requirements
For the Degree of Doctor of Philosophy
Specializing in Natural Resources

January, 2019

Defense Date: October 19, 2018
Dissertation Examination Committee:

Andrew W. Schroth, Ph.D., Advisor
William B. Bowden, Ph.D., Advisor
Arne Bomblies, Ph.D., Chairperson
James B. Shanley, Ph.D.
Cynthia J. Forehand, Ph.D., Dean of the Graduate College

ABSTRACT

Elevated nutrient concentrations present significant challenges to surface water quality management globally, and dissolved organic matter mediates several key biogeochemical processes. Storm events often dominate riverine loads of nitrate, phosphorus, and dissolved organic matter, and are expected to increase in frequency and intensity in many regions due to climate change. The recent development of in situ optical sensors has revolutionized water quality monitoring and has highlighted the important role storms play in water quality. This dissertation focuses on improving the application of in situ optical water quality sensors and interpreting the high-frequency data they produce to better understand biogeochemical and watershed processes that are critical for resource management.

We deployed in situ sensors to monitor water quality in three watersheds with contrasting land use / land cover, including agricultural, urban, and forested landscapes. The sensors measured absorbance of ultraviolet-visible light through the water column at 2.5 nanometer wavelength increments at 15-minute intervals for three years. These deployments provided a testbed to evaluate the sensors and improve models to predict concentrations of nitrate, three phosphorus fractions, and dissolved organic carbon using absorbance spectra and laboratory analyses through multivariate statistical techniques. In addition, an improved hysteresis calculation method was used to determine short-timescale storm dynamics for several parameters during 220 storm events.

Goals of each dissertation chapter were to: (1) examine the influences of seasonality, storm size, and dominant land use / land cover on storm dissolved organic carbon and nitrate hysteresis and loads; (2) evaluate the utility of the sensors to determine total, dissolved, and soluble reactive phosphorus concentrations in streams draining different land use / land covers, and perform the first statistically robust validation technique applied to optical water quality sensor calibration models; and (3) analyze storm event dissolved organic matter quantity and character dynamics by calculating hysteresis indices for DOC concentration and spectral slope ratio, and develop a novel analytical framework that leverages these high frequency measurements to infer biogeochemical and watershed processes. Each chapter includes key lessons and future recommendations for using in situ optical sensors to monitor water quality.

CITATIONS

Material from this dissertation has been published in the following form:

Vaughan, M. C. H., Bowden, W. B., Shanley, J. B., Vermilyea, A., Sleeper, R., Gold, A. J., Pradhanang, S. M., Inamdar, S. P., Levia, D. F., Andres, A. S., Birgand, F., and Schroth, A. W.. 2017. High-frequency dissolved organic carbon and nitrate measurements reveal differences in storm hysteresis and loading in relation to land cover and seasonality. Water Resources Research, v. 53, no. 7, p. 5345-5363. DOI: 10.1002/2017WR020491

Vaughan, M. C. H., Bowden, W. B., Shanley, J. B., Vermilyea, A., Wemple, B., and Schroth, A. W.. 2018. Using in situ UV-Visible spectrophotometer sensors to quantify riverine phosphorus partitioning and concentration at a high frequency. Limnology and Oceanography: Methods. DOI: 10.1002/lom3.10287

AND

Material from this dissertation has been submitted for publication in Biogeochemistry on October 10, 2018 in the following form:

Vaughan, M. C. H., Bowden, W. B., Shanley, J. B., Vermilyea, A., and Schroth, A. W.. 2018. Shining light on the storm: In-stream optics reveal hysteresis of dissolved organic matter character. Biogeochemistry.

DEDICATION

I dedicate this dissertation to my wife Rachel, our son Caleb, and our dog Pedro.

ACKNOWLEDGEMENTS

This dissertation benefited from the effort and support of many. My wife has supported me from the beginning of my career in water, and this work would not have been possible without her. Our son Caleb is a daily inspiration and a wonderful motivation to finish this work. Our faithful dog Pedro has gladly joined me on more days in the field than I could count. My parents, parents-in-law, and the rest of my large family have shown unending love and support. I also thank my co-advisors Andrew Schroth and Breck Bowden for their support and guidance throughout this work, as well as my committee members and co-authors for their numerous contributions. Additional thanks go to the Lake Champlain Basin Program team, Ryan Sleeper, Saul Blocher, Joshua Benes, Samuel Parker, Allison Jerram, Brian Pellerin, Richard Rowland, Catherine Winters, Kristen Underwood, Scott Hamshaw, Donna Rizzo, JohnFranco Saraceno, Francois Birgand, Ishi Buffam, and anonymous reviewers.

This material is based upon work supported by the National Science Foundation under VTEPSCoR Grant No. EPS-1101317, EPS-IIA1330446, and OIA 1556770, and Vermont Water Resources and Lakes Studies Center (project 2016VT80B) which is part of the National Institutes for Water Resources.

TABLE OF CONTENTS

LIST OF FIGURES

LIST OF TABLES

CHAPTER 1. PRESSING WATER QUALITY CHALLENGES AND THE BENEFITS OF IN SITU OPTICAL SENSORS

The roles of nitrogen, phosphorus, and dissolved organic matter in surface water quality issues

Eutrophication as a result of elevated nutrient concentrations is one of the most pronounced threats to water quality globally (e.g., Schindler et al. 2016), and is the most common reason for waterbody impairment in U.S. rivers (EPA 2016c), lakes (EPA 2016b), and coastal areas (EPA 2016a). Over the past century, global nitrogen and phosphorus cycles have been dramatically altered by human activities (e.g., Driscoll et al. 2003; Galloway et al. 1995; Jarvie et al. 2013), often increasing nutrient bioavailability in freshwater lakes (Smith et al. 1999) and streams (Dodds and Smith 2016). Human activities have more than doubled the rate of nitrogen fixation over natural levels in the last century (Vitousek et al. 1997). The effects of this change interact with pronounced alterations in global and regional carbon cycles, affecting both the climatic settings of freshwater systems (Guilbert et al. 2015) and the dissolved organic matter (DOM) character and quantity in waterbodies (Dhillon and Inamdar 2013). For example, eutrophication and increased temperatures have led to increased prevalence of cyanobacteria blooms worldwide (O'Neil et al. 2012), which often drive watershed management decisions (Scavia et al. 2014). Using innovative tools to gain a better understanding of freshwater nitrogen, phosphorus, and carbon dynamics in human-altered catchments will be critical to address these challenges.

Many surface water problems are the result of nitrogen from non-point sources (Boyer et al. 2002) and a disproportionate amount is delivered by storms (McClain et al. 2003). Agriculture and urban land use / land covers (LULCs) contribute non-point sources

of nitrogen and have led to elevated nitrate loads in streams (Boesch et al. 2001). These land uses can alter the storm response of a watershed from supply-limited (limited by the amount of a source constituent), typical of a forested stream, to a transport-limited condition (limited by the available water to connect the source constituent to a stream) (Carey et al. 2014; Rosenzweig et al. 2008). Elevated levels of inorganic nitrogen in surface waters, usually in the form of nitrate (NO_3^-), can cause numerous adverse effects on downstream freshwater ecosystems (Camargo and Alonso 2006; Smith et al. 1999), and coastal waters, which are often nitrogen-limited (Howarth 2008; Howarth and Marino 2006). Effects include changes in the biotic community structure and loss of biodiversity (Pardo et al. 2011), eutrophication (Smith et al. 1999), and increased acidification in forested systems (Driscoll et al. 2001) leading to increased mobilization of toxic aluminum (Baker et al. 1996). Elevated nitrogen levels also pose a risk to human health through deteriorating drinking water supply quality and ecological feedbacks to disease (Townsend et al. 2003), and has a significant detrimental impact on the economy (Camargo and Alonso 2006).

Phosphorus, another nutrient of concern, is thought to often limit cyanobacteria growth that impacts recreation, drinking water quality, property values, and ecosystem health (Carpenter et al. 1998; Conley et al. 2009). Inputs of phosphorus to aquatic systems depend greatly on LULC and have increased dramatically in the past century. Phosphorus accumulates in receiving waterbodies after the negatively charged phosphate (PO_4^{3-}) ion forms complexes with metal-containing minerals (Davison 1993). In forested systems, organic and inorganic phosphorus is primarily sourced from parent material weathering and ecosystem cycling (Likens 2013). While these processes also occur in urban and

agricultural catchments, fertilizer amendments, animal feed importation, and other human activities also contribute additional organic and inorganic phosphorus (Daloğlu et al. 2012; Wironen et al. 2018).

Phosphorus is delivered to waterbodies in several forms that can differ in bioavailability for cyanobacteria growth (Correll 1998; Isles et al. 2017). Phosphorus is most bioavailable as dissolved inorganic orthophosphate, commonly measured as soluble reactive phosphorus (SRP), or as part of the total dissolved phosphorus fraction (TDP). In addition, a portion of the organic phosphorus pool can be directly bioavailable, or can be rapidly decomposed by heterotrophic bacteria into the inorganic form that can be quickly utilized (Kane et al. 2014). Particulate phosphorus has potential bioavailability dependent upon the speciation of solid phase phosphorus and its interaction with receiving water column and pore water solutions (Giles et al. 2015; Schroth et al. 2015). Phosphorus in all forms is primarily delivered by storm events (Gerten and Adrian 2000; Pierson et al. 2013). For example, the magnitude of summer cyanobacteria blooms in Lake Erie have been shown to be positively correlated to spring river discharge and inputs of total phosphorus (TP) (Michalak et al. 2013; Stumpf et al. 2012). Quantifying phosphorus loads, the fractionation of those loads, and short- and long-term changes in these quantities will be key to meeting future water resource management goals.

Dissolved organic matter is considered a master variable that is linked to several key biogeochemical processes and water quality challenges (Stubbins et al. 2014). DOM abundance, sources, and driving processes are each altered by LULC (e.g., Parr et al. 2015; Wilson and Xenopoulos 2009). On a local scale, DOM is a major source of terrestrial carbon to receiving waterbodies (Prairie 2008), attenuates ultraviolet radiation that is

harmful to microorganisms (Bukaveckas and Robbins-Forbes 2000; Morris et al. 1995), and affects metal pollutant transport and bioavailability (Driscoll et al. 1988; Ravichandran 2004). DOM plays a key role in stream metabolism in temperate forests (Roberts et al. 2007), and its availability can limit denitrification, a microbial process that is central to maintaining high water quality (Sobczak et al. 2003). DOM also has been identified as the primary cause of harmful trihalomethane disinfectant byproduct formation during drinking water treatment (Chow et al. 2007; Kraus et al. 2008; Nguyen et al. 2013; Reckhow and Singer 1990). Globally, DOM is a significant source of carbon dioxide emissions into the atmosphere (Battin et al. 2009; Cole et al. 2007; Weyhenmeyer et al. 2012), and is a link between upland carbon sources and the oceans (Ludwig et al. 1996; Raymond and Bauer 2001). Dissolved organic carbon (DOC) loads generally have increased in the Northeast U.S. in recent decades (Monteith et al. 2007; SanClements et al. 2012; Stoddard et al. 2003). This increase has been attributed to decreased sulfate (SO_4^{2-}) concentrations and acidity in surface waters since the Clean Air Act of 1970 and Clear Air Act Amendments of 1990 greatly reduced sulfur deposition in the region (Baumgardner et al. 2002).

The natural and anthropogenically influenced pool of DOM in surface waters can contain a complex pool of thousands of compounds (Kim et al. 2006; Sleighter and Hatcher 2007; Stubbins et al. 2014). The "character" of DOM refers to the specific composition of this pool, which can differ over several temporal and spatial scales and among various ecosystem types (e.g., Jaffé et al. 2008). Human influences based on LULC can strongly influence DOM character during times of baseflow and storm events (e.g., Dalzell et al. 2005; Wilson and Xenopoulos 2008). DOM character can also have important implications for water quality management, since waters with elevated DOC concentrations and high

aromatic content have higher formation potential of disinfectant byproducts in drinking water treatment (Kitis et al. 2001; Reckhow and Singer 1990). Some types of in situ monitoring equipment offer the potential to measure DOM character independently of DOC concentration on a continuous basis to observe changes on short- and long-timescales.

Although the importance of nitrogen, phosphorus, and carbon and the influence of LULC on the supply, chemical form, and transport of these constituents is well known, more study is needed to determine how short-timescale storm nutrient and carbon dynamics differ among landscapes with various LULCs. Describing these differences may lead to opportunities for improved land use and resource management through identifying sources and pathways of pollutant delivery to stream networks.

The importance of storms and the value of high-frequency water quality monitoring

Storm events generate high stream flows that can transport considerably more nutrients and carbon to receiving water bodies than fluxes during times of baseflow (Fellman et al. 2009; Hinton et al. 1997; Inamdar et al. 2006). For example, storms can make up approximately 20% of a time period and export over 60% of the DOC load in the same time period (Oeurng et al. 2011). In addition, storms can mobilize distinct watershed and atmospherically deposited sources of nitrate through hydrologic pathways activated by storm watershed wetting; these sources can differ based on LULC and storm size (Buda and DeWalle 2009). Projections that storms in the US are expected to increase in frequency and intensity (Walsh et al. 2014) and that rapid LULC change is expected to continue (Lawler et al. 2014) together suggest that predicting future interactions of storm dynamics and LULC will be important to effectively manage water resources.

Capturing rapid water quality changes that often occur during storms can provide insight regarding watershed sources of pollutants, their hydrologic pathways during storms, and can provide the basis for more effective management. For example, quantifying the dynamic relationship between a key parameter and stream discharge during storm events can reveal solute transport pathways and active source areas (e.g. Chanat et al. 2002; Evans and Davies 1998; House and Warwick 1998). Hysteresis occurs when the parameter – discharge relationship differs on the rising limb of a storm versus the falling limb (e.g. Bowes et al. 2015; Johnson and East 1982). When a solute has higher concentrations on the rising limb versus the falling limb, a plot of these parameters forms a clockwise loop. This non-linear relationship is often the result of an exhaustible solute supply that is close in proximity to the measurement location (e.g. Bowes et al. 2009). When concentrations are higher on the falling limb versus the rising limb, an anti-clockwise hysteresis pattern emerges. This occurs when sources are more distal, have a longer transport time, stem from deeper subsurface zones, or a combination of these factors (Bieroza and Heathwaite 2015; Donn et al. 2012). In order to capture storm hysteresis effects or to determine that they do not occur, key water quality and quantity parameters must be measured on the timescale on which changes occur.

The development of in situ optical sensors has revolutionized water quality monitoring and gives researchers an improved view of the important role storms play in water quality (e.g., Kirchner et al. 2004). Storm solute loads and hysteresis dynamics are difficult to characterize with traditional "grab sampling" approaches because of the effort necessary for high-frequency sampling, and because storms are ephemeral in time and variable in space. Auto-samplers can increase temporal resolution of data, but these have

limitations. For example, they can hold a limited number of samples, and samples often sit unattended, which can compromise data quality. In situ optical water quality sensors have several advantages over these traditional methods, including: (1) sub-hourly measurement intervals to resolve rapid changes in water quality; (2) no need for hazardous chemicals to analyze solute concentrations; (3) no storage or transportation issues that can impact lab analyses of grab samples; and (4) the ability to characterize large episodic events when manual sampling may be impractical, expensive, and/or unsafe (Carey et al. 2014; Saraceno et al. 2009). Dynamics that occur on seasonal or diel timescales are also better described by this approach (Heffernan and Cohen 2010; Pellerin et al. 2012). Assessing solute export using in situ sensors can also potentially reduce error associated with discharge based load estimations due to variable event-based hysteresis (Guo et al. 2002; Pellerin et al. 2014), though the improvement over concentration-discharge measurement may be limited for some applications (Musolff et al. 2017). Optical sensors can also provide a continuous measurement record of water quality constituents to allow for greater understanding of seasonal trends, annual change, and increases the likelihood of capturing "hot moments" in a watershed (McClain et al. 2003). These continuous datasets may serve as historical benchmarks that can provide baseline conditions to monitor and evaluate environmental change due to future episodic disturbances and long-term pressures.

Ultraviolet-visible spectrophotometers have been shown to make rapid, continuous, concurrent, and accurate measurements of dissolved organic carbon, nitrate, and total suspended solids concentrations in surface waters with varying environmental conditions (Fichot and Benner 2011; Langergraber et al. 2003; Pellerin et al. 2013; Rieger et al. 2006; Sakamoto et al. 2009). These instruments measure light absorbance of the ultraviolet-

visible portion of the electromagnetic spectrum through the water column; these absorbance values can then be related to laboratory-measured concentrations through several multivariate statistical techniques. This approach also has been used to predict concentrations of non-ultraviolet-visible light absorbing solutes (e.g., P, Si, Mn) with promising results (Birgand et al. 2016). Generating algorithms to predict nutrient and DOC concentrations from water column light absorbance spectra presents a challenge due to the high dimensionality of the independent variables (light absorbance spectra) compared to the single response variable (e.g., nutrient concentration). Partial least squares regression (PLSR) is a technique that condenses independent variables into orthogonal, uncorrelated components and combines them in a multivariate model to predict the parameter of interest. This method can be used to harness the information of a rich collection of ultraviolet-visible absorbance spectra to predict a desired dependent quantity (e.g., Etheridge et al. 2014).

In addition to their current relatively high cost, there are several knowledge gaps that in part prevent the adoption of in situ ultraviolet-visible spectrophotometers by watershed managers. This technology has not been evaluated in streams draining watersheds of various LULCs in the same region, so their improvement over more traditional sampling techniques in these environments is not known. Also, previous studies evaluating this method have not presented model validation results; that is, all of the available laboratory analyses are often used to calibrate models, without verifying predictions with independent observations. In addition, though in situ spectrophotometer sensors may offer the potential to concurrently measure multiple phosphorus fraction

concentrations (e.g., TP, TDP, SRP) at a high frequency, few researchers have attempted this in a limited number of environmental conditions.

Ultraviolet-visible spectrophotometer sensors have shown promise to predict phosphorus fractions in some cases (Etheridge et al. 2014), though predictions of TP, TDP, and SRP concentrations from optical sensors have not been evaluated rigorously in a variety of systems. Studies and monitoring programs often make TP concentration estimates based on correlations of laboratory-measured TP concentration from grab samples with continuously measured discharge, turbidity, or a combination of the two. Unlike solutes such as nitrate and dissolved organic carbon, most phosphorus fractions do not directly absorb light in the ultraviolet-visible spectrum. Therefore, calibrations with concentrations of different phosphorus fractions would rely on proxy correlations alone, similar to correlations relating TP concentration to discharge. If robust proxy correlations were developed, phosphorus fractions could be monitored continuously on short timescales that capture rapid changes in hydrologic and biogeochemical processes critical to inform watershed management and nutrient reduction goals.

Overarching research questions, study design, and dissertation outline

This dissertation aims to address several overarching research questions while assessing and developing an emerging water quality monitoring technology:

1. Can in situ ultraviolet-visible spectrophotometer sensors be used in a wide variety of riverine environments to accurately and precisely monitor nitrate, phosphorus fractions, and DOM continuously and at a high frequency?

2. How does land use / land cover influence biogeochemical and watershed processes during storm events, and what are the downstream implications of these influences?
3. Can high-frequency water quality data be used to inform on sources and hydrologic pathways of nitrate and DOM?
4. How do land use / land cover, seasonality, and storm events together influence nitrate and DOM loading?

To answer these questions, monitoring stations were installed at three sites that were chosen to represent distinct end-members of LULC: agricultural, urban/suburban, and forested. Sites at Hungerford Brook (agricultural), Potash Brook (urban/suburban), and Wade Brook (forested) are located in the US state of Vermont on streams that drain to Lake Champlain. These stations were part of a larger network of sensors in the Northeast Water Resources Network (NEWRnet), which supported similar stations in the US states of Rhode Island and Delaware. Site characteristics are described in detail in the following chapters.

Each station was outfitted with an in-stream s::can Spectrolyser spectrophotometer that measured the absorbance of multiple wavelengths of ultraviolet and visible light, and a YSI EXO2 multi-parameter sonde that measured stream temperature, specific electrical conductivity, fluorescent dissolved organic matter, pH, and dissolved oxygen concentration. Each station was also equipped with a tipping bucket rain gauge, an in-stream pressure transducer, an atmospheric pressure transducer, solar panels, a datalogger, and a modem-antenna system to transmit data and troubleshoot remotely. These sites were an excellent test-bed for the next generation of water quality monitoring systems, where

researchers can see and react to water quality changes remotely and in real-time. All measurements were collected at a one measurement per 15-minute frequency, or at the rate of tip occurrence for the tipping bucket gauge. This measurement frequency was a key element of our study design that allowed for water quality changes to be characterized on the timescale on which they occur. Significant effort was put into collecting an adequate number of grab samples so that sensor measurements could be compared to laboratory analyses of nitrate, TP, TDP, SRP, and DOC concentration.

Significant thought and effort were put into the on-site sensor deployment design and installation. This design needed to accommodate dry baseflow, dangerously high stormflow, in-stream debris and sediment, temperature extremes, variable turbidity conditions, biological fouling, and both wildlife and human tampering. In-stream equipment was anchored with lag bolts into bridge infrastructure and/or cinder blocks and were always secured with redundant cables that were often activated by high stormflows. Large PVC pipe housings for sensors were reinforced with stainless steel lag bolts that allowed water, solutes, and fine sediment to flow past measurement windows while restricting the influx of in-stream debris and larger sediment. Biological fouling was minimized with silicone sensor wipers and with regular cleaning in the field. Wildlife tampering was minimized with above and underwater electrical conduit, and human tampering was minimized by disguising expensive monitoring equipment as refuse. Stream discharge measurements and stage-discharge rating curve development presented an ongoing challenge at the three sites. These challenges were due to inaccessible high flows, difficulty in the prediction of storm timing, variable groundwater contribution, and non-uniform channel morphology. Although rarely a focus of recent novel research on water

resources, accurately measuring stream discharge forms the basis of many studies in stream dynamics and considerations to reduce uncertainty in discharge should not be discounted during study design.

While high-frequency data can reveal short-timescale changes not characterized by grab sampling, the management, organization, and analysis of high-frequency data is non-trivial (e.g., Porter et al. 2012). For example, measuring a single parameter at a 15-minute interval for one year produces over 35,000 measurements; this is in contrast to 12 – 52 samples per year for the common practice of discrete monthly or weekly sampling (Pellerin et al. 2016). Code infrastructure in the R programming language was extremely useful to manage and make effective use of our large dataset. After several data management iterations, the most effective was a system based on compiling two main sets of data: (1) a dataframe containing concurrent raw sensor measurements and corresponding laboratory-measured values, and (2) a dataframe containing best 15-minute frequency estimates for all parameters of interest. For each dataframe, a row represented a single point in time, and each column represented a measurement made at that time, or analytical results from grab samples taken at that time. This system allowed for a two-step process in which models could be developed and validated from dataset (1) to relate raw sensor measurements to laboratory-measured value. These models could then be applied to create dataset (2), and derived timeseries could be used to infer watershed processes through subsequent analyses. For this work, dataframe (1) contained 649 rows and 444 columns, and dataframe (2) contained approximately 166,000 rows and 15 columns. Details on these models, validations, and analyses are presented in subsequent chapters. This approach allowed for

a “big data,” or “near-census” approach to storm response analysis that ultimately revealed a previously unknown and remarkable variability in storm dynamics of nutrients and DOM.

The subsequent chapters of this dissertation address the overarching questions using multiple approaches and both novel and established methods. The second chapter, *High-frequency dissolved organic carbon and nitrate measurements reveal differences in storm hysteresis and loading in relation to land cover and seasonality*, compares the performance of optical sensors in untested environments and uses a newly developed hysteresis metric to determine how LULC influences nitrate and DOM dynamics. Continuous monitoring for the spring, summer, and fall seasons over two years allowed us to capture and characterize 126 storm events and describe the influence of LULC and seasonal effects on nitrate and DOC loading. This number of storms is relatively high for the literature and shows a remarkable amount variability has not been observed with other techniques. This is the first study to apply this emerging technology to watersheds with varied LULCs in the same region, and we were able to directly observe what appears to be the complex interaction of farm management practices and seasonal dynamics. This chapter was published in a special section of *Water Resources Research*: “Continuous nutrient sensing in research and management: Applications and lessons learned across aquatic environments and watersheds.”

The third chapter, *Using in situ UV-Visible spectrophotometer sensors to quantify riverine phosphorus partitioning and concentration at a high frequency*, aims to evaluate the use of ultraviolet-visible spectrophotometers to monitor three different riverine phosphorus fraction concentrations: total, dissolved, and soluble reactive phosphorus. This chapter builds upon others’ work in this field by assessing the utility of this technology to

measure multiple phosphorus fraction concentrations concurrently in a variety of environmental settings. It also introduces a robust model validation technique that is recommended for future studies using optical water quality sensors. Rather than displaying model statistics using all available calibration data, robust validation requires that some data be withheld to compare model predictions with observations not used in model development. A bootstrap validation technique was used to repeat this process randomly one thousand times so the validation would not be sensitive to sampling error. Similar validation techniques are common in other scientific fields, but applied here for the first time to high-frequency water quality monitoring. The result is a robust estimate of uncertainty associated with predicting an unknown water quality parameter using established models based on ultraviolet-visible absorbance spectra. This chapter was published in *Limnology and Oceanography: Methods* in October, 2018.

The fourth chapter, *Shining light on the storm: In-stream optics reveal hysteresis of dissolved organic matter character*, builds upon the methods developed in the second and third chapters by incorporating the spectral slope ratio. The spectral slope ratio is inversely proportional to the molecular weight of DOM pool, and can be derived from the shape of an ultraviolet-visible spectrum curve. We incorporated these measurements into a novel analytical framework where storm spectral slope ratio hysteresis is plotted versus storm DOC concentration hysteresis in a four-quadrant cartesian grid. The location of each storm in this plotting space indicates the source and character of DOM during different stages of each storm, and provides context to conjecture on rapid changes in DOM provenance depending on LULC. Calculations from 220 storms again showed remarkable variability and reveal significant influences of LULC on DOM sources, processing, and

transport. This chapter was submitted for publication to *Biogeochemistry* on October 10, 2018.

This dissertation forms a basis for future work on optical water quality sensors, high-frequency environmental data analysis, and interpretation of biogeochemical processes based on near-census sampling of environmental change. Recommendations for using in situ water quality sensors and resulting data are included throughout this work in an effort to aid watershed managers in adopting this emerging technology.

References

Baker, J. P., Van Sickle, J., Gagen, C. J., DeWalle, D. R., Sharpe, W. E., Carline, R. F., Baldigo, B. P., Murdoch, P. S., Bath, D. W., Krester, W. A., Simonin, H. A., and Wigington, P. J., 1996, Episodic acidification of small streams in the Northeastern United States: Effects on fish populations: Ecological Applications, v. 6, no. 2, p. 422-437.

Battin, T. J., Luyssaert, S., Kaplan, L. A., Aufdenkampe, A. K., Richter, A., and Tranvik, L. J., 2009, The boundless carbon cycle: Nature Geosci, v. 2, no. 9, p. 598-600.

Baumgardner, R. E., Lavery, T. F., Rogers, C. M., and Isil, S. S., 2002, Estimates of the atmospheric deposition of sulfur and nitrogen species: Clean Air Status and Trends Network, 1990-2000: Environmental Science & Technology, v. 36, no. 12, p. 2614-2629.

Bieroza, M. Z., and Heathwaite, A. L., 2015, Seasonal variation in phosphorus concentration–discharge hysteresis inferred from high-frequency in situ monitoring: Journal of Hydrology, v. 524, p. 333-347.

Birgand, F., Aveni-Deforge, K., Smith, B., Maxwell, B., Horstman, M., Gerling, A. B., and Carey, C. C., 2016, First report of a novel multiplexer pumping system coupled to a water quality probe to collect high temporal frequency in situ water chemistry measurements at multiple sites: Limnology and Oceanography: Methods, v. 14, no. 12, p. 767-783.

Boesch, D. F., Brinsfield, R. B., and Magnien, R. E., 2001, Chesapeake Bay eutrophication: Scientific understanding, ecosystem restoration, and challenges for agriculture: Journal of Environmental Quality, v. 30, no. 2, p. 303-320.

Bowes, M. J., Jarvie, H. P., Halliday, S. J., Skeffington, R. A., Wade, A. J., Loewenthal, M., Gozzard, E., Newman, J. R., and Palmer-Felgate, E. J., 2015, Characterising phosphorus and nitrate inputs to a rural river using high-frequency concentration–flow relationships: Science of The Total Environment, v. 511, p. 608-620.

Bowes, M. J., Smith, J. T., and Neal, C., 2009, The value of high-resolution nutrient monitoring: A case study of the River Frome, Dorset, UK: Journal of Hydrology, v. 378, no. 1–2, p. 82-96.

Boyer, E., Goodale, C., Jaworski, N., and Howarth, R., 2002, Anthropogenic nitrogen sources and relationships to riverine nitrogen export in the northeastern U.S.A: Biogeochemistry, v. 57-58, no. 1, p. 137-169.

Buda, A. R., and DeWalle, D. R., 2009, Dynamics of stream nitrate sources and flow pathways during stormflows on urban, forest and agricultural watersheds in central Pennsylvania, USA: Hydrological Processes, v. 23, no. 23, p. 3292-3305.

Bukaveckas, P. A., and Robbins-Forbes, M., 2000, Role of dissolved organic carbon in the attenuation of photosynthetically active and ultraviolet radiation in Adirondack lakes: Freshwater Biology, v. 43, no. 3, p. 339-354.

Camargo, J. A., and Alonso, Á., 2006, Ecological and toxicological effects of inorganic nitrogen pollution in aquatic ecosystems: A global assessment: Environment International, v. 32, no. 6, p. 831-849.

Carey, R. O., Wollheim, W. M., Mulukutla, G. K., and Mineau, M. M., 2014, Characterizing storm-event nitrate fluxes in a fifth order suburbanizing watershed using in situ sensors: Environmental Science & Technology, v. 48, no. 14, p. 7756-7765.

Carpenter, S. R., Caraco, N. F., Correll, D. L., Howarth, R. W., Sharpley, A. N., and Smith, V. H., 1998, Nonpoint pollution of surface waters with phosphorus and nitrogen: Ecological Applications, v. 8, no. 3, p. 559-568.

Chanat, J. G., Rice, K. C., and Hornberger, G. M., 2002, Consistency of patterns in concentration-discharge plots: Water Resources Research, v. 38, no. 8, p. 22-21-22-10.

Chow, A. T., Dahlgren, R. A., and Harrison, J. A., 2007, Watershed sources of disinfection byproduct precursors in the Sacramento and San Joaquin Rivers, California: Environmental Science & Technology, v. 41, no. 22, p. 7645-7652.

Cole, J. J., Prairie, Y. T., Caraco, N. F., McDowell, W. H., Tranvik, L. J., Striegl, R. G., Duarte, C. M., Kortelainen, P., Downing, J. A., Middelburg, J. J., and Melack, J., 2007, Plumbing the Global Carbon Cycle: Integrating Inland Waters into the Terrestrial Carbon Budget: Ecosystems, v. 10, no. 1, p. 172-185.

Conley, D. J., Paerl, H. W., Howarth, R. W., Boesch, D. F., Seitzinger, S. P., Havens, K. E., Lancelot, C., and Likens, G. E., 2009, Controlling Eutrophication: Nitrogen and Phosphorus: Science, v. 323, no. 5917, p. 1014-1015.

Correll, D. L., 1998, The Role of Phosphorus in the Eutrophication of Receiving Waters: A Review: Journal of Environmental Quality, v. 27, p. 261-266.

Daloğlu, I., Cho, K. H., and Scavia, D., 2012, Evaluating Causes of Trends in Long-Term Dissolved Reactive Phosphorus Loads to Lake Erie: Environmental Science & Technology, v. 46, no. 19, p. 10660-10666.

Dalzell, B. J., Filley, T. R., and Harbor, J. M., 2005, Flood pulse influences on terrestrial organic matter export from an agricultural watershed: Journal of Geophysical Research-Biogeosciences, v. 110, no. G2.

Davison, W., 1993, Iron and manganese in lakes: Earth-Science Reviews, v. 34, no. 2, p. 119-163.

Dhillon, G. S., and Inamdar, S., 2013, Extreme storms and changes in particulate and dissolved organic carbon in runoff: Entering uncharted waters?: Geophysical Research Letters, v. 40, no. 7.

Dodds, W. K., and Smith, V. H., 2016, Nitrogen, phosphorus, and eutrophication in streams: Inland Waters, v. 6, no. 2, p. 155-164.

Donn, M. J., Barron, O. V., and Barr, A. D., 2012, Identification of phosphorus export from low-runoff yielding areas using combined application of high frequency water quality data and MODHMS modelling: Science of The Total Environment, v. 426, p. 264-271.

Driscoll, C. T., Fuller, R. D., and Simone, D. M., 1988, Longitudinal variations in trace-metal concentrations in a northern forested ecosystem: Journal of Environmental Quality, v. 17, no. 1, p. 101-107.

Driscoll, C. T., Lawrence, G. B., Bulger, A. J., Butler, T. J., Cronan, C. S., Eagar, C., Lambert, K. F., Likens, G. E., Stoddard, J. L., and Weathers, K. C., 2001, Acidic deposition in the Northeastern United States: Sources and inputs, ecosystem effects, and management strategies: BioScience, v. 51, no. 3, p. 180-198.

Driscoll, C. T., Whitall, D., Aber, J., Boyer, E., Castro, M., Cronan, C., Goodale, C. L., Groffman, P., Hopkinson, C., Lambert, K., Lawrence, G., and Ollinger, S., 2003, Nitrogen pollution in the Northeastern United States: Sources, effects, and management options: BioScience, v. 53, no. 4, p. 357-374.

EPA, U. S., 2016a, National coastal condition assessment 2010: U.S. Environmental Protection Agency, Office of Water, Office of Research and Development, EPA 841-R-15-006.

EPA, U. S., 2016b, National lakes assessment 2012: A collaborative survey of lakes in the United States, EPA 841-R-16-113.

-, 2016c, National rivers and streams assessment 2008-2009: A collaborative survey: U.S. Environmental Protection Agency, Office of Water, Office of Research and Development, EPA/841/R-16/007.

Etheridge, J. R., Birgand, F., Osborne, J. A., Osburn, C. L., Burchell, M. R., II, and Irving, J., 2014, Using in situ ultraviolet-visual spectroscopy to measure nitrogen,

carbon, phosphorus, and suspended solids concentrations at a high frequency in a brackish tidal marsh: Limnology and Oceanography-Methods, v. 12, p. 10-22.

Evans, C., and Davies, T. D., 1998, Causes of concentration/discharge hysteresis and its potential as a tool for analysis of episode hydrochemistry: Water Resources Research, v. 34, no. 1, p. 129-137.

Fellman, J. B., Hood, E., Edwards, R. T., and D'Amore, D. V., 2009, Changes in the concentration, biodegradability, and fluorescent properties of dissolved organic matter during stormflows in coastal temperate watersheds: Journal of Geophysical Research: Biogeosciences, v. 114, no. G1, p. G01021.

Fichot, C. G., and Benner, R., 2011, A novel method to estimate DOC concentrations from CDOM absorption coefficients in coastal waters: Geophysical Research Letters, v. 38.

Galloway, J. N., Schlesinger, W. H., Levy, H., Michaels, A., and Schnoor, J. L., 1995, Nitrogen fixation: Anthropogenic enhancement-environmental response: Global Biogeochemical Cycles, v. 9, no. 2, p. 235-252.

Gerten, D., and Adrian, R., 2000, Climate-driven changes in spring plankton dynamics and the sensitivity of shallow polymictic lakes to the North Atlantic Oscillation: Limnology and Oceanography, v. 45, no. 5, p. 1058-1066.

Giles, C. D., Lee, L. G., Cade-Menun, B. J., Hill, J. E., Isles, P. D. F., Schroth, A. W., and Druschel, G. K., 2015, Characterization of Organic Phosphorus Form and Bioavailability in Lake Sediments using 31P Nuclear Magnetic Resonance and Enzymatic Hydrolysis: Journal of Environmental Quality, v. 44, p. 882-894.

Guilbert, J., Betts, A. K., Rizzo, D. M., Beckage, B., and Bomblies, A., 2015, Characterization of increased persistence and intensity of precipitation in the northeastern United States: Geophysical Research Letters, v. 42, no. 6, p. 2015GL063124.

Guo, Y., Markus, M., and Demissie, M., 2002, Uncertainty of nitrate-N load computations for agricultural watersheds: Water Resources Research, v. 38, no. 10, p. 3-1-3-12.

Heffernan, J. B., and Cohen, M. J., 2010, Direct and indirect coupling of primary production and diel nitrate dynamics in a subtropical spring-fed river: Limnology and Oceanography, v. 55, no. 2, p. 677-688.

Hinton, M. J., Schiff, S. L., and English, M. C., 1997, The significance of storms for the concentration and export of dissolved organic carbon from two Precambrian Shield catchments: Biogeochemistry, v. 36, no. 1, p. 67-88.

House, W. A., and Warwick, M. S., 1998, Hysteresis of the solute concentration/discharge relationship in rivers during storms: Water Research, v. 32, no. 8, p. 2279-2290.

Howarth, R. W., 2008, Coastal nitrogen pollution: A review of sources and trends globally and regionally: Harmful Algae, v. 8, no. 1, p. 14-20.

Howarth, R. W., and Marino, R., 2006, Nitrogen as the limiting nutrient for eutrophication in coastal marine ecosystems: Evolving views over three decades: Limnology and Oceanography, v. 51, no. 1part2, p. 364-376.

Inamdar, S. P., O'Leary, N., Mitchell, M. J., and Riley, J. T., 2006, The impact of storm events on solute exports from a glaciated forested watershed in western New York, USA: Hydrological Processes, v. 20, no. 16, p. 3423-3439.

Isles, P. D. F., Xu, Y., Stockwell, J. D., and Schroth, A. W., 2017, Climate-driven changes in energy and mass inputs systematically alter nutrient concentration and stoichiometry in deep and shallow regions of Lake Champlain: Biogeochemistry, v. 133, no. 2, p. 201-217.

Jaffé, R., McKnight, D., Maie, N., Cory, R., McDowell, W. H., and Campbell, J. L., 2008, Spatial and temporal variations in DOM composition in ecosystems: The importance of long-term monitoring of optical properties: Journal of Geophysical Research: Biogeosciences, v. 113, no. G4, p. G04032.

Jarvie, H. P., Sharpley, A. N., Spears, B., Buda, A. R., May, L., and Kleinman, P. J. A., 2013, Water Quality Remediation Faces Unprecedented Challenges from "Legacy Phosphorus": Environmental Science & Technology, v. 47, no. 16, p. 8997-8998.

Johnson, F. A., and East, J. W., 1982, Cyclical relationships between river discharge and chemical concentration during flood events: Journal of Hydrology, v. 57, no. 1, p. 93-106.

Kane, D. D., Conroy, J. D., Peter Richards, R., Baker, D. B., and Culver, D. A., 2014, Re-eutrophication of Lake Erie: Correlations between tributary nutrient loads and phytoplankton biomass: Journal of Great Lakes Research, v. 40, no. 3, p. 496-501.

Kim, S., Kaplan, L. A., and Hatcher, P. G., 2006, Biodegradable dissolved organic matter in a temperate and a tropical stream determined from ultra-high resolution mass spectrometry: Limnology and Oceanography, v. 51, no. 2, p. 1054-1063.

Kirchner, J. W., Feng, X. H., Neal, C., and Robson, A. J., 2004, The fine structure of water-quality dynamics: the (high-frequency) wave of the future: Hydrological Processes, v. 18, no. 7, p. 1353-1359.

Kitis, M., Karanfil, T., Kilduff, J. E., and Wigton, A., 2001, The reactivity of natural organic matter to disinfection byproducts formation and its relation to specific ultraviolet absorbance: Water Science and Technology, v. 43, no. 2, p. 9-16.

Kraus, T. E. C., Bergamaschi, B. A., Hernes, P. J., Spencer, R. G. M., Stepanauskas, R., Kendall, C., Losee, R. F., and Fujii, R., 2008, Assessing the contribution of wetlands and subsided islands to dissolved organic matter and disinfection byproduct precursors in the Sacramento–San Joaquin River Delta: A geochemical approach: Organic Geochemistry, v. 39, no. 9, p. 1302-1318.

Langergraber, G., Fleischmann, N., and Hofstadter, F., 2003, A multivariate calibration procedure for UV/VIS spectrometric quantification of organic matter and nitrate in wastewater: Water Science and Technology, v. 47, no. 2, p. 63-71.

Lawler, J. J., Lewis, D. J., Nelson, E., Plantinga, A. J., Polasky, S., Withey, J. C., Helmers, D. P., Martinuzzi, S., Pennington, D., and Radeloff, V. C., 2014, Projected land-use change impacts on ecosystem services in the United States: Proceedings of the National Academy of Sciences.

Likens, G. E., 2013, Biogeochemistry of a forested ecosystem, New York, NY, Springer, 208 p.:

Ludwig, W., Probst, J.-L., and Kempe, S., 1996, Predicting the oceanic input of organic carbon by continental erosion: Global Biogeochemical Cycles, v. 10, no. 1, p. 23-41.

McClain, M. E., Boyer, E. W., Dent, C. L., Gergel, S. E., Grimm, N. B., Groffman, P. M., Hart, S. C., Harvey, J. W., Johnston, C. A., Mayorga, E., McDowell, W. H., and Pinay, G., 2003, Biogeochemical Hot Spots and Hot Moments at the Interface of Terrestrial and Aquatic Ecosystems: Ecosystems, v. 6, no. 4, p. 301-312.

Michalak, A. M., Anderson, E. J., Beletsky, D., Boland, S., Bosch, N. S., Bridgeman, T. B., Chaffin, J. D., Cho, K., Confesor, R., Daloğlu, I., DePinto, J. V., Evans, M. A., Fahnenstiel, G. L., He, L., Ho, J. C., Jenkins, L., Johengen, T. H., Kuo, K. C., LaPorte, E., Liu, X., McWilliams, M. R., Moore, M. R., Posselt, D. J., Richards, R. P., Scavia, D., Steiner, A. L., Verhamme, E., Wright, D. M., and Zagorski, M. A., 2013, Record-setting algal bloom in Lake Erie caused by agricultural and meteorological trends consistent with expected future conditions: Proceedings of the National Academy of Sciences, v. 110, no. 16, p. 6448-6452.

Monteith, D. T., Stoddard, J. L., Evans, C. D., de Wit, H. A., Forsius, M., Hogasen, T., Wilander, A., Skjelkvale, B. L., Jeffries, D. S., Vuorenmaa, J., Keller, B., Kopacek, J., and Vesely, J., 2007, Dissolved organic carbon trends resulting from changes in atmospheric deposition chemistry: Nature, v. 450, no. 7169, p. 537-U539.

Morris, D. P., Zagarese, H., Williamson, C. E., Balseiro, E. G., Hargreaves, B. R., Modenutti, B., Moeller, R., and Queimalinos, C., 1995, The attentuation of solar UV radiation in lakes and the role of dissolved organic carbon: Limnology and Oceanography, v. 40, no. 8, p. 1381-1391.

Musolff, A., Fleckenstein, J. H., Rao, P. S. C., and Jawitz, J. W., 2017, Emergent archetype patterns of coupled hydrologic and biogeochemical responses in catchments: Geophysical Research Letters, v. 44, no. 9, p. 4143-4151.

Nguyen, H. V.-M., Lee, M.-H., Hur, J., and Schlautman, M. A., 2013, Variations in spectroscopic characteristics and disinfection byproduct formation potentials of dissolved organic matter for two contrasting storm events: Journal of Hydrology, v. 481, no. 0, p. 132-142.

O'Neil, J. M., Davis, T. W., Burford, M. A., and Gobler, C. J., 2012, The rise of harmful cyanobacteria blooms: The potential roles of eutrophication and climate change: Harmful Algae, v. 14, p. 313-334.

Oeurng, C., Sauvage, S., Coynel, A., Maneux, E., Etcheber, H., and Sánchez-Pérez, J.-M., 2011, Fluvial transport of suspended sediment and organic carbon during flood events in a large agricultural catchment in southwest France: Hydrological Processes, v. 25, no. 15, p. 2365-2378.

Pardo, L. H., Fenn, M. E., Goodale, C. L., Geiser, L. H., Driscoll, C. T., Allen, E. B., Baron, J. S., Bobbink, R., Bowman, W. D., Clark, C. M., Emmett, B., Gilliam, F. S., Greaver, T. L., Hall, S. J., Lilleskov, E. A., Liu, L., Lynch, J. A., Nadelhoffer, K. J., Perakis, S. S., Robin-Abbott, M. J., Stoddard, J. L., Weathers, K. C., and Dennis, R. L., 2011, Effects of nitrogen deposition and empirical nitrogen critical loads for ecoregions of the United States: Ecological Applications, v. 21, no. 8, p. 3049-3082.

Parr, T. B., Cronan, C. S., Ohno, T., Findlay, S. E. G., Smith, S. M. C., and Simon, K. S., 2015, Urbanization changes the composition and bioavailability of dissolved organic matter in headwater streams: Limnology and Oceanography, p. n/a-n/a.

Pellerin, B. A., Bergamaschi, B. A., Downing, B. D., Saraceno, J. F., Garrett, J. A., and Olsen, L. D., 2013, Optical techniques for the determination of nitrate in environmental waters: Guidelines for instrument selection, operation, deployment, maintenance, quality assurance, and data reporting, U.S. Geological Survey Techniques and Methods 1-D5.

Pellerin, B. A., Bergamaschi, B. A., Gilliom, R. J., Crawford, C. G., Saraceno, J., Frederick, C. P., Downing, B. D., and Murphy, J. C., 2014, Mississippi River Nitrate Loads from High Frequency Sensor Measurements and Regression-Based Load Estimation: Environmental Science & Technology, v. 48, no. 21, p. 12612-12619.

Pellerin, B. A., Saraceno, J. F., Shanley, J. B., Sebestyen, S. D., Aiken, G. R., Wollheim, W. M., and Bergamaschi, B. A., 2012, Taking the pulse of snowmelt: in situ sensors reveal seasonal, event and diurnal patterns of nitrate and dissolved organic matter variability in an upland forest stream: Biogeochemistry, v. 108, no. 1, p. 183-198.

Pellerin, B. A., Stauffer, B. A., Young, D. A., Sullivan, D. J., Bricker, S. B., Walbridge, M. R., Clyde, G. A., and Shaw, D. M., 2016, Emerging Tools for Continuous Nutrient Monitoring Networks: Sensors Advancing Science and Water Resources Protection: JAWRA Journal of the American Water Resources Association, v. 52, no. 4, p. 993-1008.

Pierson, D. C., Samal, N. R., Owens, E. M., Schneiderman, E. M., and Zion, M. S., 2013, Changes in the timing of snowmelt and the seasonality of nutrient loading: can models simulate the impacts on freshwater trophic status?: Hydrological Processes, v. 27, no. 21, p. 3083-3093.

Porter, J. H., Hanson, P. C., and Lin, C.-C., 2012, Staying afloat in the sensor data deluge: Trends in Ecology & Evolution, v. 27, no. 2, p. 121-129.

Prairie, Y. T., 2008, Carbocentric limnology: looking back, looking forward: Canadian Journal of Fisheries and Aquatic Sciences, v. 65, no. 3, p. 543-548.

Ravichandran, M., 2004, Interactions between mercury and dissolved organic matter - a review: Chemosphere, v. 55, no. 3, p. 319-331.

Raymond, P. A., and Bauer, J. E., 2001, Riverine export of aged terrestrial organic matter to the North Atlantic Ocean: Nature, v. 409, no. 6819, p. 497-500.

Reckhow, D. A., and Singer, P. C., 1990, Chlorination by-products in drinking waters - from formation potentials to finished water concentrations: Journal American Water Works Association, v. 82, no. 4, p. 173-180.

Rieger, L., Langergraber, G., and Siegrist, H., 2006, Uncertainties of spectral in situ measurements in wastewater using different calibration approaches: Water Science and Technology, v. 53, no. 12, p. 187-197.

Roberts, B., Mulholland, P., and Hill, W., 2007, Multiple Scales of Temporal Variability in Ecosystem Metabolism Rates: Results from 2 Years of Continuous Monitoring in a Forested Headwater Stream: Ecosystems, v. 10, no. 4, p. 588-606.

Rosenzweig, B. R., Moon, H. S., Smith, J. A., Baeck, M. L., and Jaffe, P. R., 2008, Variation in the instream dissolved inorganic nitrogen response between and within rainstorm events in an urban watershed: Journal of Environmental Science and Health, Part A, v. 43, no. 11, p. 1223-1233.

Sakamoto, C. M., Johnson, K. S., and Coletti, L. J., 2009, Improved algorithm for the computation of nitrate concentrations in seawater using an in situ ultraviolet spectrophotometer: Limnology and Oceanography-Methods, v. 7, p. 132-143.

SanClements, M. D., Oelsner, G. P., McKnight, D. M., Stoddard, J. L., and Nelson, S. J., 2012, New Insights into the Source of Decadal Increases of Dissolved Organic Matter in Acid-Sensitive Lakes of the Northeastern United States: Environmental Science & Technology, v. 46, no. 6, p. 3212-3219.

Saraceno, J. F., Pellerin, B. A., Downing, B. D., Boss, E., Bachand, P. A. M., and Bergamaschi, B. A., 2009, High-frequency in situ optical measurements during a storm event: Assessing relationships between dissolved organic matter, sediment concentrations, and hydrologic processes: Journal of Geophysical Research-Biogeosciences, v. 114.

Scavia, D., David Allan, J., Arend, K. K., Bartell, S., Beletsky, D., Bosch, N. S., Brandt, S. B., Briland, R. D., Daloğlu, I., DePinto, J. V., Dolan, D. M., Evans, M. A., Farmer, T. M., Goto, D., Han, H., Höök, T. O., Knight, R., Ludsin, S. A., Mason, D., Michalak, A. M., Peter Richards, R., Roberts, J. J., Rucinski, D. K., Rutherford, E., Schwab, D. J., Sesterhenn, T. M., Zhang, H., and Zhou, Y., 2014,

Assessing and addressing the re-eutrophication of Lake Erie: Central basin hypoxia: Journal of Great Lakes Research, v. 40, no. 2, p. 226-246.

Schindler, D. W., Carpenter, S. R., Chapra, S. C., Hecky, R. E., and Orihel, D. M., 2016, Reducing Phosphorus to Curb Lake Eutrophication is a Success: Environmental Science & Technology, v. 50, no. 17, p. 8923-8929.

Schroth, A. W., Giles, C. D., Isles, P. D. F., Xu, Y., Perzan, Z., and Druschel, G. K., 2015, Dynamic Coupling of Iron, Manganese, and Phosphorus Behavior in Water and Sediment of Shallow Ice-Covered Eutrophic Lakes: Environmental Science & Technology, v. 49, no. 16, p. 9758-9767.

Sleighter, R. L., and Hatcher, P. G., 2007, The application of electrospray ionization coupled to ultrahigh resolution mass spectrometry for the molecular characterization of natural organic matter: Journal of Mass Spectrometry, v. 42, no. 5, p. 559-574.

Smith, V. H., Tilman, G. D., and Nekola, J. C., 1999, Eutrophication: impacts of excess nutrient inputs on freshwater, marine, and terrestrial ecosystems: Environmental Pollution, v. 100, no. 1–3, p. 179-196.

Sobczak, W., Findlay, S., and Dye, S., 2003, Relationships between DOC bioavailability and nitrate removal in an upland stream: An experimental approach: Biogeochemistry, v. 62, no. 3, p. 309-327.

Stoddard, J. L., Kahl, J. S., Deviney, F. A., DeWalle, D. R., Driscoll, C. T., Herlihy, A. T., Kellogg, J. H., Murdoch, P. S., Webb, J. R., and Webster, K. E., 2003, Response of Surface Water Chemistry to the Clean Air Act Amendments of 1990: U.S. Environmental Protection Agency.

Stubbins, A., Lapierre, J. F., Berggren, M., Prairie, Y. T., Dittmar, T., and del Giorgio, P. A., 2014, What's in an EEM? Molecular signatures associated with dissolved organic fluorescence in Boreal Canada: Environmental Science & Technology, v. 48, no. 18, p. 10598-10606.

Stumpf, R. P., Wynne, T. T., Baker, D. B., and Fahnenstiel, G. L., 2012, Interannual Variability of Cyanobacterial Blooms in Lake Erie: PLoS ONE, v. 7, no. 8, p. e42444.

Townsend, A. R., Howarth, R. W., Bazzaz, F. A., Booth, M. S., Cleveland, C. C., Collinge, S. K., Dobson, A. P., Epstein, P. R., Holland, E. A., Keeney, D. R., Mallin, M. A., Rogers, C. A., Wayne, P., and Wolfe, A. H., 2003, Human health effects of a changing global nitrogen cycle: Frontiers in Ecology and the Environment, v. 1, no. 5, p. 240-246.

Vitousek, P. M., Aber, J. D., Howarth, R. W., Likens, G. E., Matson, P. A., Schindler, D. W., Schlesinger, W. H., and Tilman, D. G., 1997, Human alteration of the global nitrogen cycle: Sources and consequences: Ecological Applications, v. 7, no. 3, p. 737-750.

Walsh, J., Dwuebbles, K., Hayhoe, K., Kossin, J., Kunkel, K., Stephens, G., Thorne, P., Vose, R., Wehner, M., Willis, J., Anderson, D., Doney, S., Feely, R., Hennon, P., Kharin, V., Knutson, T., Landerer, F., Lenton, T., Kennedy, J., and Somerville, R., 2014, Climate change impacts in the United States: The third national climate assessment: US Global Change Research Program.

Weyhenmeyer, G. A., Fröberg, M., Karltun, E., Khalili, M., Kothawala, D., Temnerud, J., and Tranvik, L. J., 2012, Selective decay of terrestrial organic carbon during transport from land to sea: Global Change Biology, v. 18, no. 1, p. 349-355.

Wilson, H., and Xenopoulos, M., 2008, Ecosystem and Seasonal Control of Stream Dissolved Organic Carbon Along a Gradient of Land Use: Ecosystems, v. 11, no. 4, p. 555-568.

Wilson, H. F., and Xenopoulos, M. A., 2009, Effects of agricultural land use on the composition of fluvial dissolved organic matter: Nature Geosci, v. 2, no. 1, p. 37-41.

Wironen, M. B., Bennett, E. M., and Erickson, J. D., 2018, Phosphorus flows and legacy accumulation in an animal-dominated agricultural region from 1925 to 2012: Global Environmental Change, v. 50, p. 88-99.

CHAPTER 2. HIGH-FREQUENCY DISSOLVED ORGANIC CARBON AND NITRATE MEASUREMENTS REVEAL DIFFERENCES IN STORM HYSTERESIS AND LOADING IN RELATION TO LAND COVER AND SEASONALITY

Abstract

Storm events dominate riverine loads of dissolved organic carbon (DOC) and nitrate, and are expected to increase in frequency and intensity in many regions due to climate change. We deployed three high-frequency (15-minute) *in-situ* absorbance spectrophotometers to monitor DOC and nitrate concentration for 126 storms in three watersheds with agricultural, urban, and forested land use / land cover. We examined intrastorm hysteresis and the influences of seasonality, antecedent conditions, storm size, and dominant land use / land cover on storm DOC and nitrate loads. DOC hysteresis was generally anti-clockwise at all sites, indicating distal and plentiful sources for all three streams despite varied DOC character and sources. Nitrate hysteresis was generally clockwise for urban and forested sites, but anti-clockwise for the agricultural site, indicating an exhaustible, proximal source of nitrate in the urban and forested sites, and more distal and plentiful sources of nitrate in the agricultural site. The agricultural site had significantly higher storm nitrate yield per water yield and higher storm DOC yield per water yield than the urban or forested sites. Seasonal effects were important for storm nitrate yield in all three watersheds and farm management practices likely caused complex interactions with seasonality at the agricultural site. Hysteresis indices did not improve predictions of storm nitrate yields at any site. We discuss key lessons from using high-frequency *in-situ* optical sensors.

Introduction

Storms transport considerably more carbon and nutrients to receiving water bodies than during times of baseflow (Fellman et al. 2009; Inamdar et al. 2006). Understanding fluxes during storm events is critical since storms in the US are expected to increase in frequency and intensity in the future (Walsh et al. 2014). Storms are difficult to characterize with traditional "grab sampling" approaches because they are ephemeral in time and variable in space. The development of *in-situ* optical sensors has revolutionized water quality monitoring and gives researchers an improved view into the important and dynamic role that storms play in water quality. These instruments have several advantages over traditional hand or automatic grab sampling to characterize storms, including: (1) sub-hourly measurement intervals to resolve rapid changes in water quality; (2) no need for hazardous chemicals to analyze solute concentrations; (3) no storage or transportation issues that can impact lab analyses of grab samples; and (4) the ability to continuously monitor streamwater chemistry so that rare and episodic events can be characterized. Assessing solute export using *in-situ* sensors also reduces error associated with discharge based load estimations, since discharge-solute relationships can break down during extreme precipitation events or due to variable event-based hysteresis loops (Dhillon and Inamdar 2013).

Recently, *in-situ* spectrophotometers have been used to measure streamwater dissolved organic carbon (DOC) and nitrate (NO_3^-) concentrations, two important water quality characteristics. DOC is transported from terrestrial sources of carbon to receiving water bodies (Prairie 2008), attenuates ultraviolet radiation that is harmful to microorganisms (Bukaveckas and Robbins-Forbes 2000; Morris et al. 1995), affects metal

pollutant transport and bioavailability (Driscoll et al. 1988; Ravichandran 2004), and has been identified as the primary cause of harmful trihalomethane disinfectant byproduct formation during drinking water treatment (Chow et al. 2007; Kraus et al. 2008; Nguyen et al. 2013; Reckhow and Singer 1990). Nitrate is an essential nutrient to aquatic ecosystems; however, when supply exceeds ecosystem demand, elevated concentrations in surface waters cause numerous adverse effects on downstream freshwater ecosystems (Camargo and Alonso 2006; Smith et al. 1999), including changes in the biotic community structure and loss of biodiversity (Pardo et al. 2011), eutrophication (Smith et al. 1999), increased acidification in forested systems (Driscoll et al. 2001) leading to increased mobilization of toxic aluminum (Baker et al. 1996), and deterioration of drinking water supply quality (Townsend et al. 2003). Therefore, *in-situ* high-frequency measurements of these key parameters have exciting potential to inform our understanding of a diverse suite of water quality issues operating across multiple spatial and temporal scales.

Quantifying the dynamic relationship between solute concentration and stream discharge can improve understanding of solute transport pathways and active source areas (e.g. Chanat et al. 2002; Evans and Davies 1998; House and Warwick 1998). Hysteresis occurs when the concentration – discharge relationship differs on the rising limb of a storm versus the falling limb (e.g. Bowes et al. 2015; Johnson and East 1982). When a solute has higher concentrations on the rising limb versus the falling limb, a plot of these parameters forms a clockwise loop. This non-linear relationship is often the result of an exhaustible solute supply that is close in proximity to the measurement location (e.g. Bowes et al. 2009). When concentrations are higher on the falling limb versus the rising limb, an anti-clockwise hysteresis pattern emerges. This occurs when sources are more distal, have a

longer transport time, stem from deeper subsurface zones, or a combination of these factors (Bieroza and Heathwaite 2015; Donn et al. 2012). Hysteresis relationships can provide some indication of the general sources of solutes during storms, though it is not clear whether hysteresis dynamics correlate with solute loading.

Seasonal effects can have significant influences on storm DOC and nitrate export. During spring snowmelt, high water table levels activate upper organic soil horizons during storms, causing greater export of DOC, especially from riparian soils (Boyer et al. 1997; Raymond and Saiers 2010). This is also a season in which nitrate export loads tend to be higher because nitrate stored in the snowpack is transported to the stream during rain-on-snow events, and biological uptake has not yet begun (Driscoll et al. 2003). In the summer months, stream water DOC loads tend to decrease because lower precipitation and drier soils result in fewer storms that activate flow paths in upper soil horizons that leach DOC. Stream water nitrate concentrations also tend to fall at this time as biological uptake increases dramatically (Likens 2013).

Land use / land cover (LULC) also plays a key role in determining the amount of DOC and nitrate that is exported during storms. Studies in small agricultural watersheds often note elevated baseflow DOC concentrations relative to other streams in the same region and increases in DOC concentration during storm events (Dalzell et al. 2005; Royer and David 2005; Saraceno et al. 2009; Vidon et al. 2008) because agricultural activities alter the source of stream water DOC and lead to greater in-stream DOC production due to greater fertility (Stanley et al. 2012; Wilson and Xenopoulos 2008). A significant portion of nitrogen delivered to water bodies during storms is from non-point sources, stemming from agricultural practices and atmospheric deposition due to human activities (Boyer et

al. 2002). Agriculture and urban land use change have been shown to contribute to increased nitrate loads in streams (Boesch et al. 2001), and can alter the storm response of a watershed from supply-limited, typical of a forested stream, to a transport-limited condition (Carey et al. 2014; Rosenzweig et al. 2008). Urbanization often has a substantial impact on stream hydrology (Walsh et al. 2005), and can result in elevated organic carbon loading in streams (Newcomer et al. 2012; Sickman et al. 2007). Increased DOC loads in urban streams during storms can be sourced from wastewater inputs (Aitkenhead-Peterson et al. 2009; Sickman et al. 2007), organic material deposited onto impervious surfaces, human and animal waste, and grass clippings from home lawns, all combined with greater hydrologic response (Sickman et al. 2007). These numerous sources are in addition to decomposing organic matter that accumulates in soil layers, as in unaltered systems. Even so, there is no consensus on the overall effects of urbanization on DOC concentrations and loads. Studies suggest that urbanization causes DOC export to either increase (Kaushal and Belt 2012), decrease (Kominoski and Rosemond 2011), or provide a compensatory mechanism where internal production balances decrease of external inputs, resulting in no net change (Parr et al. 2015).

The Northeast Water Resources Network (NEWRnet) was created in Spring 2014 to better understand water quality dynamics in the Northeast US by using emerging optical water quality sensor technology. Our sensor array provided an excellent resource to see how several of the factors summarized above influence storm DOC and nitrate dynamics. Continuous monitoring in the spring, summer, and fall seasons over 19 months using *in-situ* spectrophotometers allowed us to quantify DOC and nitrate storm exports using high-frequency measurements. We use these data to address the following research objectives:

(1) evaluate the use of *in-situ* spectrophotometers to quantify DOC and nitrate storm hysteresis and exports using high-frequency measurements in streams with varied LULCs; (2) compare intrastorm DOC and nitrate hysteresis relationships between watersheds of differing LULCs to determine differences in source areas and solute transport processes; (3) compare the influence of agricultural, urban/suburban, and forested LULCs on storm DOC and nitrate exports; and (4) determine what factors, including hysteresis, might explain the variance in storm DOC and nitrate exports. Through these analyses, we develop a more holistic perspective of how land use, seasonality, and storm event water yield impact storm event loading and the temporal evolution of water chemistry during storms.

Study areas

We compared streams draining watersheds with various primary LULCs to characterize the influence of LULC on storm hysteresis and exports of DOC and nitrate. The study sites were in the Lake Champlain Basin of Vermont in the northeastern US (Table 2.1, Figure 2.1). Hungerford Brook is a primarily agricultural catchment, including dairy, row crops, hay, and pasture. Potash Brook is situated near the city of Burlington, Vermont's densest population center. Its watershed is primarily characterized by urban and suburban development (54%), though there is some agricultural and forest cover (29% and 11%, respectively). The Wade Brook catchment is primarily forested (95%) and is situated on the western slope of Vermont's Green Mountain chain. Hungerford Brook and Wade Brook eventually drain to the Missisquoi River and Lake Champlain; Potash Brook drains directly to Lake Champlain. Precipitation totals in the Wade Brook catchment are higher

than the catchments of Hungerford Brook and Potash Brook due to orographic effects (Table 2.1).

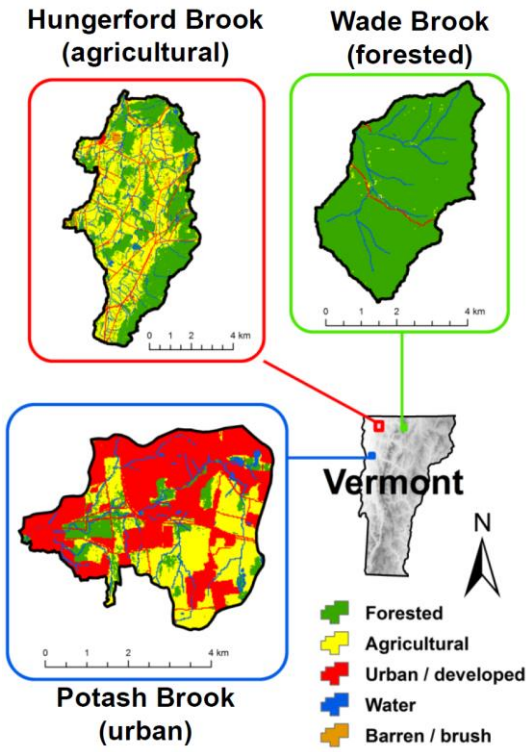

Figure 2.1. Map showing location and land use / land cover of the three study areas.

Table 2.1. Summary of study area characteristics

	Hungerford Brook	Potash Brook	Wade Brook
Primary land cover	Agricultural	Urban / Suburban	Forest
Watershed area (km^2)	48.1	18.4	16.7
Percentage forested	40.5	10.6	95.1
Percentage agricultural	44.8	29.1	0.6
Percentage urban	5.6	53.5	0.8
Percentage impervious area	2.3	23.9	0
Sensor elevation (m)	80	42	320
Maximum watershed elevation (m)	354	143	981
Mean watershed slope (%)	5.6	5.3	26
Mean air temperature (°C)	6.7	7.8	4.2
Mean precipitation (mm yr^{-1})	1000	961	1453
Mean annual atmospheric nitrogen deposition (kg N km^{-2})	450	340	570
Sensor optical path length (mm)	5	5	15
Coordinates (WGS 1984)	44.918403° N, 73.055664° W	44.444331° N, 73.214482° W	44.864468° N, 72.552904° W
Soil and Surficial Geology	Sandy, silty, and stony loams	Sandy and silty loams, clay	Glacial till, sandy loam
Vegetation	Agricultural, mixed northern hardwoods and conifer	Urban / suburban landscaping, mixed northern hardwoods and conifer, agricultural	Mixed northern hardwoods and conifer

Methods

In-situ methods

We used s::can Spectrolyser UV-Vis spectrophotometers (s::can Messtechnik GmbH, Vienna, Austria) in each stream, deployed from June 2014 to December 2015 for spring, summer, and fall seasons. The sensors were housed in PVC tubing for protection during high flows, were solar powered for autonomous operation, and transmitted data in real time through a cellular data network. The spectrophotometers measure light absorbance at wavelengths ranging from 220 to 750 nm at 2.5 nm increments and were programmed to take measurements every 15 minutes. Optical path lengths were either 5 or 15 mm, depending on the typical turbidity of each stream (Table 2.1), and absorbance spectra were normalized by optical path length for comparison. Sensor measurement windows were automatically cleaned before each measurement with a silicone wiper and cleaned manually in the field at least every two weeks using pure ethanol. To focus on dissolved constituents, absorbance spectra were corrected for the effects of turbidity by fitting a third-order polynomial in the visible range of the spectrum, extrapolating into the UV portion, and then subtracting the extrapolated absorbance from the raw spectrum (Avagyan et al. 2014; Langergraber et al. 2003). Discharge measurements were acquired from a U.S. Geological Survey gaging station where available (Hungerford Brook Station 04293900), or calculated from discharge-depth rating curves developed with velocity-area calculations (Turnipseed and Sauer 2010), salt dilutions (Moore 2005), and 15-minute stage measurements using atmospherically compensated pressure transducers.

Lab measurements

Manual grab samples were collected during baseflow and storms to compare and calibrate *in-situ* absorbance spectrophotometer measurements to laboratory measurements. A total of 226 grab samples were taken over the duration of this study. Each sample was filtered using rinsed glass fiber GF/F filters (nominal pore size of 0.7 µm) into new HDPE bottles. Samples were stored on ice in the field, then DOC samples were stored in a cooler at 2 ºC (for DOC samples), and nitrate samples were stored in a freezer at -23 ºC until analysis. Lab DOC measurements were made using a Shimadzu TOC-L analyzer using the combustion catalytic oxidation method. Lab nitrate-N measurements were made using the QuickChem method 31-107-04-1E on a Latchat analyzer.

Preparation of in-situ sensor data

Because of the high dimensionality of absorbance spectra, dimension reduction combined with multiple regression techniques have proven effective in recent studies to predict DOC and nitrate concentrations (Avagyan et al. 2014; Etheridge et al. 2014). We used an identical approach to Etheridge et al. (2014), where partial least squares regression is employed with the pls package in R to generate calibration algorithms (Mevik et al. 2015; R Core Team 2015). To validate calibrations, we ensured that a randomly chosen subset representing 10% of each calibration dataset could be adequately predicted using the remaining data. Once validated, the full dataset was used for each calibration. Spectral slope ratio (Helms et al. 2008) was calculated for all grab samples and compared among sites to determine how DOC character might influence calibrations. Spectral slope was calculated using the equation

$$a_\lambda = a_{\lambda_{ref}} e^{-S(\lambda - \lambda_{ref})}\ , \quad (1)$$

where S is the best fit spectral slope (nm^{-1}), a is the Naperian absorption coefficient (m^{-1}), λ is wavelength (nm), and λ_{ref} is the reference wavelength (285 nm). The spectral slope ratio was then found by dividing the spectral slope over the 275-295 nm range by the spectral slope in the 350-400 nm range.

Time series of DOC and nitrate-N concentration (mg L^{-1}) were generated using each calibration, and short data gaps (< 2 hr) were filled using cubic spline interpolation to produce a continuous dataset for the analyzed storms. We then multiplied predicted concentration by concurrent discharge ($m^3\ s^{-1}$) to estimate DOC and nitrate-N load (g s^{-1}).

Storms were delineated by baseflow separation using the filter method outlined in Arnold et al. (1995). This filtering approach partitions the streamflow hydrograph into baseflow and direct runoff components. A minimum rise criterion determined the start of each storm and the end of the storm was chosen manually as a point on the falling limb where storm event discharge approached antecedent or inter-event levels (Figure 2.2). Manual selection of the inflection point was used since we found that analyses were not sensitive to minor differences in the designated ending point of the storm. Geographic separation of sites and differences in hydrologic response for each watershed resulted in differing numbers of observed storms for each site.

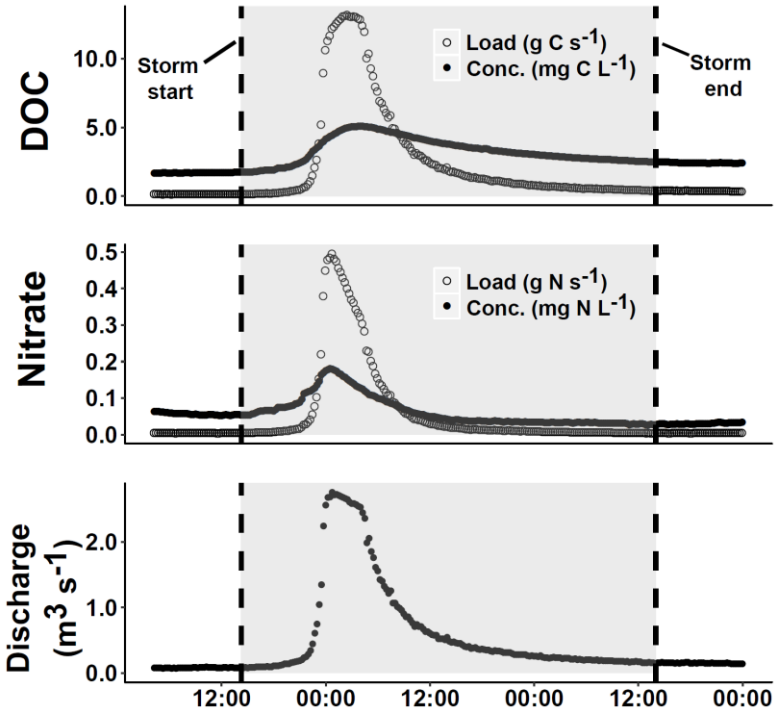

Figure 2.2. Plot of high frequency (15-min) data from a storm at the forested site on October 4 – 6, 2014. DOC and nitrate concentrations were measured with the s::can spectrophotometer and load was calculated by the product of concentration and concurrent discharge. The shaded region between the dashed lines shows the period of the record that was considered for this storm; the DOC and nitrate loads were integrated over this period, and then divided by watershed area to determine storm DOC and nitrate yield.

Calculation of hysteresis indices

We used a recently improved hysteresis index to quantify temporal solute concentration dynamics for each storm and compare across our sites (Lloyd et al. 2016). This hysteresis index is based on normalized discharge and storm solute concentrations, as follows:

$$Q_{i,norm} = \frac{Q_i - Q_{min}}{Q_{max} - Q_{min}} \quad (2)$$

$$C_{i,norm} = \frac{C_i - C_{min}}{C_{max} - C_{min}}, \quad (3)$$

where Q_i and C_i are the discharge and solute concentration values at timestep i, Q_{max} and Q_{min} are the maximum and minimum discharge values in the storm, and C_{max} and C_{min} are

the maximum and minimum solute concentrations in the storm. Then, we found an interpolated solute concentration C_j by linear regression of $Ci_{,norm}$ at 2% intervals of $Qi_{,norm}$ on both the rising and falling limbs at interval j using two adjacent measurements. The hysteresis index at each discharge interval was determined by subtracting the falling limb from the rising limb:

$$HI_j = C_{j,rising} - C_{j,falling}. \quad (4)$$

HI_j was only calculated for intervals where data existed for both rising and falling limbs because not all storms returned to their initial discharge condition. An overall hysteresis index for each storm event was determined by calculating the mean of all HI_j values (Figure 2.3a - b). This value is conveniently scaled from -1 to 1, where negative values indicate anti-clockwise hysteresis, positive values indicate clockwise hysteresis, and the magnitude of *HI* indicates the amount of difference between the rising and falling limbs. We compared these measures using the non-parametric Kruskal-Wallis test for differences in the medians (Kruskal and Wallis 1952), and Levene's test for equality of variances among sites (Levene 1960).

Storms were further characterized using a flushing index *FI* similar to the one used by Butturini et al. (2008):

$$FI = C_{Qpeak,norm} - C_{initial,norm}, \quad (5)$$

where $C_{Qpeak,norm}$ and $C_{initial,norm}$ are the normalized solute concentrations at the point of peak discharge and the beginning of the storm, respectively. This index also conveniently ranges from -1 to 1, where negative values indicate a diluting effect on the rising limb, and positive values indicate an increase in concentration, or "flushing" effect on the rising limb. *FI* values are equal to the slope of the line that intersects the first normalized solute

concentration measured in a storm and the normalized solute concentration at peak discharge (Figure 2.3c).

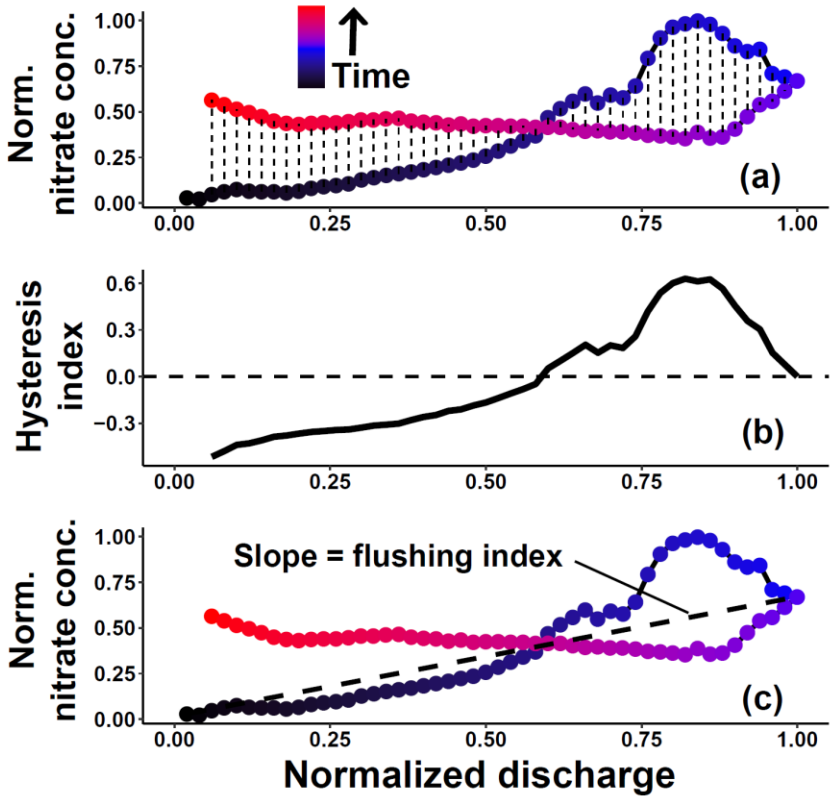

Figure 2.3. Plot of (a) normalized nitrate concentration vs. normalized discharge, (b) hysteresis index, and (c) flushing index illustration for a storm at the agricultural site on September 30 – October 2, 2015. We calculated hysteresis index HI_j by subtracting the normalized solute concentration on the falling limb from that of the rising limb for each 2% of normalized discharge, and the storm hysteresis *HI* is the mean of these values. Flushing index *FI* is the slope of the line that intersects the normalized solute concentration at the beginning and at the point of peak discharge of the storm. For this storm, nitrate *HI* = -0.03 and *FI* = 0.64.

Statistical analyses for storm nitrate and DOC yield

For each storm, we integrated DOC and nitrate-N load from the beginning to the end of the event to determine export mass (kg) of each solute. This was divided by watershed area to calculate DOC and nitrate-N yield (kg km^{-2}) for comparison among sites. We also integrated discharge for each storm to calculate the amount of runoff and then divided by watershed area to determine water yield (mm). The ratio of storm DOC yield to

water yield (kg C km^{-2} mm^{-1}), and the ratio of storm nitrate yield to water yield (kg N km^{-2} mm^{-1}) were also calculated for each storm. The non-parametric Kruskal-Wallis test was employed to detect significant differences in population medians (Walford 2011).

To explore the relationship between both storm DOC yield and water yield, and storm nitrate yield and water yield, least squares linear regression was performed for each, grouped by site. When less than 90% of variance was explained, additional regressions were performed by grouping storms by season. Since storm DOC and nitrate yields are calculated using stream discharge, they are intrinsically auto-correlated with storm water yield. This means that if solute concentration is constant, we would expect a perfectly linear correlation. A weak correlation is indicative of greater variability in solute concentration that is related to other factors besides stream discharge. Difference in correlation coefficients between sites stems from differences in solute concentrations during and among storms.

Regression coefficients between these subgroups were tested for statistically significant differences using the equation

$$Z = \frac{b_1 - b_2}{\sqrt{{SE_1}^2 + {SE_2}^2}}, \quad (6)$$

where b_1 and b_2 are the regression coefficients of each model, and SE_1, SE_2 are the associated standard errors (Paternoster et al. 1998). Models with regression coefficients that were not significantly different were then tested for categorical differences using analysis of covariance (ANCOVA). For this test and all others in the paper, we used $p \leq 0.05$ as significant.

Results

Sensor performance

The partial least squares regression technique used sensor absorbance spectra to predict nitrate-N concentrations with excellent comparison to lab measured values. Over 99% of the variance in laboratory measured concentrations was explained by sensor predictions at all three sites, with a standard error of ± 0.0078 mg N L^{-1} (Figure 2.4a).

Spectral slope ratios of grab samples were significantly different among sites ($p < 0.0001$) (Figure 2.5), and calibrations to predict DOC concentrations were optimal when data were grouped by site (Figure 2.4b - d). The sensors explained 96%, 95%, and 97% of the variance in lab measured DOC concentrations at the agricultural, urban, and forested sites, respectively. The standard error was highest at the agricultural site with a value of ± 0.045 mg C L^{-1}, and was lowest at the forested site with a value of ± 0.025 mg C L^{-1}.

Storm DOC hysteresis

We observed 126 storms, including 40 at the agricultural site, 26 at the urban site, and 60 at the forested site (Supporting Figure 2.S1). The DOC hysteresis loop pattern varied greatly from storm to storm, and the median DOC hysteresis index was negative for all three sites, indicating a typical anti-clockwise loop pattern (Figure 2.6a). The median DOC hysteresis indices were not significantly different among sites, though the variances were significantly different among sites by Levene's test ($p = 0.013$). The agricultural stream had the highest variance in DOC hysteresis index ($\sigma^2 = 0.09$), which was more than double that of the urban and forested sites ($\sigma^2 = 0.04$ for each).

Plotting DOC storm hysteresis index vs. DOC storm flushing index revealed that most storms at all three sites increased in concentration on the rising limb, and had falling

limbs that were even higher in concentration than the rising limb. There was notable variability in this relationship for all three sites (Figure 2.6c). We found no apparent patterns relating storm DOC hysteresis or flushing index to seasonal or other measured variables.

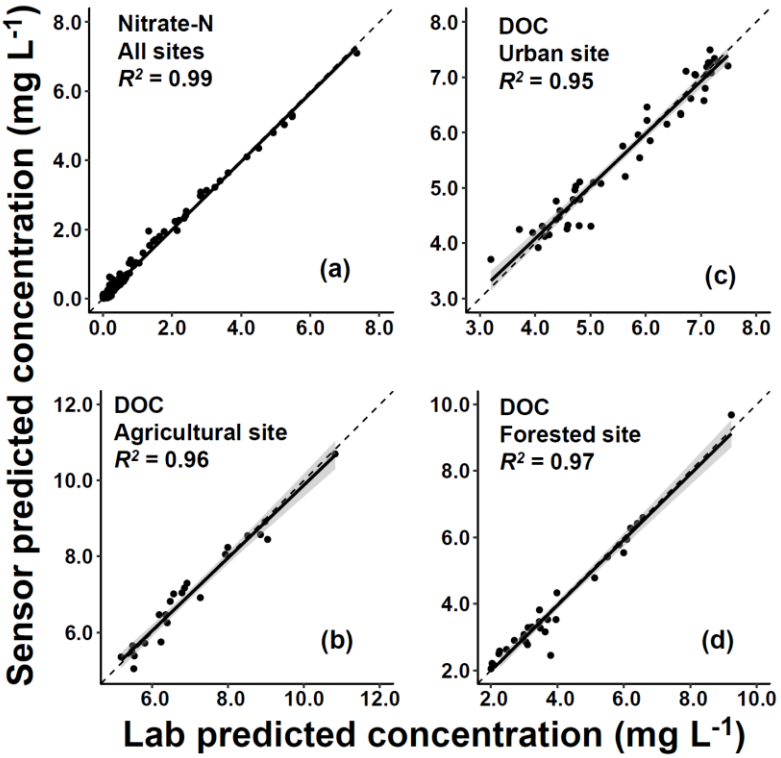

Figure 2.4. Plots of sensor predicted (a) nitrate and (b-d) DOC concentrations vs. lab measured values. Shaded regions indicate 95% confidence intervals. The partial least squares calibration algorithm causes all regression lines to assume the equation y = x, and the dashed line is 1:1. All relationships were highly significant ($p < 0.0001$).

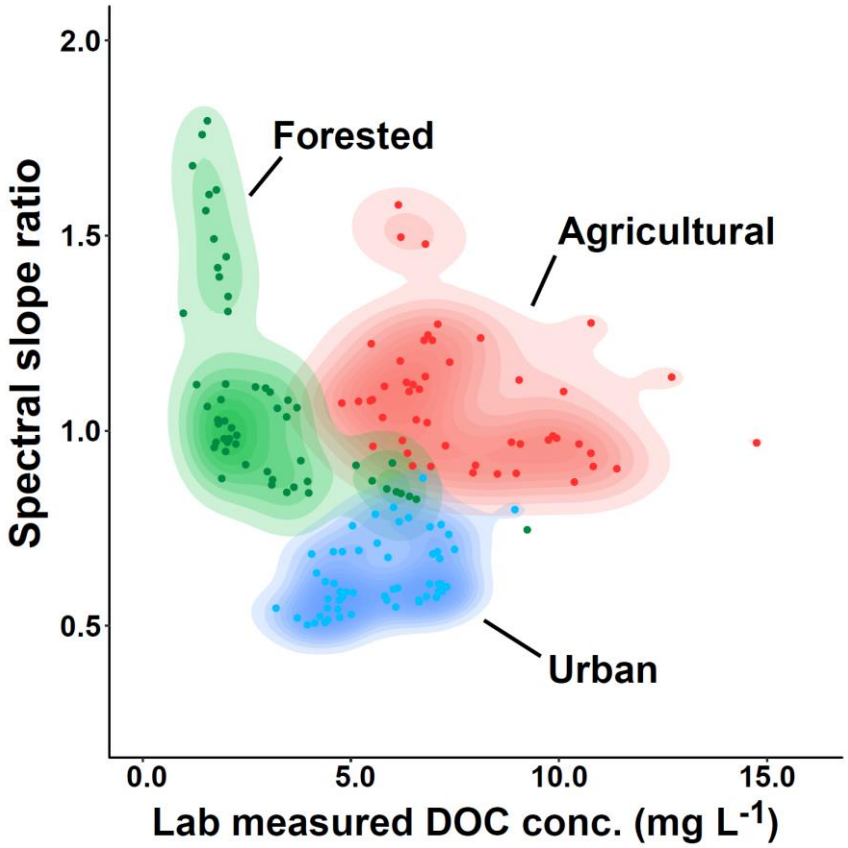

Figure 2.5. Plot of spectral slope ratio versus lab measured DOC concentration. Shaded areas show high density regions for each site.

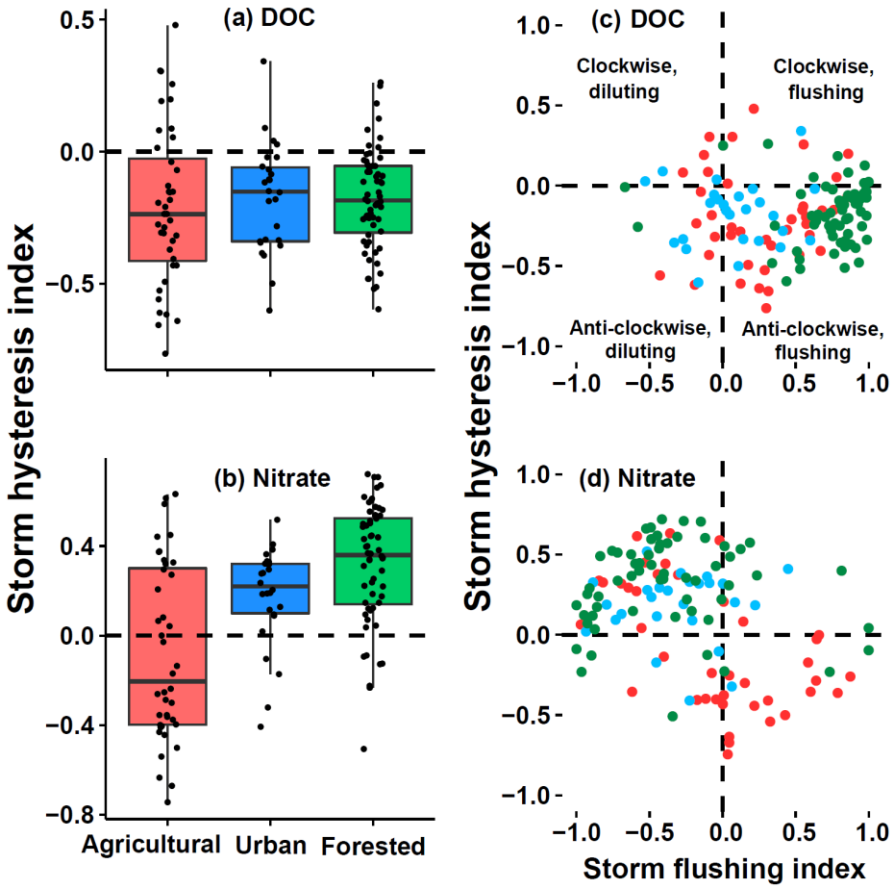

Figure 2.6. Box and whisker plots of storm hysteresis indices for (a) DOC and (b) nitrate, and plots of storm hysteresis index vs. storm flushing index at the agricultural (red), urban (blue), and forested (green) sites for (c) DOC and (d) nitrate.

Storm nitrate hysteresis

The nitrate hysteresis analysis for the 126 storms revealed differences among the sites. The median nitrate hysteresis indices were negative for the agricultural site (anti-clockwise loop pattern), positive (clockwise loop pattern) for the urban and forested sites, and were significantly different by the Kruskal-Wallis test ($p < 0.0001$). The forested site had a higher positive median hysteresis index than the urban site, indicating larger clockwise loop patterns (Figure 2.6b). The agricultural stream had the highest variance in nitrate hysteresis index ($\sigma^2 = 0.15$), and was two to three times higher than variances for the urban and forested sites ($\sigma^2 = 0.05$ and 0.08, respectively).

Plotting nitrate storm hysteresis index vs. nitrate storm flushing index revealed remarkable variability among sites. Most storms at the urban and forested streams showed decreasing nitrate concentrations on the rising limbs, and even lower nitrate concentrations on the falling limbs. The agricultural stream showed greater variability than the others though tended toward clockwise hysteresis and negative flushing index, or anti-clockwise hysteresis and positive flushing index (Figure 2.6d). We found no apparent patterns relating storm nitrate hysteresis or flushing index to seasonal or other measured variables.

Storm DOC yield

The median ratio of storm DOC yield to water yield was statistically different at each site, as revealed by a Kruskal-Wallis test ($p < 0.0001$). The highest median ratio is at the agricultural (8.39 kg C km^{-2} mm^{-1}), followed by the urban (5.37 kg C km^{-2} mm^{-1}), and is lowest at the forested site (2.98 kg C km^{-2} mm^{-1}). Water yield alone explains a large portion of the variance in storm DOC yield for each of the three monitored sites. With respect to DOC yield per storm water yield, the agricultural stream was largest, followed by the urban and finally the forested streams. By equation (6), differences in slope are statistically significant between the agricultural and the other two sites ($p < 0.0001$), but not between the urban and forested sites ($p = 0.16$) (Figure 2.7a). The lack of a significant difference in slope qualifies these sites for an ANCOVA test, which reveals that there is a statistically significant difference in the relationship between storm DOC yield and storm water yield for the urban and forested stream.

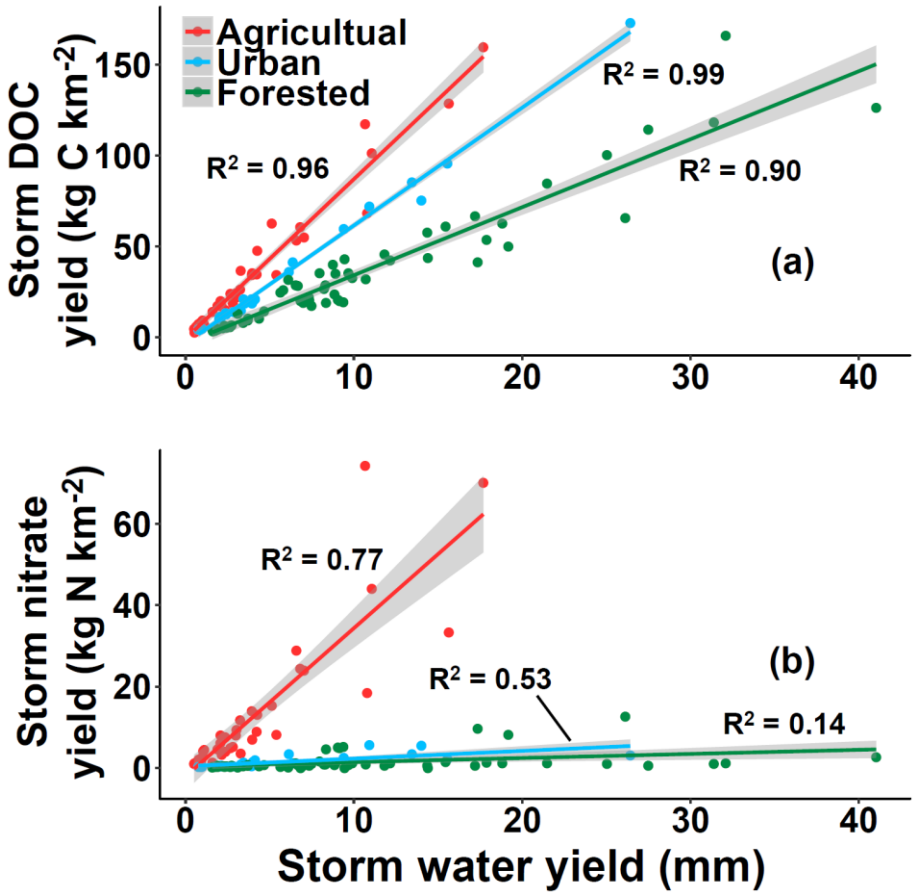

Figure 2.7. Plot of (a) storm DOC yield vs. storm water yield and (b) storm nitrate yield vs. storm water yield for all 126 storms observed during the 2014 – 2015 field seasons. Shaded regions indicate 95% confidence intervals. For storm DOC yield, relationships were highly significant for each site ($p < 0.0001$), and hypothesis tests comparing the sites showed significant differences between each site. For storm nitrate yield, the agricultural site had a significantly steeper slope than the forested and urban sites, and no significant differences were apparent between the urban and forested sites.

Storm nitrate yield

The median ratio of storm nitrate yield to water yield is statistically different at each site, as revealed by a Kruskal-Wallis rank sum test ($p < 0.0001$). The highest median ratio is at the agricultural (2.52 kg km^{-2} mm^{-1}), followed by the urban (0.27 kg km^{-2} mm^{-1}), and is lowest at the forested site (0.12 kg km^{-2} mm^{-1}). Among the three sites, a large portion of the variance in storm nitrate yield can be explained at the agricultural site with storm water yield through linear regression ($R^2 = 0.77$). However, only 53% and 14% of the variance

can be explained by storm water yield for the urban and forested sites, respectively (Figure 2.7b).

In general, the agricultural site exports higher storm nitrate yield per water yield than the urban site, and the forested site exports the lowest amount of storm nitrate yield per storm water yield of the three. Differences in storm nitrate yield among sites became more pronounced with increased storm water yield. The regression slopes between the agricultural and urban sites, and between the agricultural and forested sites were significantly different by equation (6) ($p < 0.0001$). The difference in regression slopes for the urban and forested stream were not significant, however ($p = 0.076$), and an ANCOVA test showed no significant difference between the regressions ($p = 0.39$).

Seasonal effects on storm nitrate yield

At the agricultural site, a larger portion of the variance in storm nitrate yield could be explained by storm water yield when the storms were grouped by spring, summer, and fall seasons. In addition, the regression slope coefficient between storm nitrate yield and storm water yield was significantly greater for summer than spring storms ($p < 0.0001$), greater for summer than fall storms ($p = 0.016$), and greater for fall storms than spring storms ($p = 0.024$) by equation (6) (Figure 2.8a).

A larger portion of the variance in storm nitrate yield at the urban site could be explained by storm water yield when grouped by season (Figure 2.8b). Equation (6) also revealed that the regression slope at the urban site was significantly higher for spring storms than summer storms ($p = 0.027$), but not significantly different between other storms. This qualified these subgroups for an ANCOVA test, which revealed that there is a significant categorical difference between spring and fall storms ($p < 0.0001$). The

ANCOVA test showed no significant differences between summer and fall storms at the urban site.

Grouping storms by season at the forested site showed a significant difference in regression slopes between spring storms and the other two seasons ($p < 0.0001$), though not between summer and fall storms (Figure 2.8c) ($p = 0.14$), and the ANCOVA test showed no significant categorical difference between summer and fall storms.

Plotting the ratio of storm nitrate yield to water yield for each storm reveals that there are large differences among sites and that seasonal trends differ (Figure 2.9). At the agricultural site, this ratio increases through the spring, decreases through the summer, then increases once again in the fall. While swings in this ratio are less pronounced at the urban site, there is a decrease through the spring, the ratio stays low in the summer, then increases again in the fall. At the forested site, this ratio is by far highest in the early spring, then decreases throughout the year.

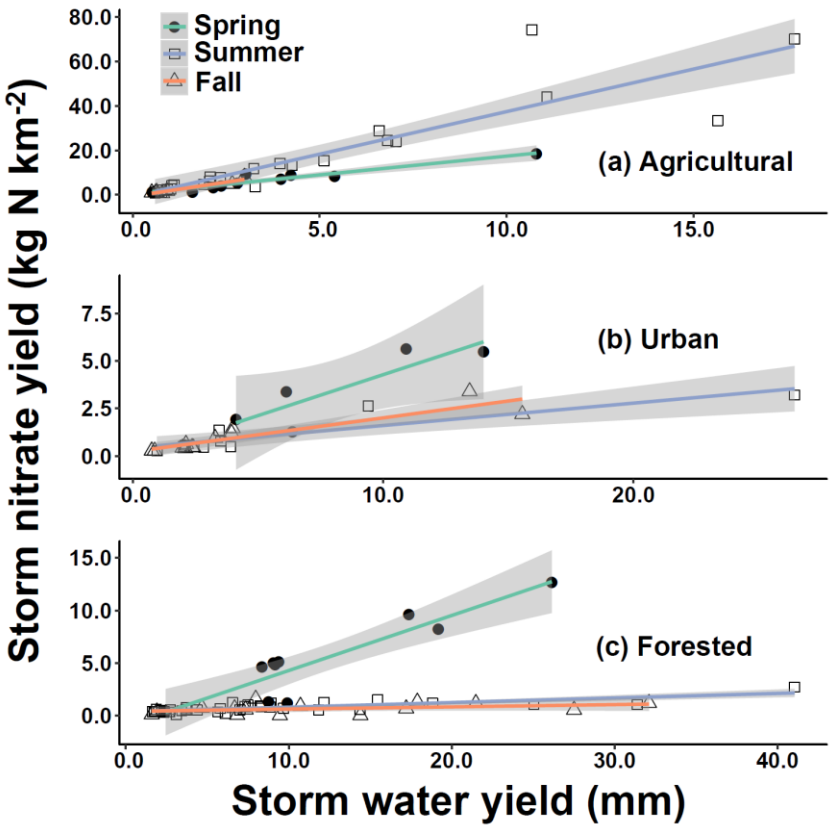

Figure 2.8. Plots of storm nitrate yield vs. water yield grouped by season for the (a) agricultural, (b) urban, and (c) forested streams. Shaded regions indicate 95% confidence intervals.

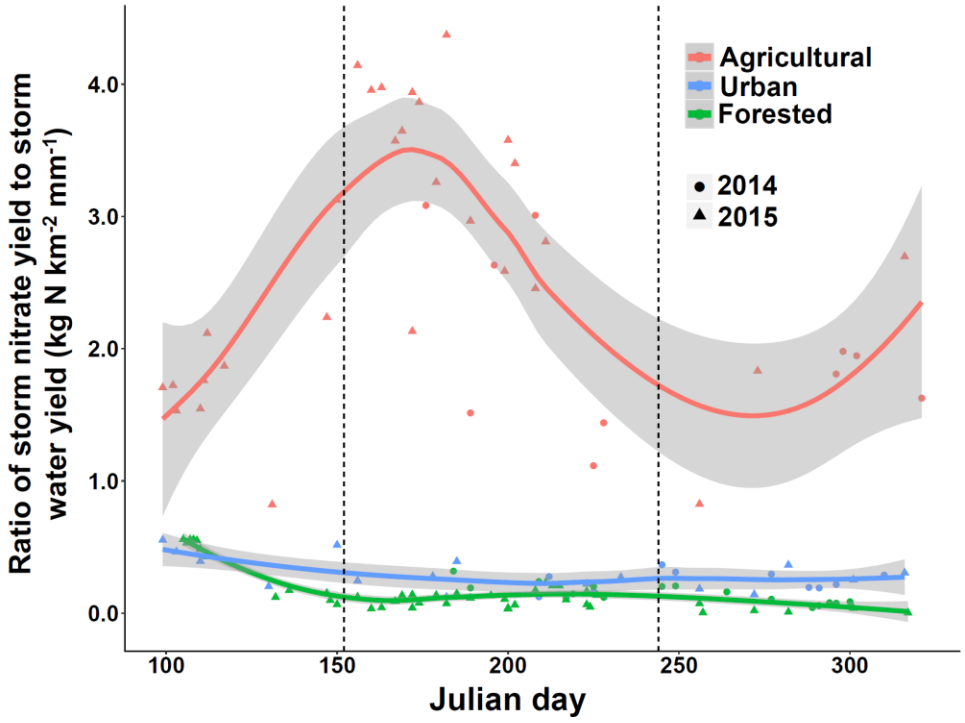

Figure 2.9. Plot of the ratio of storm nitrate yield to storm water yield versus the Julian day that the storm started. Lines were created with high-order polynomial regression. Shaded regions indicate 95% confidence intervals. One outlier was removed from plot for clarity, but remained for analyses (Agricultural, Julian day 152, 6.9 kg N km^{-2} mm^{-1}).

Discussion

Effects of LULC on optical sensor calibrations

This study is the first to apply UV-Vis spectrophotometry to determine DOC and nitrate concentrations in agricultural, urban, and forested catchments in the same region, and lessons learned in utilizing these sensors may be applicable to others who wish to monitor water quality parameters in a variety of settings at a high frequency. The s::can Spectrolyser sensors provided accurate and precise *in-situ* UV-Vis spectra, though we found that local calibrations for DOC and nitrate based on our own lab analyses performed better than the "global calibration" algorithms provided by the vendor (Supporting Figure 2.S2). The partial least squares regression calibration technique was successful in using the

high dimensional UV-Vis spectra to predict DOC and nitrate concentrations in a variety of conditions (Figure 2.4a-d), so we recommend using this approach.

Nitrate concentrations were predicted well in all sites using one common algorithm generated by partial least squares regression, despite differences in optical properties of stream water between sites (Figure 2.4a). This is not surprising since the nitrate molecule consistently absorbs UV light near λ = 220 nm (Johnson and Coletti 2002). In contrast, significant differences in DOC pool composition among sites did necessitate site-specific DOC calibrations. The DOC pool likely represents thousands of molecules absorbing light in the UV-Vis spectrum (Stubbins et al. 2014), and diversity in the composition of this pool can influence the calibration used to predict DOC concentration from UV-Vis absorbance spectra. Agricultural and urban land uses have been shown to influence DOC character (e.g., Wilson and Xenopoulos 2009), and the spectral slope ratio, a proxy that is inversely related to molecular weight, was significantly different among the sites (Figure 5). In addition, studies measuring DOC export character in a variety of land use conditions have found that aromatic and humic content increases significantly during storms (Inamdar et al. 2011; Saraceno et al. 2009; Yoon and Raymond 2012). It is therefore quite likely that both cross-site differences (due to LULC) and intra-site variability (due to shifts in DOC sources during storm events) in DOC composition necessitated individual calibrations at each site. These issues are likely broadly applicable and should be considered by any investigator seeking to study storm event DOC dynamics using this technology.

Calibrations were also affected by the method of sample collection. Automated programmable pump samplers (e.g., ISCO samplers) are popular as a means to collect water samples remotely when researchers are not able to be in the field. However, we found

that including samples from automated samplers resulted in lab results that were less reliable for calibration purposes. This impact was more pronounced for DOC than for nitrate (Supporting Figure 2.S3). We suspect that this effect may be due to unstable storage temperature and the variable amount of time between sample collection and filtration. If these challenges can be addressed with remote filtration and refrigerated storage, then perhaps automatic samplers could be useful in expanding calibration datasets for future studies.

Effects of LULC on storm DOC and nitrate hysteresis

This study applied the recently improved hysteresis index metric outlined by Lloyd et al. (2016) to DOC and nitrate dynamics for a large number of storms, and we calculated hysteresis indices at finer resolution than previously used (2% intervals of storm discharge). Hysteresis patterns for DOC and nitrate were highly variable (Figure 2.6a - b) and did not correlate with seasonal or other measured variables. The three sites exhibited high variability in storm DOC dynamics, though all sites showed generally similar storm DOC anti-clockwise hysteresis and positive flushing behavior (Figure 2.6a, c). The positive flushing index suggests that proximal DOC sources are plentiful enough to increase streamwater concentration on the rising limb, while the anti-clockwise loop pattern suggests that DOC concentrations are higher on the falling limb than the rising limb, and that distal sources of DOC are activated later in the storm as hydrologic pathways connect, and/or that transport time for DOC is greater than that of water in the stream channel. This finding differs from the findings of some small forested catchments (Buffam et al. 2001; Hood et al. 2006; Raymond and Saiers 2010), though it is similar to results of other forested catchments (Brown et al. 1999; McGlynn and McDonnell 2003; Moore and Jackson 1989;

Pellerin et al. 2012), and at least one study in an agricultural catchment (Morel et al. 2009). The dynamics we observed fit well with the conceptual model described by McGlynn and McDonnell (2003). They found that source waters shifted from riparian to hillslope waters during storm events, and that the rising concentrations from hillslope waters occurred as soil became sufficiently saturated to connect upslope sources to the stream. While our different sites have distinct upland sources of DOC, it appears that they all share a similar dynamic, in that these sources are likely distal and hydrologically connected to the stream later in the storm cycle. This is remarkable, considering the differing sources of DOC and hydrologic pathways among the three watersheds. Urban systems, for example, are heavily affected by sewers, ditches, gutters, and runoff from impervious surfaces (Kaushal and Belt 2012). Watershed DOC sources range from manure and residual crop matter in agricultural fields, to wetlands and upland organic soils in the forested catchment, to sewer bacterial communities and grass clippings in the urban stream, yet the relative timing of connectivity and possibly the mechanism for delivery is not significantly different among the three sites.

The agricultural watershed displayed high variability in storm nitrate hysteresis (Figure 2.6b), though tended toward an anti-clockwise pattern. This pattern coupled with a positive flushing index for many storms (Figure 2.6d) suggests the transport of plentiful proximal sources early in storm cycles, followed by enrichment from distal and plentiful sources of nitrate. Others have attributed this pattern to the rise of the water table to the upper horizons that store accumulated nitrate from fertilizer application (Oeurng et al. 2010). While differences in watershed characteristics may be a contributing factor in differing storm nitrate dynamics, soil nitrate enrichment from fertilizer application may be a primary driver. While results on nitrate hysteresis in agricultural areas reported by others

vary, our results generally agree with many that also report anti-clockwise nitrate hysteresis patterns (Oeurng et al. 2010; Outram et al. 2014; Van Herpe and Troch 2000). In contrast, Bowes et al. (2015) observed clockwise nitrate hysteresis for 21 out of 36 storms in an agricultural watershed in southern England. While this does not reflect the trend toward anti-clockwise hysteresis behavior we observed, both this study and ours observed a high amount of variance in agricultural nitrate hysteresis behavior. Interestingly, Darwiche-Criado et al. (2015) also observed a wide variety of storm nitrate hysteresis patterns in an agricultural area in the Flumen River, Spain. Though agricultural practices in that region differ greatly from those of our study area, they identified possible linkages between fertilization and irrigation practices with hysteresis patterns.

The median nitrate hysteresis index at the forested site was positive (clockwise) and the flushing index was generally negative, which suggests a proximal nitrate supply that is quickly depleted from riparian soils (Creed and Band 1998). Others' observations vary on the direction of nitrate hysteresis found in forested streams. Studies find clockwise behavior (Zhang et al. 2007), anti-clockwise behavior (Buffam et al. 2001; Rusjan et al. 2008), and at times no consistent pattern (Andrea et al. 2006). Storms at our urban site also had a positive median nitrate hysteresis index and generally negative flushing index. To our knowledge, only one other study has investigated storm nitrate hysteresis in urban streams, in which case the stream exhibited clockwise nitrate hysteresis for 14 out of the 17 storms observed (Carey et al. 2014), which is in agreement with the nitrate hysteresis pattern at our urban site. Any nitrate sources that have accumulated on impervious surfaces will quickly transport to the urban stream network due to artificially increased drainage density, in addition to nitrogen pools accumulated in riparian soils, as in the forested

system. In both the urban and forested systems, the combination of general clockwise hysteresis and negative flushing index patterns suggest that distal nitrate sources are not plentiful enough, and/or do not hydrologically connect to the stream network sufficiently to increase streamwater concentrations at the point of measurement.

The breadth of our dataset shows what is possible with continuous high-frequency water quality data and new methods to quantify storm hysteresis. However, the remarkable variability that we observed in instrastorm hysteresis dynamics within and across sites highlights the need for continuously monitoring many storms, since sampling error is likely when inferring hysteresis patterns and suggested biogeochemical processes if only a few storms are observed. This level of detail in hysteresis calculations and the emergence of optical sensor technology will allow for better hysteresis measurement and comparisons in the future, but the dramatic variability and unpredictable hysteresis trajectories when comparing 126 storms across LULC clearly illustrates that there is much work needed to understand what controls the behavior of solutes within specific storm events over time and space.

Effects of LULC on storm DOC yield

The high proportion of the variance in storm DOC yield explained by water yield at our sites suggests that DOC flux is driven by storm water yield for each LULC, and is not influenced by the exhaustibility of these source areas (Figure 2.7a). The wetting of soil columns during storms connects DOC source areas to streams, and this process of DOC delivery appeared to be similar among sites. However, we found statistically significant differences in storm DOC yield versus water yield relationships, indicating that LULC drives the relationship between storm DOC yield and water yield across these sites by

essentially setting a concentration range for stormwater. This storm water concentration range is likely determined by the relative abundance, nature and connectivity of DOC sources within each catchment, which is impacted heavily by LULC. Other factors such as seasonality and the antecedent conditions we observed did not have a substantial impact on storm DOC yield. While storm water yield is known to be subject to shifts in seasonal patterns, the DOC that we expect to be exported at each site with a given water yield does not vary significantly in our study areas.

It has been established that human activities in agricultural areas alter the source of fluvial DOC and lead to greater autochthonous DOC production (Stanley et al. 2012; Wilson and Xenopoulos 2008), and the differences we observed in storm DOC yield between land uses are similar to what others have recently found (Caverly et al. 2013; e.g. Yoon and Raymond 2012). Urban and suburban development has also been shown to alter sources of DOC (e.g., Sickman et al. 2007). Our results also suggest that urban and suburban development increase the storm export of DOC over undeveloped forest land cover, which is similar to the findings of Kaushal and Belt (2012) in the city of Baltimore, Maryland. This increase has been attributed to increased hydrologic connectivity and greater drainage density following installations of underground pipe networks, gutters, and ditches (Elmore and Kaushal 2008), and additional DOC sources not found in forested catchments, such as sewage, lawn clippings, and more prevalent algal communities (Kaushal and Belt 2012).

Effects of LULC and seasonality on storm nitrate yield

The relationships between storm nitrate yield and water yield suggest that LULC has a dramatic impact on storm nitrate yield in the study areas. Our results comparing

agricultural to urban and forested LULC is consistent with others', as nitrate concentrations are often elevated in agricultural areas due to nitrogen amendment (Carpenter et al. 1998). The regression slopes between storm nitrate yield and water yield were significantly different between the agricultural site and the other sites, suggesting that the effect of agricultural LULC on nitrate loads is enhanced by larger storms (Figure 2.7b). In addition to increasing nitrate loads through direct fertilizer application, agricultural practices also alter the hydrology of watersheds by influencing evapotranspiration, and by developing tile drainage, which bypasses potential nitrogen retention hotspots (Royer et al. 2006). Agricultural tile drainage could potentially be a key driver for the higher nitrate yield in this system, as it forms direct pathways to transport leached nitrate to streams (Dinnes et al. 2002; Hatfield et al. 1998). Tile drainage is currently unregulated in the study area and the precise extent is unknown, though extent estimates for the agricultural site range from 60 – 76% (Winchell et al. 2011).

Urbanization is known to cause an increase in nitrate loading due to the production of new nitrate sources, and the alteration of hydrologic pathways due to impervious surfaces that bypass nitrogen retention hotspots, such as wetlands and riparian zones (Groffman et al. 2002; Kaushal et al. 2008; Rosenzweig et al. 2008). While the median ratios of storm nitrate yield to water yield were shown to be significantly different among sites, the slope of the correlation between the storm nitrate yield and water yield was not significantly different between the urban and forested sites (Figure 2.7b). Increased DOC concentrations in urban streams have also been shown to increase biological uptake and denitrification of nitrogen (Kaushal and Belt 2012; Sivirichi et al. 2011), so although we

might expect increased inputs of inorganic nitrogen to the urban stream, the altered DOC dynamics may create a compensatory mechanism to curb this impact.

Interestingly, the seasonal effects on the relationship of storm nitrate yield vs. water yield caused opposing trends between the agricultural and the other two sites. Regression slopes at the agricultural stream ranked from highest to lowest in the summer, fall, and spring, respectively. At the urban and forested sites, the descending order of regression slopes was spring, fall, and summer (Figure 2.8). The seasonal fluctuations in the ratio of storm nitrate yield to water yield we observed at the agricultural site (Figure 2.9) may be a signature of agricultural land use practices interacting with seasonal dynamics. A winter ban on manure application is lifted annually on April 1, leading to widespread application during the spring. During this time, the ratio of storm nitrate yield to water yield increased throughout the spring season and peaked just after the beginning of the summer season. This pattern may be affected by biological uptake from field crops, which likely begins to increase substantially at this time. Through the summer growing season, this ratio decreased; we suggest that this may be due to a decrease in fertilizer application to fields, while concurrent biological uptake continues. In addition, the groundwater flux is likely lower during this time, causing the thickness of the unsaturated zone to increase, and the temperature is seasonally higher – all leading to higher rates of biogeochemical cycling and longer retention times. The ratio eventually reached a second minimum following the beginning of the fall season. When harvest occurred and biological uptake slowed, the greater leaching potential may have caused the ratio to increase again into late fall. Fall storms are also likely to be influenced by increased hydrological connectivity due to wetter soils following lower crop transpiration, and by the common practice of late season manure

application prior to the winter ban that begins on December 15. Manure is often applied in the fall due to the availability of labor, favorable weather, and lower fertilizer prices (Dinnes et al. 2002), although the majority of the nitrogen applied at this time is lost through pathways other than crop production before the subsequent growing season (Sanchez and Blackmer 1988).

The ratio of storm nitrate yield to water yield was generally lower at the forested stream, and the seasonal pattern differed from the other sites. The ratio was highest during the few spring snowmelt events we observed, which may be when a pulse of atmospherically deposited nitrate is released from the melting snow pack, as inferred by Pellerin et al. (2012) at the Sleepers River in Vermont. Decreases in this ratio throughout the spring may be due to increasing vegetative nitrogen uptake across the catchment with green-up, leaving less nitrate available to be transported during storm events. This downward trajectory continues into the fall season, and the very low values of this ratio in the fall may be due to low nitrate concentrations during the litterfall period. Studies have observed lower baseflow nitrate concentrations during this time of year, which has been attributed to increased heterotrophic uptake and denitrification of in-stream nitrate following the leaching of labile DOC from leaves in streams (Goodale et al. 2009; Sebestyen et al. 2014; Sobczak et al. 2003; Webster et al. 2009). Patterns in storm nitrate yield versus storm water yield in our studied forested catchment underscore the importance of atmospherically deposited nitrogen stored in forest snowpack and frozen soils released during spring storms, and the biological uptake of mineral nitrogen in the summer and fall which may lower the nitrate yield of storms.

Challenges and recommendations for high-frequency storm monitoring

This study combines emerging optical sensor technology with recently developed methods for characterizing storms, and sheds light on the large amount of variation and complexity possible in DOC and nitrate storm dynamics. Many studies previously documenting DOC and nitrate hysteresis were conducted using grab samples, and often only considered a few storms. Therefore, comparing our results to those with smaller sample sizes may be problematic due to the potential for sampling error, and limited storm coverage and scope.

There are differences in watershed characteristics between our study areas that may confound LULC comparisons. Agricultural and urban areas have developed on flat valleys in the Northeast US, while steep mountain catchments remain forested, largely due to the difficulty to develop them and greater distance from population centers. Differences in topography, surficial soils, and hydrologic pathways are likely to impact our results, though the magnitude of the difference between agricultural and other LULCs presented here is compelling evidence that a significant portion can be attributed to LULC. As *in-situ* water quality sensors become more affordable and accessible, future studies that investigate the influence of LULC would benefit from deploying sensors across a wider variety of agricultural, urban, and forested systems.

Collecting continuous, high-frequency data was critical to the success of this study, though we encountered several challenges in maintaining sensors due to biological fouling, flood damage, vandalism, and wildlife tampering. Significant effort was required for regular site visits to ensure data quality, and for troubleshooting when hardware or software failed. Also, calibration results show that regular and storm grab samples were needed to

validate *in-situ* measurements, so sensors are not able to completely replace manual grab samples at this point. We make the following recommendations as lessons learned for future studies employing *in-situ* sensors:

1. We recommend using manual grab samples in place of automatically pumped samples that are stored unfiltered and unrefrigerated. We found that samples from our automatic samplers made the comparison to UV-Vis absorbance spectra unreliable for DOC calibrations (Supporting Figure 2.S3).
2. We recommend reinforcing submerged wires to protect from aquatic wildlife and flood damage.
3. Maintaining the cleanliness of the optical measurement windows and wiper mechanism is critical for obtaining reliable UV-Vis absorbance spectra. For the s::can Spectrolyser, we found that cleaning with pure ethanol and deionized water worked well to clear biological fouling in most situations. A thorough cleaning every two weeks was usually sufficient, though more frequent cleaning was necessary when stream conditions fostered high rates of biological production.
4. We recommend a system design that transmits data remotely. This was extremely useful in order to monitor data in real-time, react promptly to problems, store data offsite, and even troubleshoot remotely. In our sensor installations, Campbell Scientific CR1000 dataloggers with modems and antennas allowed us to access measured data through cellular networks via a laptop or handheld device.
5. We relied on solar power, which generally worked very well. Power supply was an issue at times, especially when daylight hours decline in the late fall season. If relying on solar power, we recommend careful selection of solar panel array and

battery storage, and thoughtful installation with full exposure to the sun. A gridded power system could be ideal, though this would still necessitate a battery backup since storms are often when power grids fail.

6. While the s::can Spectrolyser is field-rugged, we recommend constructing a secondary housing unit for stream installation. We used large PVC piping and steel carriage bolts, which protected the sensors from damage during several large flood events, but also allowed water and sediment to pass through unobstructed. This housing was also secured to land-based anchors via a steel cable to prevent loss of equipment during the largest events. This safety line proved useful on several occasions.

Conclusions

High-frequency measurements allowed for a new hysteresis calculation method to be applied to 126 storms and provided highly accurate and precise solute yield estimates. We observed remarkable variability in DOC storm dynamics and general trends in storm DOC hysteresis were similar in general among the three sites despite distinct DOC sources and hydrologic pathways. In addition, we found that the amount and timing of nitrate delivery to streams during storms differed significantly among the LULCs. We attribute this to land use practices generating more distal and plentiful nitrate source areas in the agricultural system, while nitrate depletion from more proximal riparian sources is more common in the urban and forested systems. We observed several differences among our sites of varied LULCs for storm DOC and nitrate loading. Both storm DOC and nitrate yields were elevated in the agricultural stream, and seasonal patterns reflected the complex interaction of land use practices, biogeochemical cycling, and climatic drivers. We also

found that larger storm size magnifies differences between all LULCs for storm DOC yield and for storm nitrate yield in the agricultural site compared to the others.

While future work should include monitoring more storms during years with varied hydrologic inputs, more study areas are needed to put these findings into a cohesive context. As *in-situ* optical sensor technology becomes more widely used, we can expect the cost of obtaining and maintaining these instruments to drop significantly. By incorporating sites with varied degrees of each end-member LULC type, we could better isolate land use effects from other watershed characteristics. Also, coupling *in-situ* sensors with terrestrial sensor networks may help to better characterize the spatial distribution and temporal dynamics of source areas for DOC and nitrate, and aid in interpretation of integrated watershed signals.

Acknowledgements

This material is based upon work supported by the National Science Foundation under VTEPSCoR Grant No. EPS-1101317, EPS-IIA1330446, and OIA 1556770. Any opinions, findings, and conclusions or recommendations expressed in this material are those of the author(s) and do not necessarily reflect the views of the National Science Foundation or Vermont EPSCoR. We appreciate thoughtful reviews from Ishi Buffam and two anonymous reviewers that greatly improved this work. We thank Joshua Benes, Samuel Parker, Allison Jerram, Brian Pellerin, Richard Rowland, Catherine Winters, Kristen Underwood, Scott Hamshaw, and Donna Rizzo for their helpful contributions to this work. Any use of trade, firm, or product names is for descriptive purposes only and does not imply endorsement by the U.S. Government. The data used in this publication are freely available on HydroShare (https://goo.gl/R5u3HR).

Supporting information

Supporting Text S1

To explain remaining variance in storm nitrate yield, additional measured parameters were combined with water yield in multiple linear regression models (Supporting Table 2.S1). Julian day for the start of each storm was transformed by the equations:

$$D_{sin} = \sin\frac{2\pi J}{365.25} \quad (7)$$

$$D_{cos} = \cos\frac{2\pi J}{365.25}, \quad (8)$$

where J is the Julian date. If either D_{sin} or D_{cos} was significant, both were included together in models to account for seasonal phases (Aulenbach et al. 2016). For all models, standard assumptions for multiple linear regressions were checked, including autocorrelation of independent variables, and normality and homoscedasticity of residuals. Variables containing information on solute concentrations during a given storm were excluded from models that predicted storm export of that solute.

Supporting Text S2

Multiple linear regression models revealed that neither DOC nor nitrate storm hysteresis indices were significant in predicting nitrate loading for any of the sites. The models also showed that 79% of the variance in storm nitrate yield at the urban site could be explained by combining the seasonality variables and the time duration from storm start to discharge peak with water yield for that storm (Supporting Table 2.S2). The time

duration from storm start to discharge peak variable had a positive coefficient in the model, indicating that storms with similar water yield may export a higher nitrate yield if the storm takes a longer period of time to reach peak discharge.

Multiple linear regression revealed that 81% of the variance in storm nitrate yield could be explained at the forested site by combining the seasonal variables, the initial nitrate concentration at the start of storm, and the peak nitrate concentration of the previous storm. Each of these predictors had positive coefficients in the model. No additional variables increased the amount of variance in storm nitrate yield for the agricultural site that did not violate auto-correlation assumptions.

Supporting Text S3

Multiple linear regression models were successful in improving prediction of storm nitrate yield for the urban and forested sites, though different factors were important for each. At the urban site, the time duration from the storm start to Q peak improved the model when combined with the D_{sin} seasonality variable (Eq. 7) and storm water yield (Supporting Table 2.S2). On a storm to storm basis, the time duration of the rising limb is a function of rainfall intensity, antecedent moisture conditions, and the evapotranspiration potential of the watershed, so it is possible that the correlation with the timing is indicative of a proxy variable for factors that were not directly measured. In addition, this could be caused by a process in which storms with a slower onset may cause greater watershed connectivity, so that it is not just the first flush of impervious surfaces that is contributing to the storm nitrate yield.

At the forested site, the seasonal variables, the initial nitrate concentration, and the peak nitrate concentration from the previous storm all combined with water yield to predict

storm nitrate yield quite well (Adjusted R^2 = 0.81, Supporting Table 2.S2). The improvement over the model with water yield alone (R^2 = 0.14) was dramatic. While the initial nitrate concentration does vary seasonally, this variable did not correlate with seasonal variables included in the model. In addition, since the nitrate peak concentration from the previous storm was significant in the model, we conjecture that this may be a proxy for watershed wetness, where hydrologic pathways to significant nitrate sources are activated. It is remarkable that storm hysteresis indices did not significantly improve prediction of storm nitrate yield at any of the sites.

Supporting Table 2.S1. Variables tested in multiple linear regression models to predict storm nitrate yield

Variable	Units
Storm water yield	mm
Storm DOC hysteresis index	-
Storm nitrate hysteresis index	-
Julian day of storm start	-
D_{sin} (Eq. 7)	-
D_{cos} (Eq. 8)	-
Storm initial DOC conc.	mg L^{-1}
Storm initial stream stage	m
Storm initial stream discharge	m^3 s^{-1}
Storm initial nitrate conc.	mg L^{-1}
Storm minimum DOC conc.	mg L^{-1}
Storm minimum nitrate conc.	mg L^{-1}
Storm maximum DOC conc.	mg L^{-1}
Storm maximum nitrate conc.	mg L^{-1}
Storm initial water temperature	ºC
Time duration from storm start to Q peak	hr
Time duration from Q peak to storm end	hr
Time duration from Q peak to DOC conc. peak	hr
Time duration from Q peak to nitrate conc. peak	hr
Time duration of storm	days
Ratio of water yield to time duration of storm	mm $days^{-1}$
Storm range of DOC conc.	mg L^{-1}
Storm range of nitrate conc.	mg L^{-1}
Time duration since previous storm started	days
Time duration since previous storm ended	days
Water yield of previous storm	mm
Maximum nitrate conc. of previous storm	mg L^{-1}
Maximum DOC conc. of previous storm	mg L^{-1}

Supporting Table 2.S2. Summary of results for the multiple linear regression models to predict storm nitrate yield (kg N km^{-2})

Urban site: Adjusted R^2 = 0.79; Std. Error = 0.78; p < 0.0001			
Variable	Coefficient	Std. Error	*p*
Storm water yield (mm)	0.14	0.03	< **0.0001**
D_{sin}	0.70	0.30	**0.028**
D_{cos}	0.41	0.33	0.22
Time duration from storm start to Q peak	0.04	0.02	**0.018**
Intercept	0.61	0.37	0.12

Forested site: Adjusted R^2 = 0.81; Std. Error = 1.1; p < 0.0001			
Variable	Coefficient	Std. Error	*p*
Storm water yield (mm)	0.094	0.020	< **0.0001**
D_{sin}	0.75	0.33	**0.030**
D_{cos}	0.94	0.37	**0.015**
Storm initial nitrate concentration (mg L^{-1})	7.5	1.6	**0.018**
Maximum nitrate conc. of previous storm (mg L^{-1})	3.7	1.5	**0.017**
Intercept	-1.1	0.61	0.074

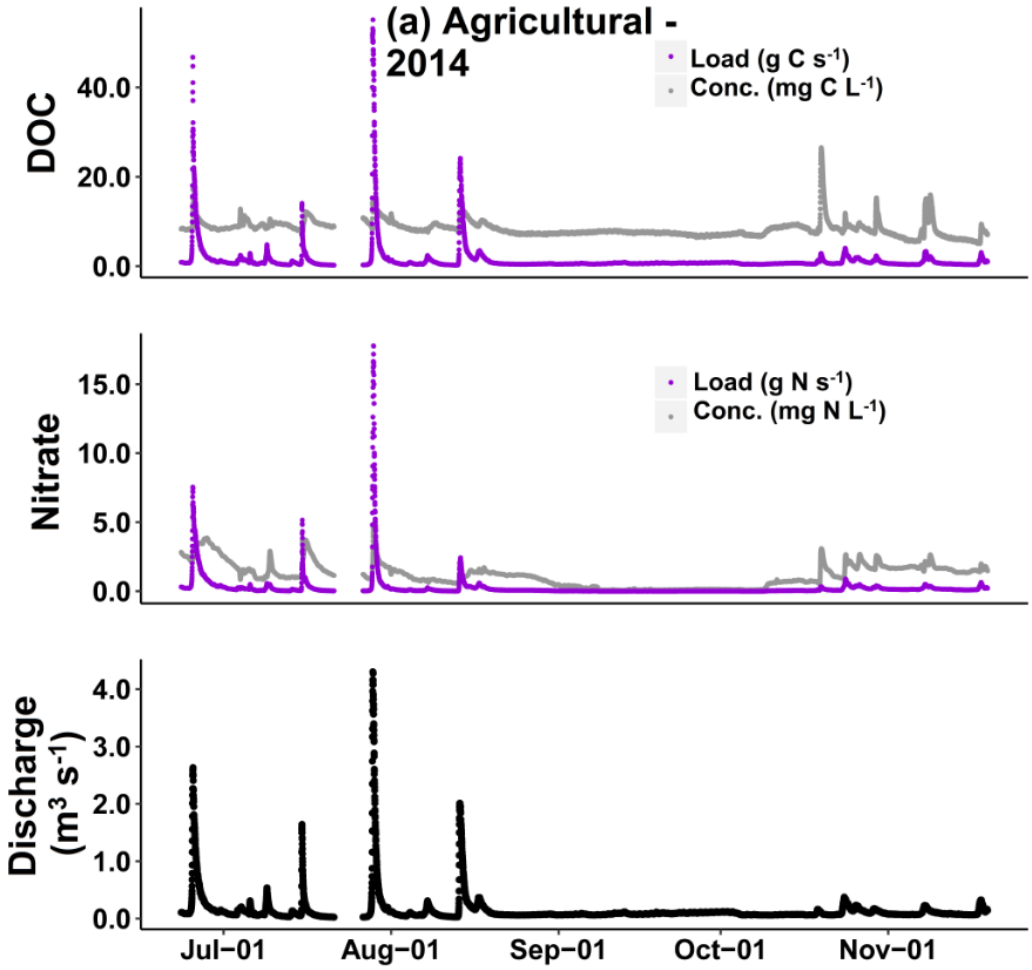
(a) Agricultural - 2014
DOC
Load (g C s-1)
Conc. (mg C L-1)
40.0
20.0
0.0
Nitrate
Load (g N s-1)
Conc. (mg N L-1)
15.0
10.0
5.0
0.0
Discharge (m3 s-1)
4.0
3.0
2.0
1.0
0.0
Jul−01
Aug−01
Sep−01
Oct−01
Nov−01

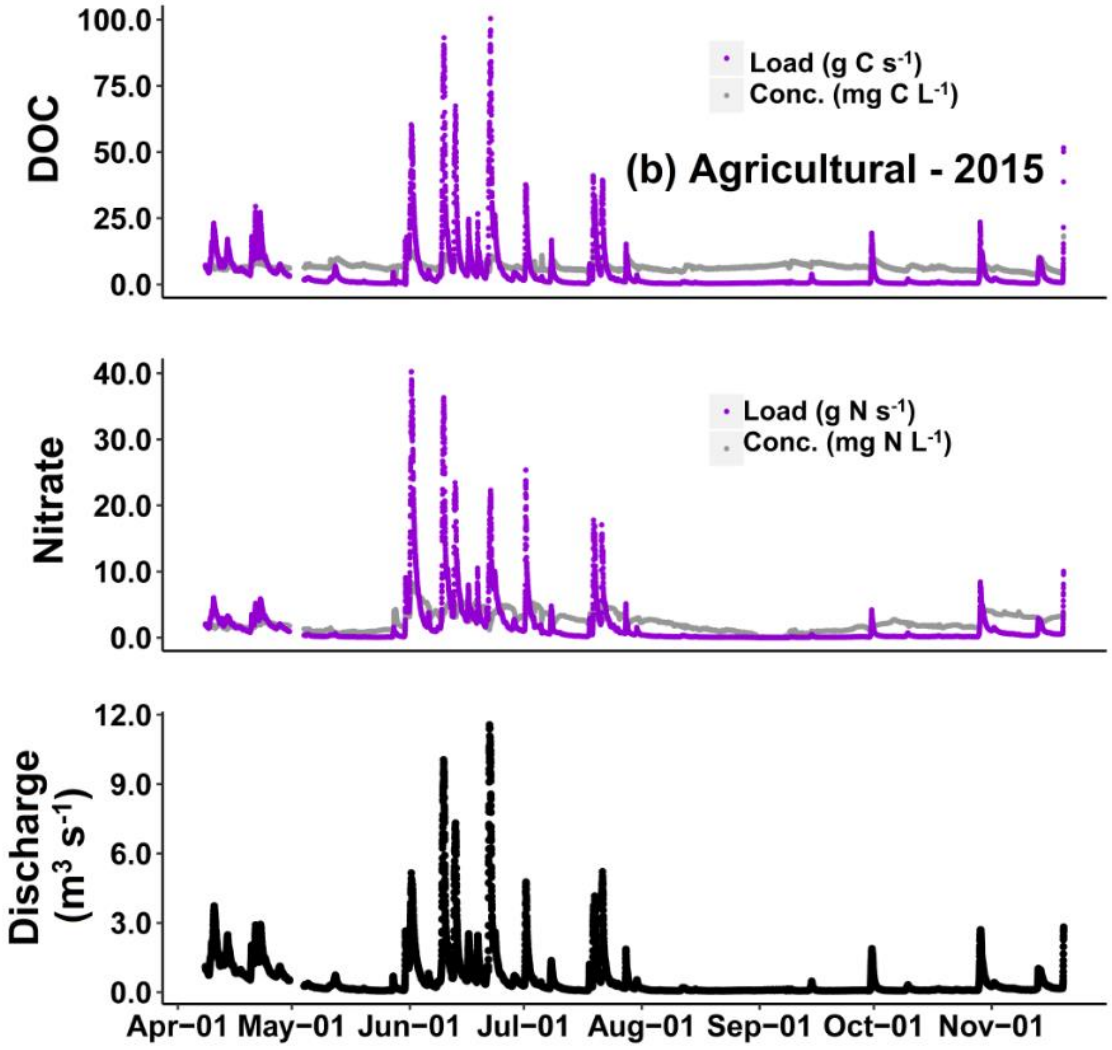
DOC
100.0
75.0
50.0
25.0
0.0
Load (g C s-1)
Conc. (mg C L-1)
(b) Agricultural - 2015
Nitrate
40.0
30.0
20.0
10.0
0.0
Load (g N s-1)
Conc. (mg N L-1)
Discharge (m3 s-1)
12.0
9.0
6.0
3.0
0.0
Apr−01 May−01 Jun−01 Jul−01 Aug−01 Sep−01 Oct−01 Nov−01

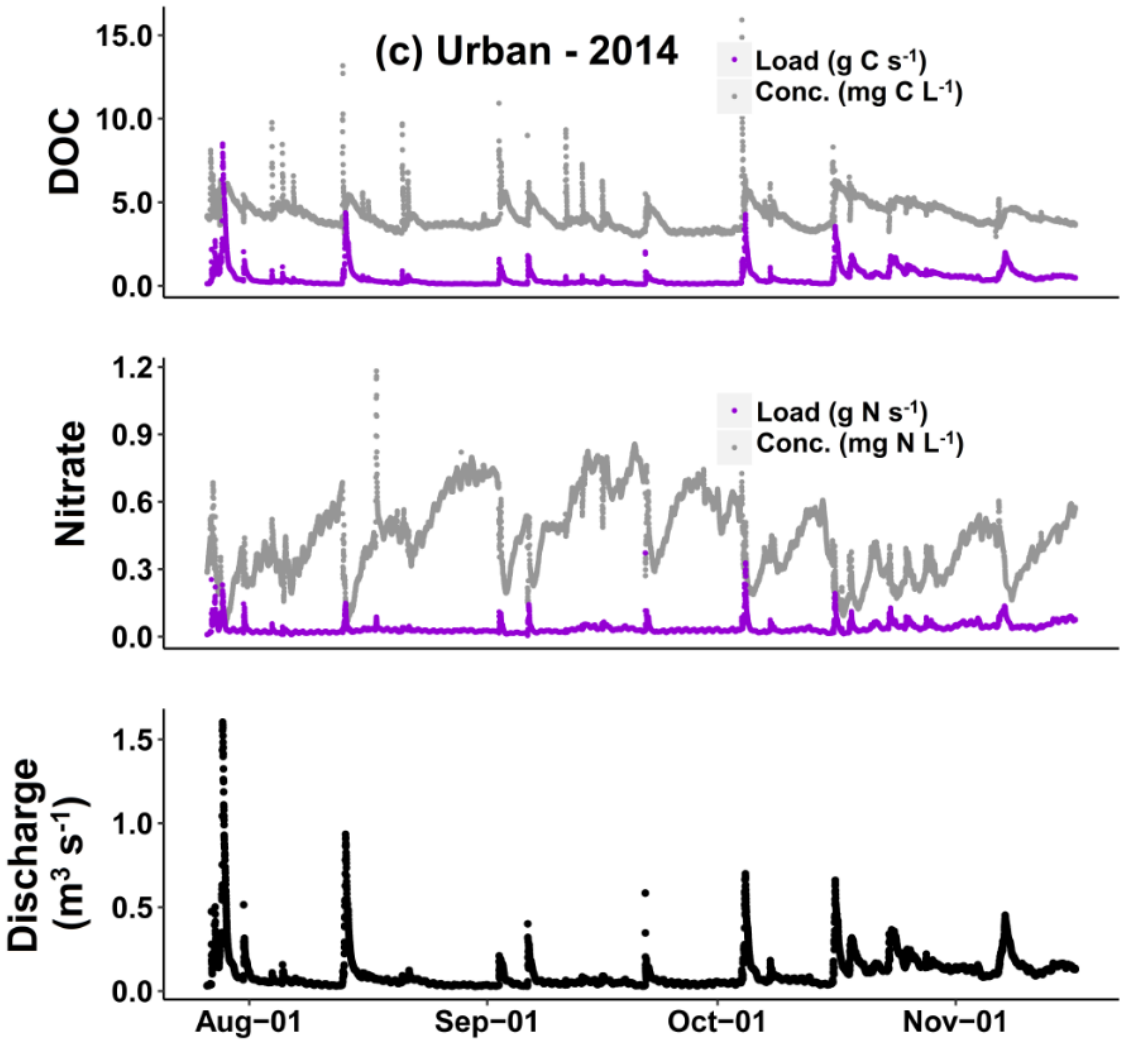
(c) Urban - 2014
Load (g C s-1)
Conc. (mg C L-1)
DOC
15.0
10.0
5.0
0.0
Load (g N s-1)
Conc. (mg N L-1)
Nitrate
1.2
0.9
0.6
0.3
0.0
Discharge (m3 s-1)
1.5
1.0
0.5
0.0
Aug−01
Sep−01
Oct−01
Nov−01

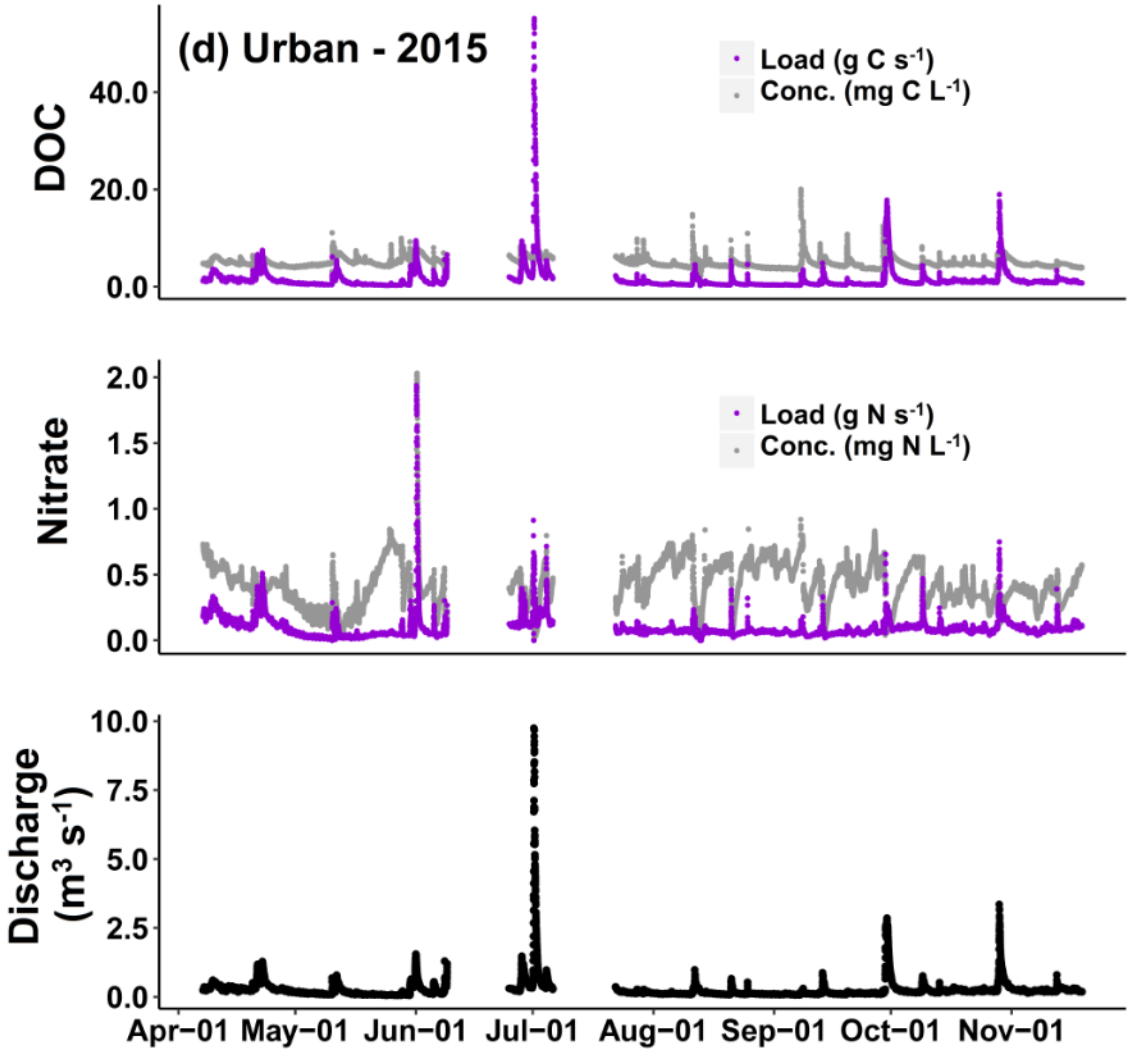
(d) Urban - 2015
DOC
40.0
20.0
0.0
Load (g C s-1)
Conc. (mg C L-1)
Nitrate
2.0
1.5
1.0
0.5
0.0
Load (g N s-1)
Conc. (mg N L-1)
Discharge (m3 s-1)
10.0
7.5
5.0
2.5
0.0
Apr−01
May−01
Jun−01
Jul−01
Aug−01
Sep−01
Oct−01
Nov−01

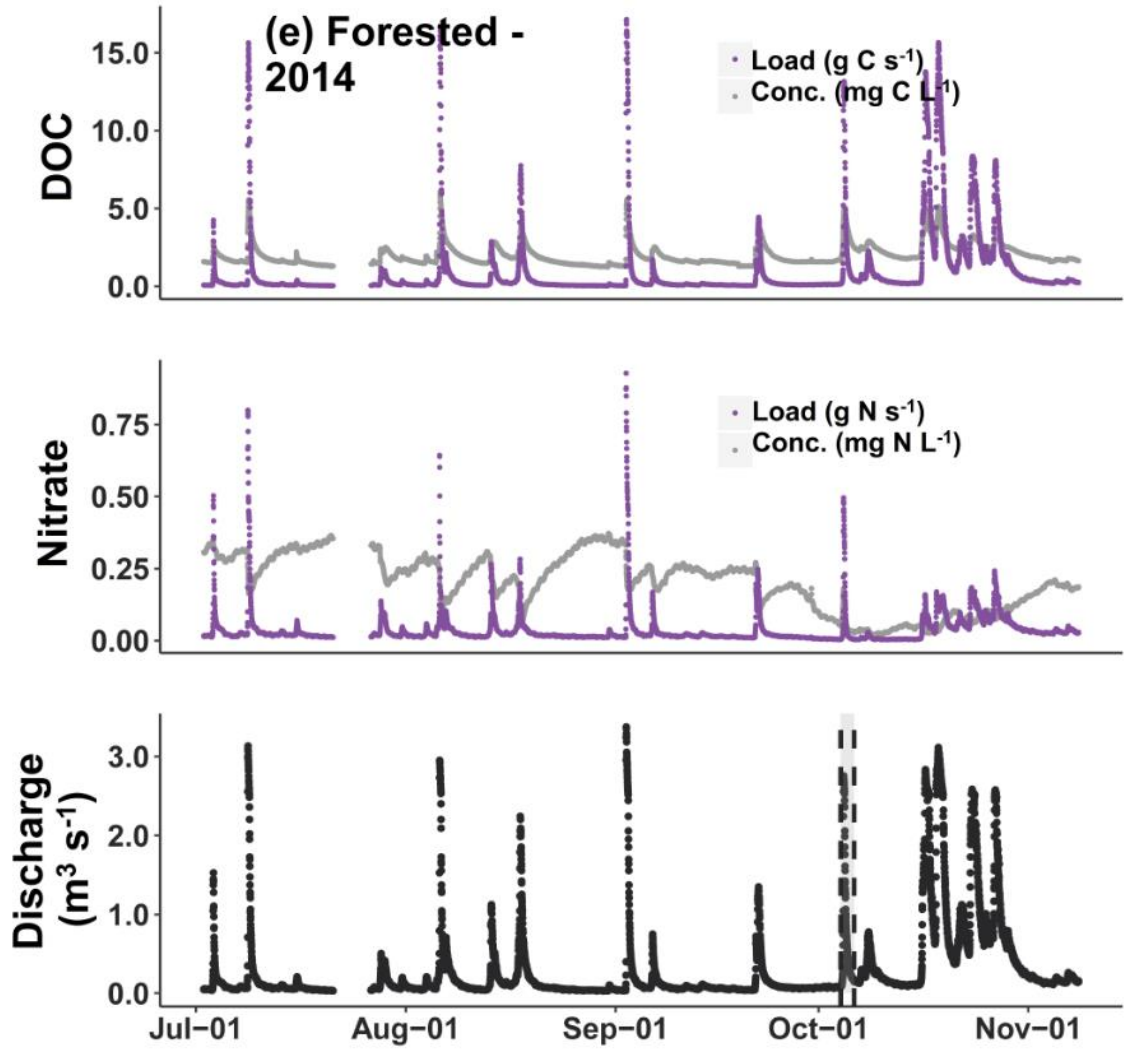
(e) Forested - 2014
DOC
15.0
10.0
5.0
0.0
Load (g C s-1)
Conc. (mg C L-1)
Nitrate
0.75
0.50
0.25
0.00
Load (g N s-1)
Conc. (mg N L-1)
Discharge (m3 s-1)
3.0
2.0
1.0
0.0
Jul−01
Aug−01
Sep−01
Oct−01
Nov−01

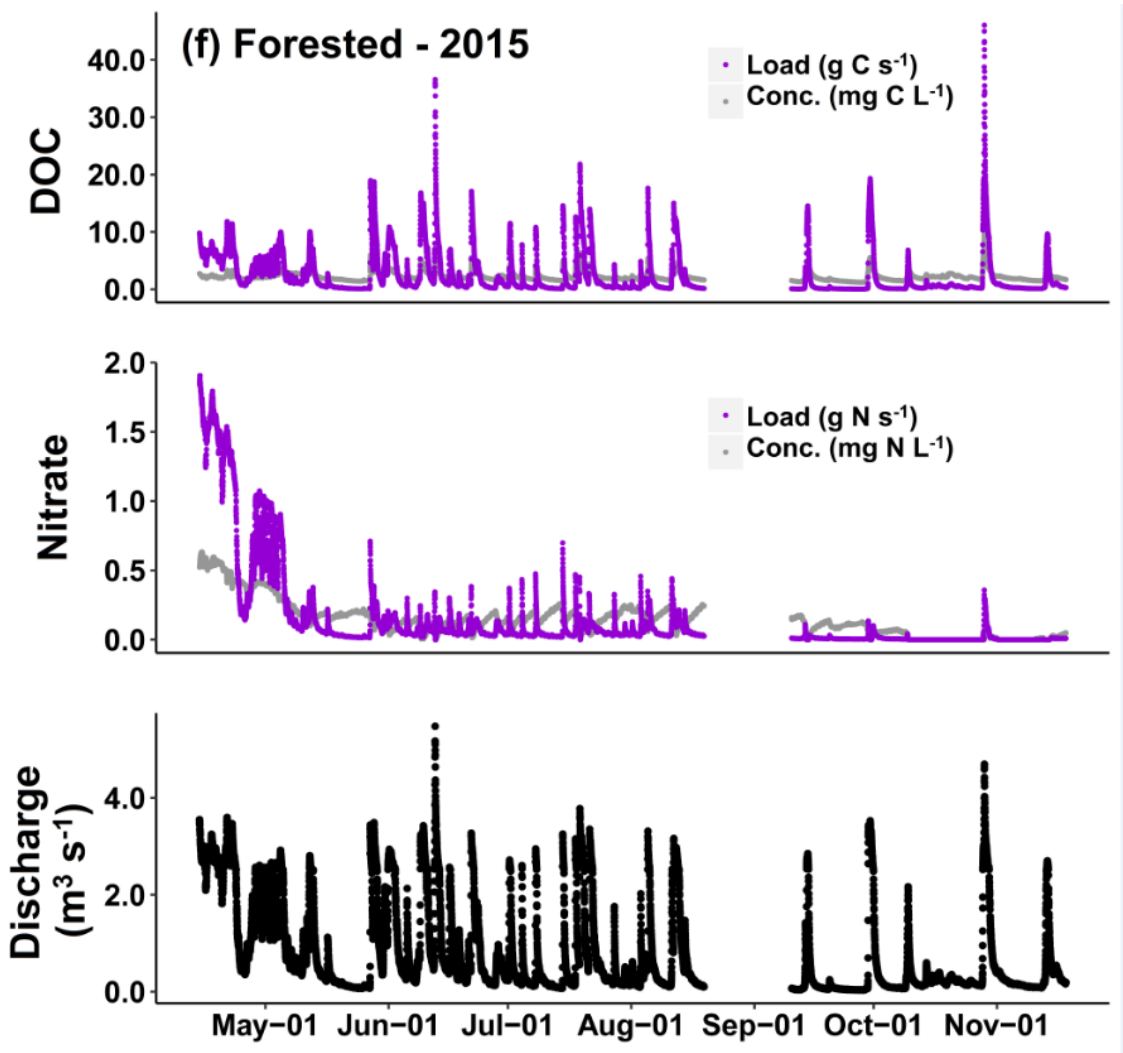

Supporting Figure 2.S1. Time-series plots of DOC and nitrate load and concentration, and discharge for the (a-b) agricultural, (c-d) urban, and (e-f) forested sites throughout the 2014 and 2015 field seasons. The shaded region in plot (e) is the storm featured in Figure 2.2.

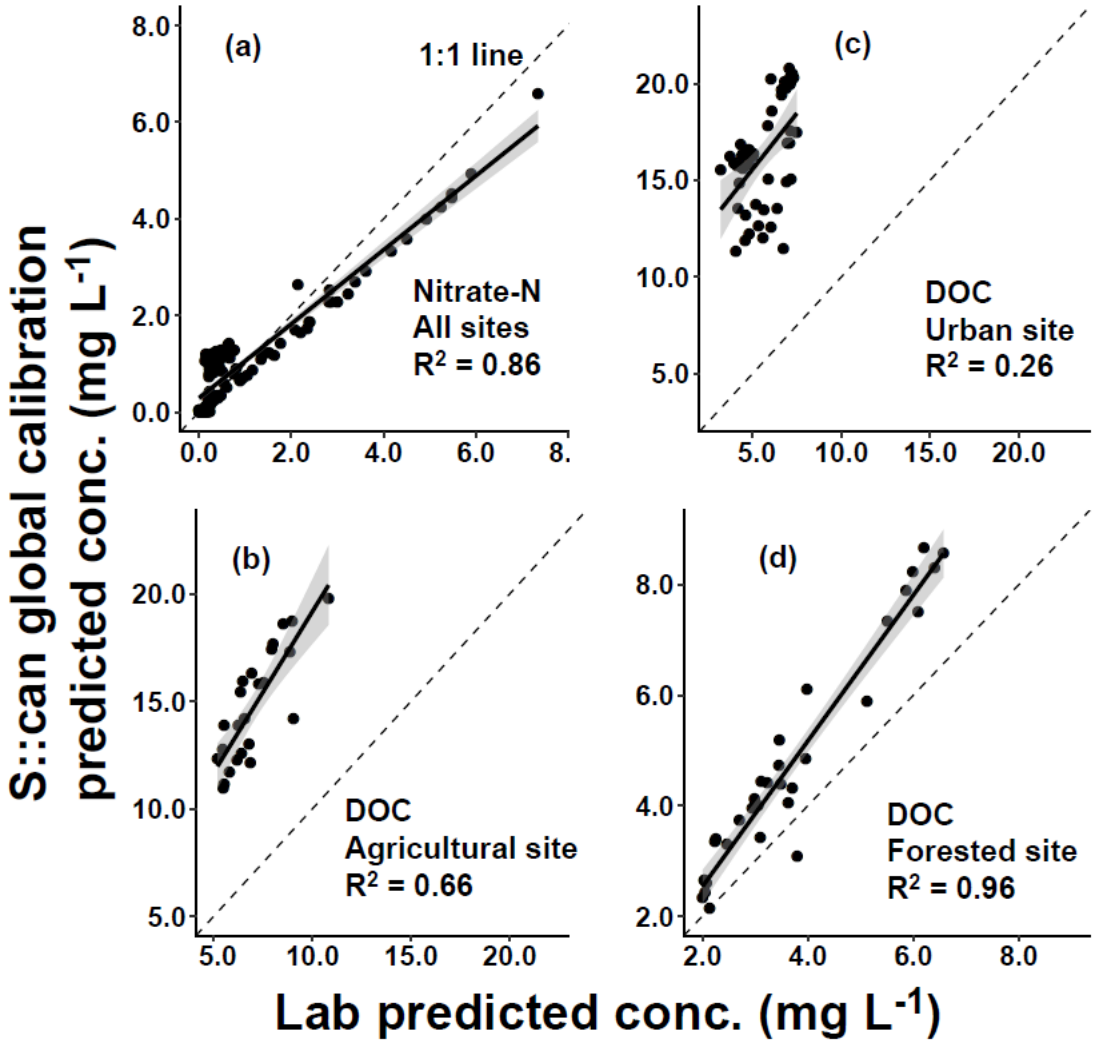

Supporting Figure 2.S2. Plots of s::can sensor proprietary global calibration predicted (a) nitrate and (b-d) DOC concentrations vs. lab measured values. Shaded regions indicate 95% confidence intervals and the dashed line is 1:1.

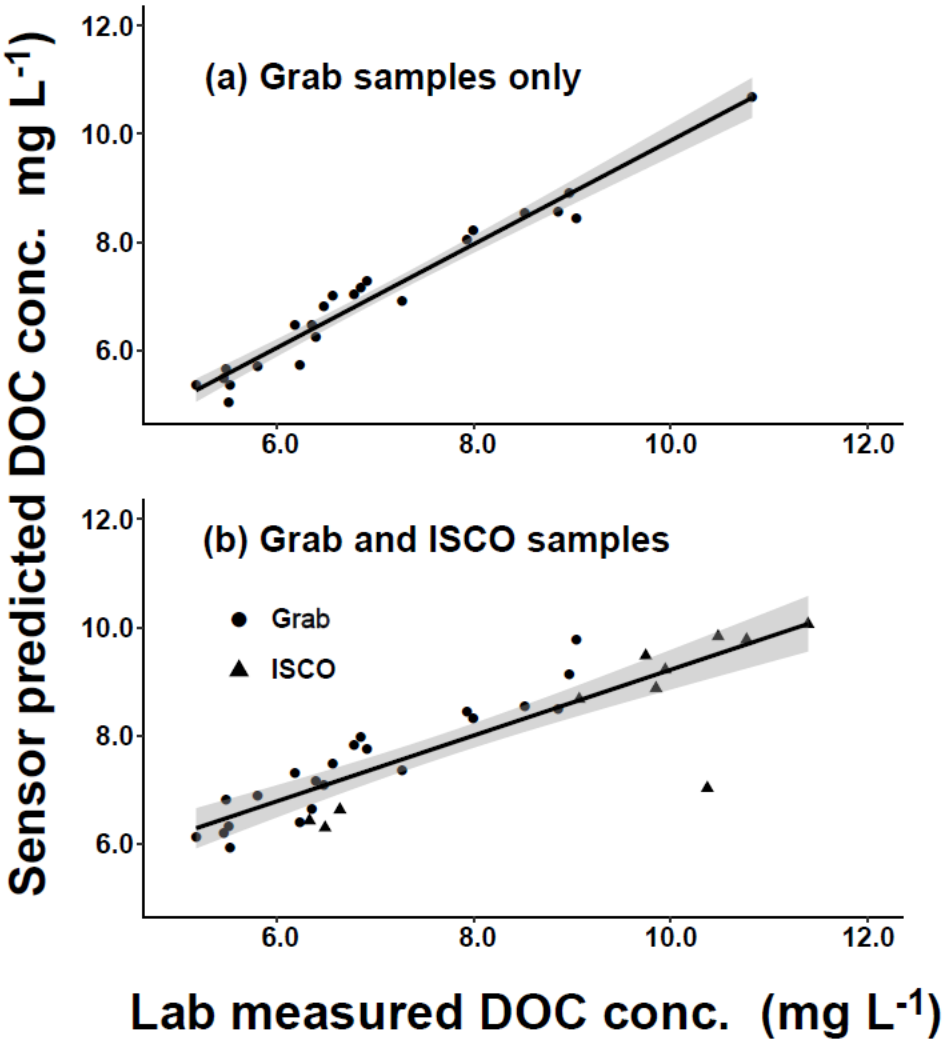

Supporting Figure 2.S3. Plot of sensor DOC calibration at the agricultural site (a) with manual grab samples only, and (b) with both manual grab samples and automatically collected samples using an ISCO collector.

References

Aitkenhead-Peterson, J. A., Steele, M. K., Nahar, N., and Santhy, K., 2009, Dissolved organic carbon and nitrogen in urban and rural watersheds of south-central Texas: land use and land management influences: Biogeochemistry, v. 96, no. 1-3, p. 119-129.

Andrea, B., Francesc, G., Jérôme, L., Eusebi, V., and Francesc, S., 2006, Cross-site comparison of variability of DOC and Nitrate c–q hysteresis during the autumn–winter period in three mediterranean headwater streams: A synthetic approach: Biogeochemistry, v. 77, no. 3, p. 327-349.

Arnold, J. G., Allen, P. M., Muttiah, R., and Bernhardt, G., 1995, Automated base-flow separation and recession analysis techniques: Ground Water, v. 33, no. 6, p. 1010-1018.

Aulenbach, B. T., Burns, D. A., Shanley, J. B., Yanai, R. D., Bae, K., Wild, A. D., Yang, Y., and Yi, D., 2016, Approaches to stream solute load estimation for solutes with varying dynamics from five diverse small watersheds: Ecosphere, v. 7, no. 6, p. n/a-n/a.

Avagyan, A., Runkle, B. R. K., and Kutzbach, L., 2014, Application of high-resolution spectral absorbance measurements to determine dissolved organic carbon concentration in remote areas: Journal of Hydrology, v. 517, p. 435-446.

Baker, J. P., Van Sickle, J., Gagen, C. J., DeWalle, D. R., Sharpe, W. E., Carline, R. F., Baldigo, B. P., Murdoch, P. S., Bath, D. W., Krester, W. A., Simonin, H. A., and Wigington, P. J., 1996, Episodic acidification of small streams in the Northeastern United States: Effects on fish populations: Ecological Applications, v. 6, no. 2, p. 422-437.

Bieroza, M. Z., and Heathwaite, A. L., 2015, Seasonal variation in phosphorus concentration–discharge hysteresis inferred from high-frequency in situ monitoring: Journal of Hydrology, v. 524, p. 333-347.

Boesch, D. F., Brinsfield, R. B., and Magnien, R. E., 2001, Chesapeake Bay eutrophication: Scientific understanding, ecosystem restoration, and challenges for agriculture: Journal of Environmental Quality, v. 30, no. 2, p. 303-320.

Bowes, M. J., Jarvie, H. P., Halliday, S. J., Skeffington, R. A., Wade, A. J., Loewenthal, M., Gozzard, E., Newman, J. R., and Palmer-Felgate, E. J., 2015, Characterising phosphorus and nitrate inputs to a rural river using high-frequency concentration–flow relationships: Science of The Total Environment, v. 511, p. 608-620.

Bowes, M. J., Smith, J. T., and Neal, C., 2009, The value of high-resolution nutrient monitoring: A case study of the River Frome, Dorset, UK: Journal of Hydrology, v. 378, no. 1–2, p. 82-96.

Boyer, E., Goodale, C., Jaworski, N., and Howarth, R., 2002, Anthropogenic nitrogen sources and relationships to riverine nitrogen export in the northeastern U.S.A: Biogeochemistry, v. 57-58, no. 1, p. 137-169.

Boyer, E. W., Hornberger, G. M., Bencala, K. E., and McKnight, D. M., 1997, Response characteristics of DOC flushing in an alpine catchment: Hydrological Processes, v. 11, no. 12, p. 1635-1647.

Brown, V. A., McDonnell, J. J., Burns, D. A., and Kendall, C., 1999, The role of event water, a rapid shallow flow component, and catchment size in summer stormflow: Journal of Hydrology, v. 217, no. 3–4, p. 171-190.

Buffam, I., Galloway, J. N., Blum, L. K., and McGlathery, K. J., 2001, A stormflow/baseflow comparison of dissolved organic matter concentrations and

bioavailability in an Appalachian stream: Biogeochemistry, v. 53, no. 3, p. 269-306.

Bukaveckas, P. A., and Robbins-Forbes, M., 2000, Role of dissolved organic carbon in the attenuation of photosynthetically active and ultraviolet radiation in Adirondack lakes: Freshwater Biology, v. 43, no. 3, p. 339-354.

Butturini, A., Alvarez, M., Bernal, S., Vazquez, E., and Sabater, F., 2008, Diversity and temporal sequences of forms of DOC and NO3-discharge responses in an intermittent stream: Predictable or random succession?: Journal of Geophysical Research: Biogeosciences, v. 113, no. G3, p. n/a-n/a.

Camargo, J. A., and Alonso, Á., 2006, Ecological and toxicological effects of inorganic nitrogen pollution in aquatic ecosystems: A global assessment: Environment International, v. 32, no. 6, p. 831-849.

Carey, R. O., Wollheim, W. M., Mulukutla, G. K., and Mineau, M. M., 2014, Characterizing storm-event nitrate fluxes in a fifth order suburbanizing watershed using in situ sensors: Environmental Science & Technology, v. 48, no. 14, p. 7756-7765.

Carpenter, S. R., Caraco, N. F., Correll, D. L., Howarth, R. W., Sharpley, A. N., and Smith, V. H., 1998, Nonpoint pollution of surface waters with phosphorus and nitrogen: Ecological Applications, v. 8, no. 3, p. 559-568.

Caverly, E., Kaste, J. M., Hancock, G. S., and Chambers, R. M., 2013, Dissolved and particulate organic carbon fluxes from an agricultural watershed during consecutive tropical storms: Geophysical Research Letters, v. 40, no. 19, p. 5147-5152.

Chanat, J. G., Rice, K. C., and Hornberger, G. M., 2002, Consistency of patterns in concentration-discharge plots: Water Resources Research, v. 38, no. 8, p. 22-21-22-10.

Chow, A. T., Dahlgren, R. A., and Harrison, J. A., 2007, Watershed sources of disinfection byproduct precursors in the Sacramento and San Joaquin Rivers, California: Environmental Science & Technology, v. 41, no. 22, p. 7645-7652.

Creed, I. F., and Band, L. E., 1998, Export of nitrogen from catchments within a temperate forest: Evidence for a unifying mechanism regulated by variable source area dynamics: Water Resources Research, v. 34, no. 11, p. 3105-3120.

Dalzell, B. J., Filley, T. R., and Harbor, J. M., 2005, Flood pulse influences on terrestrial organic matter export from an agricultural watershed: Journal of Geophysical Research-Biogeosciences, v. 110, no. G2.

Darwiche-Criado, N., Comin, F. A., Sorando, R., and Sanchez-Perez, J. M., 2015, Seasonal variability of NO3- mobilization during flood events in a Mediterranean catchment: The influence of intensive agricultural irrigation: Agriculture Ecosystems & Environment, v. 200, p. 208-218.

Dhillon, G. S., and Inamdar, S., 2013, Extreme storms and changes in particulate and dissolved organic carbon in runoff: Entering uncharted waters?: Geophysical Research Letters, v. 40, no. 7.

Dinnes, D. L., Karlen, D. L., Jaynes, D. B., Kaspar, T. C., Hatfield, J. L., Colvin, T. S., and Cambardella, C. A., 2002, Nitrogen management strategies to reduce nitrate leaching in tile-drained Midwestern soils: Agronomy Journal, v. 94, p. 153-171.

Donn, M. J., Barron, O. V., and Barr, A. D., 2012, Identification of phosphorus export from low-runoff yielding areas using combined application of high frequency water quality data and MODHMS modelling: Science of The Total Environment, v. 426, p. 264-271.

Driscoll, C. T., Fuller, R. D., and Simone, D. M., 1988, Longitudinal variations in trace-metal concentrations in a northern forested ecosystem: Journal of Environmental Quality, v. 17, no. 1, p. 101-107.

Driscoll, C. T., Lawrence, G. B., Bulger, A. J., Butler, T. J., Cronan, C. S., Eagar, C., Lambert, K. F., Likens, G. E., Stoddard, J. L., and Weathers, K. C., 2001, Acidic deposition in the Northeastern United States: Sources and inputs, ecosystem effects, and management strategies: BioScience, v. 51, no. 3, p. 180-198.

Driscoll, C. T., Whitall, D., Aber, J., Boyer, E., Castro, M., Cronan, C., Goodale, C. L., Groffman, P., Hopkinson, C., Lambert, K., Lawrence, G., and Ollinger, S., 2003, Nitrogen pollution in the Northeastern United States: Sources, effects, and management options: BioScience, v. 53, no. 4, p. 357-374.

Elmore, A. J., and Kaushal, S. S., 2008, Disappearing headwaters: patterns of stream burial due to urbanization: Frontiers in Ecology and the Environment, v. 6, no. 6, p. 308-312.

Etheridge, J. R., Birgand, F., Osborne, J. A., Osburn, C. L., Burchell, M. R., II, and Irving, J., 2014, Using in situ ultraviolet-visual spectroscopy to measure nitrogen, carbon, phosphorus, and suspended solids concentrations at a high frequency in a brackish tidal marsh: Limnology and Oceanography-Methods, v. 12, p. 10-22.

Evans, C., and Davies, T. D., 1998, Causes of concentration/discharge hysteresis and its potential as a tool for analysis of episode hydrochemistry: Water Resources Research, v. 34, no. 1, p. 129-137.

Fellman, J. B., Hood, E., Edwards, R. T., and D'Amore, D. V., 2009, Changes in the concentration, biodegradability, and fluorescent properties of dissolved organic matter during stormflows in coastal temperate watersheds: Journal of Geophysical Research: Biogeosciences, v. 114, no. G1, p. G01021.

Goodale, C. L., Thomas, S. A., Fredriksen, G., Elliott, E. M., Flinn, K. M., Butler, T. J., and Walter, M. T., 2009, Unusual seasonal patterns and inferred processes of nitrogen retention in forested headwaters of the Upper Susquehanna River: Biogeochemistry, v. 93, no. 3, p. 197-218.

Groffman, P. M., Boulware, N. J., Zipperer, W. C., Pouyat, R. V., Band, L. E., and Colosimo, M. F., 2002, Soil nitrogen cycle processes in urban riparian zones: Environ Sci Technol, v. 36, no. 21, p. 4547-4552.

Hatfield, J., Prueger, J., and Jaynes, D., Environmental impacts of agricultural drainage in the Midwest, *in* Proceedings Proceedings of the 7th Annual Drainage Symposium, Orlando, FL. American Society of Agricultural Engineers, St. Joseph, MI. pp. 28ñ351998.

Helms, J. R., Stubbins, A., Ritchie, J. D., Minor, E. C., Kieber, D. J., and Mopper, K., 2008, Absorption spectral slopes and slope ratios as indicators of molecular weight, source, and photobleaching of chromophoric dissolved organic matter: Limnology and Oceanography, v. 53, no. 3, p. 955-969.

Hood, E., Gooseff, M. N., and Johnson, S. L., 2006, Changes in the character of stream water dissolved organic carbon during flushing in three small watersheds, Oregon: Journal of Geophysical Research: Biogeosciences, v. 111, no. G1, p. n/a-n/a.

House, W. A., and Warwick, M. S., 1998, Hysteresis of the solute concentration/discharge relationship in rivers during storms: Water Research, v. 32, no. 8, p. 2279-2290.

Inamdar, S., Singh, S., Dutta, S., Levia, D., Mitchell, M., Scott, D., Bais, H., and McHale, P., 2011, Fluorescence characteristics and sources of dissolved organic matter for stream water during storm events in a forested mid-Atlantic watershed: Journal of Geophysical Research-Biogeosciences, v. 116.

Inamdar, S. P., O'Leary, N., Mitchell, M. J., and Riley, J. T., 2006, The impact of storm events on solute exports from a glaciated forested watershed in western New York, USA: Hydrological Processes, v. 20, no. 16, p. 3423-3439.

Johnson, F. A., and East, J. W., 1982, Cyclical relationships between river discharge and chemical concentration during flood events: Journal of Hydrology, v. 57, no. 1, p. 93-106.

Johnson, K. S., and Coletti, L. J., 2002, In situ ultraviolet spectrophotometry for high resolution and long-term monitoring of nitrate, bromide and bisulfide in the ocean: Deep Sea Research Part I: Oceanographic Research Papers, v. 49, no. 7, p. 1291-1305.

Kaushal, S. S., and Belt, K. T., 2012, The urban watershed continuum: evolving spatial and temporal dimensions: Urban Ecosystems, v. 15, no. 2, p. 409-435.

Kaushal, S. S., Groffman, P. M., Band, L. E., Shields, C. A., Morgan, R. P., Palmer, M. A., Belt, K. T., Swan, C. M., Findlay, S. E. G., and Fisher, G. T., 2008, Interaction between urbanization and climate variability amplifies watershed nitrate export in Maryland: Environmental Science & Technology, v. 42, no. 16, p. 5872-5878.

Kominoski, J. S., and Rosemond, A. D., 2011, Conservation from the bottom up: forecasting effects of global change on dynamics of organic matter and management needs for river networks: Freshwater Science, v. 31, no. 1, p. 51-68.

Kraus, T. E. C., Bergamaschi, B. A., Hernes, P. J., Spencer, R. G. M., Stepanauskas, R., Kendall, C., Losee, R. F., and Fujii, R., 2008, Assessing the contribution of wetlands and subsided islands to dissolved organic matter and disinfection byproduct precursors in the Sacramento–San Joaquin River Delta: A geochemical approach: Organic Geochemistry, v. 39, no. 9, p. 1302-1318.

Kruskal, W. H., and Wallis, W. A., 1952, Use of ranks in one-criterion variance analysis: Journal of the American Statistical Association, v. 47, no. 260, p. 583-621.

Langergraber, G., Fleischmann, N., and Hofstadter, F., 2003, A multivariate calibration procedure for UV/VIS spectrometric quantification of organic matter and nitrate in wastewater: Water Science and Technology, v. 47, no. 2, p. 63-71.

Levene, H., 1960, Robust tests for equality of variances, *in* Olkin, I., ed., Contributions to Probability and Statistics: Essays in Honor of Harold Hotelling, Stanford University Press, p. 278-292.

Likens, G. E., 2013, Biogeochemistry of a forested ecosystem, New York, NY, Springer, 208 p.:

Lloyd, C. E. M., Freer, J. E., Johnes, P. J., and Collins, A. L., 2016, Technical Note: Testing an improved index for analysing storm discharge–concentration hysteresis: Hydrol. Earth Syst. Sci., v. 20, no. 2, p. 625-632.

McGlynn, B. L., and McDonnell, J. J., 2003, Quantifying the relative contributions of riparian and hillslope zones to catchment runoff: Water Resources Research, v. 39, no. 11, p. 1310.

Mevik, B., Wehrens, R., and Liland, K. H., 2015, pls: Partial Least Squares and Principal Component Regression.

Moore, R. D., 2005, Slug injection using salt in solution: Streamline Watershed Management Bulletin, v. 8, no. 2, p. 1-6.

Moore, T. R., and Jackson, R. J., 1989, Dynamics of dissolved organic carbon in forested and disturbed catchments, Westland, New Zealand: 2. Larry River: Water Resources Research, v. 25, no. 6, p. 1331-1339.

Morel, B., Durand, P., Jaffrezic, A., Gruau, G., and Molenat, J., 2009, Sources of dissolved organic carbon during stormflow in a headwater agricultural catchment: Hydrological Processes, v. 23, no. 20, p. 2888-2901.

Morris, D. P., Zagarese, H., Williamson, C. E., Balseiro, E. G., Hargreaves, B. R., Modenutti, B., Moeller, R., and Queimalinos, C., 1995, The attentuation of solar UV radiation in lakes and the role of dissolved organic carbon: Limnology and Oceanography, v. 40, no. 8, p. 1381-1391.

Newcomer, T. A., Kaushal, S. S., Mayer, P. M., Shields, A. R., Canuel, E. A., Groffman, P. M., and Gold, A. J., 2012, Influence of natural and novel organic carbon sources on denitrification in forest, degraded urban, and restored streams: Ecological Monographs, v. 82, no. 4, p. 449-466.

Nguyen, H. V.-M., Lee, M.-H., Hur, J., and Schlautman, M. A., 2013, Variations in spectroscopic characteristics and disinfection byproduct formation potentials of dissolved organic matter for two contrasting storm events: Journal of Hydrology, v. 481, no. 0, p. 132-142.

Oeurng, C., Sauvage, S., and Sánchez-Pérez, J.-M., 2010, Temporal variability of nitrate transport through hydrological response during flood events within a large agricultural catchment in south-west France: Science of The Total Environment, v. 409, no. 1, p. 140-149.

Outram, F. N., Lloyd, C. E. M., Jonczyk, J., Benskin, C. M. H., Grant, F., Perks, M. T., Deasy, C., Burke, S. P., Collins, A. L., Freer, J., Haygarth, P. M., Hiscock, K. M., Johnes, P. J., and Lovett, A. L., 2014, High-frequency monitoring of nitrogen and phosphorus response in three rural catchments to the end of the 2011–2012 drought in England: Hydrol. Earth Syst. Sci., v. 18, no. 9, p. 3429-3448.

Pardo, L. H., Fenn, M. E., Goodale, C. L., Geiser, L. H., Driscoll, C. T., Allen, E. B., Baron, J. S., Bobbink, R., Bowman, W. D., Clark, C. M., Emmett, B., Gilliam, F. S., Greaver, T. L., Hall, S. J., Lilleskov, E. A., Liu, L., Lynch, J. A., Nadelhoffer, K. J., Perakis, S. S., Robin-Abbott, M. J., Stoddard, J. L., Weathers, K. C., and Dennis, R. L., 2011, Effects of nitrogen deposition and empirical nitrogen critical loads for ecoregions of the United States: Ecological Applications, v. 21, no. 8, p. 3049-3082.

Parr, T. B., Cronan, C. S., Ohno, T., Findlay, S. E. G., Smith, S. M. C., and Simon, K. S., 2015, Urbanization changes the composition and bioavailability of dissolved organic matter in headwater streams: Limnology and Oceanography, p. n/a-n/a.

Paternoster, R., Brame, R., Mazerolle, P., and Piquero, A., 1998, Using the correct statistical test for the equality of regression coefficients: Criminology, v. 36, no. 4, p. 859-866.

Pellerin, B. A., Saraceno, J. F., Shanley, J. B., Sebestyen, S. D., Aiken, G. R., Wollheim, W. M., and Bergamaschi, B. A., 2012, Taking the pulse of snowmelt: in situ sensors reveal seasonal, event and diurnal patterns of nitrate and dissolved organic matter variability in an upland forest stream: Biogeochemistry, v. 108, no. 1, p. 183-198.

Prairie, Y. T., 2008, Carbocentric limnology: looking back, looking forward: Canadian Journal of Fisheries and Aquatic Sciences, v. 65, no. 3, p. 543-548.

R Core Team, 2015, R: A language and environment for statistical computing.: Vienna, Austria, R Foundation for Statistical Computing.

Ravichandran, M., 2004, Interactions between mercury and dissolved organic matter - a review: Chemosphere, v. 55, no. 3, p. 319-331.

Raymond, P., and Saiers, J., 2010, Event controlled DOC export from forested watersheds: Biogeochemistry, v. 100, no. 1-3, p. 197-209.

Reckhow, D. A., and Singer, P. C., 1990, Chlorination by-products in drinking waters - from formation potentials to finished water concentrations: Journal American Water Works Association, v. 82, no. 4, p. 173-180.

Rosenzweig, B. R., Moon, H. S., Smith, J. A., Baeck, M. L., and Jaffe, P. R., 2008, Variation in the instream dissolved inorganic nitrogen response between and within rainstorm events in an urban watershed: Journal of Environmental Science and Health, Part A, v. 43, no. 11, p. 1223-1233.

Royer, T. V., and David, M. B., 2005, Export of dissolved organic carbon from agricultural streams in Illinois, USA: Aquatic Sciences, v. 67, no. 4, p. 465-471.

Royer, T. V., David, M. B., and Gentry, L. E., 2006, Timing of riverine export of nitrate and phosphorus from agricultural watersheds in Illinois: Implications for reducing nutrient loading to the Mississippi River: Environmental Science & Technology, v. 40, no. 13, p. 4126-4131.

Rusjan, S., Brilly, M., and Mikoš, M., 2008, Flushing of nitrate from a forested watershed: An insight into hydrological nitrate mobilization mechanisms through seasonal high-frequency stream nitrate dynamics: Journal of Hydrology, v. 354, no. 1–4, p. 187-202.

Sanchez, C. A., and Blackmer, A. M., 1988, Recovery of anhydrous ammonia-derived nitrogen-15 during three years of corn production in Iowa: Agronomy Journal, v. 80, p. 102-108.

Saraceno, J. F., Pellerin, B. A., Downing, B. D., Boss, E., Bachand, P. A. M., and Bergamaschi, B. A., 2009, High-frequency in situ optical measurements during a storm event: Assessing relationships between dissolved organic matter, sediment concentrations, and hydrologic processes: Journal of Geophysical Research-Biogeosciences, v. 114.

Sebestyen, S. D., Shanley, J. B., Boyer, E. W., Kendall, C., and Doctor, D. H., 2014, Coupled hydrological and biogeochemical processes controlling variability of nitrogen species in streamflow during autumn in an upland forest: Water Resources Research, v. 50, no. 2, p. 1569-1591.

Sickman, J. O., Zanoli, M. J., and Mann, H. L., 2007, Effects of urbanization on organic carbon loads in the Sacramento River, California: Water Resources Research, v. 43, no. 11, p. W11422.

Sivirichi, G. M., Kaushal, S. S., Mayer, P. M., Welty, C., Belt, K. T., Newcomer, T. A., Newcomb, K. D., and Grese, M. M., 2011, Longitudinal variability in streamwater chemistry and carbon and nitrogen fluxes in restored and degraded

urban stream networks: Journal of Environmental Monitoring, v. 13, no. 2, p. 288-303.

Smith, V. H., Tilman, G. D., and Nekola, J. C., 1999, Eutrophication: impacts of excess nutrient inputs on freshwater, marine, and terrestrial ecosystems: Environmental Pollution, v. 100, no. 1–3, p. 179-196.

Sobczak, W., Findlay, S., and Dye, S., 2003, Relationships between DOC bioavailability and nitrate removal in an upland stream: An experimental approach: Biogeochemistry, v. 62, no. 3, p. 309-327.

Stanley, E. H., Powers, S. M., Lottig, N. R., Buffam, I., and Crawford, J. T., 2012, Contemporary changes in dissolved organic carbon (DOC) in human-dominated rivers: is there a role for DOC management?: Freshwater Biology, v. 57, p. 26-42.

Stubbins, A., Lapierre, J. F., Berggren, M., Prairie, Y. T., Dittmar, T., and del Giorgio, P. A., 2014, What's in an EEM? Molecular signatures associated with dissolved organic fluorescence in Boreal Canada: Environmental Science & Technology, v. 48, no. 18, p. 10598-10606.

Townsend, A. R., Howarth, R. W., Bazzaz, F. A., Booth, M. S., Cleveland, C. C., Collinge, S. K., Dobson, A. P., Epstein, P. R., Holland, E. A., Keeney, D. R., Mallin, M. A., Rogers, C. A., Wayne, P., and Wolfe, A. H., 2003, Human health effects of a changing global nitrogen cycle: Frontiers in Ecology and the Environment, v. 1, no. 5, p. 240-246.

Turnipseed, D. P., and Sauer, V. B., 2010, Discharge measurements at gaging stations: U.S. Geological Survey, 2328-7055.

Van Herpe, Y., and Troch, P. A., 2000, Spatial and temporal variations in surface water nitrate concentrations in a mixed land use catchment under humid temperate climatic conditions: Hydrological Processes, v. 14, no. 14, p. 2439-2455.

Vidon, P., Wagner, L. E., and Soyeux, E., 2008, Changes in the character of DOC in streams during storms in two Midwestern watersheds with contrasting land uses: Biogeochemistry, v. 88, no. 3, p. 257-270.

Walford, N., 2011, Practical statistics for geographers and earth scientists, Oxford, UK ; Hoboken, NJ, Wiley-Blackwell, xxiii, 416 p. p.:

Walsh, C. J., Roy, A. H., Feminella, J. W., Cottingham, P. D., Groffman, P. M., and Morgan, R. P., 2005, The urban stream syndrome: current knowledge and the search for a cure: Journal of the North American Benthological Society, v. 24, no. 3, p. 706-723.

Walsh, J., Dwuebbles, K., Hayhoe, K., Kossin, J., Kunkel, K., Stephens, G., Thorne, P., Vose, R., Wehner, M., Willis, J., Anderson, D., Doney, S., Feely, R., Hennon, P., Kharin, V., Knutson, T., Landerer, F., Lenton, T., Kennedy, J., and Somerville, R., 2014, Climate change impacts in the United States: The third national climate assessment: US Global Change Research Program.

Webster, J. R., Newbold, J. D., Thomas, S. A., Valett, H. M., and Mulholland, P. J., 2009, Nutrient uptake and mineralization during leaf decay in streams – a model simulation: International Review of Hydrobiology, v. 94, no. 4, p. 372-390.

Wilson, H., and Xenopoulos, M., 2008, Ecosystem and Seasonal Control of Stream Dissolved Organic Carbon Along a Gradient of Land Use: Ecosystems, v. 11, no. 4, p. 555-568.

Wilson, H. F., and Xenopoulos, M. A., 2009, Effects of agricultural land use on the composition of fluvial dissolved organic matter: Nature Geosci, v. 2, no. 1, p. 37-41.

Winchell, M., Meals, D., Folle, S., Moore, J., Braun, D., DeLeo, C., Budreski, K., and Schiff, R., 2011, Identification of critical source areas of phosphorus within the Vermont sector of the Missisquoi Bay Basin: Lake Champlain Basin Program.

Yoon, B., and Raymond, P. A., 2012, Dissolved organic matter export from a forested watershed during Hurricane Irene: Geophysical Research Letters, v. 39.

Zhang, Z., Fukushima, T., Onda, Y., Gomi, T., Fukuyama, T., Sidle, R., Kosugi, K., and Matsushige, K., 2007, Nutrient runoff from forested watersheds in central Japan during typhoon storms: implications for understanding runoff mechanisms during storm events: Hydrological Processes, v. 21, no. 9, p. 1167-1178.

CHAPTER 3. USING IN SITU UV-VISIBLE SPECTROPHOTOMETER SENSORS TO QUANTIFY RIVERINE PHOSPHORUS PARTITIONING AND CONCENTRATION AT A HIGH FREQUENCY

Abstract

Accurate riverine phosphorus concentration measurements are often critical to meet watershed management goals. Phosphorus monitoring programs often rely on proxy variables such as turbidity and discharge and have limited ability to accurately estimate concentrations of dissolved phosphorus fractions that are most bioavailable. Optical water quality sensors can make sub-hourly measurements and have been shown to reduce uncertainty in load estimates and reveal high-frequency storm dynamics for nitrate and dissolved organic carbon. We evaluated the utility of in situ UV-Visible spectrophotometers to predict total, dissolved, and soluble reactive phosphorus concentrations in streams draining agricultural, urban, and forested land use / land covers. We present the first statistically validated application of optical water quality sensors to demonstrate how sensors may perform in predicting phosphorus fraction concentrations through training set models. Total phosphorus predictions from UV-Visible spectra were optimal when models were site-specific, and the proportion of variance explained was generally as high as or higher than the results of other studies that rely only on discharge and turbidity. However, root mean square errors for total phosphorus models were relatively high compared to the median concentrations at each site. Models to predict dissolved and soluble reactive phosphorus explained a greater proportion of the variance than any other known proxy variable technique, and results varied by land use / land cover. Though accuracy limitations remain, this approach has potential to predict concurrent total,

dissolved, and soluble reactive phosphorus concentrations at a high frequency for many applications in water quality research and management communities.

Introduction

Elevated phosphorus concentrations cause persistent problems such as eutrophication and potentially toxic cyanobacteria growth in many fresh waterbodies that impact recreation, drinking water quality, property values, and ecosystem health (Carpenter et al. 1998; Conley et al. 2009). To address these challenges, watersheds are often managed to reduce tributary total phosphorus (TP) loads (Djodjic et al. 2002; Sharpley et al. 1994). Accurate tributary phosphorus load estimation is critical to meet these management goals, and TP load estimates assess the efficacy of watershed-scale phosphorus reduction efforts (Medalie 2016). Episodic storm events are particularly important to capture, since they deliver disproportionately large loads of water, sediment, and phosphorus (Jordan et al. 2007; Sharpley et al. 2008) and phosphorus concentrations change rapidly during storms (Correll et al. 1999).

TP is delivered to waterbodies in several forms that can differ in bioavailability for cyanobacteria growth (Correll 1998; Giles et al. 2015; Isles et al. 2017). Phosphorus is most bioavailable as dissolved inorganic orthophosphate (PO_4^{3-}), commonly measured as soluble reactive phosphorus (SRP), or as part of the total dissolved phosphorus fraction (TDP). A portion of the organic phosphorus pool can also be directly bioavailable, or can be rapidly decomposed by heterotrophic bacteria into the inorganic form that can be quickly utilized (Kane et al. 2014). Particulate phosphorus has potential bioavailability dependent upon the speciation of solid phase phosphorus and its interaction with receiving water column and pore water solutions (Giles et al. 2015; Schroth et al. 2015). Because

each phosphorus fraction has differing degrees of bioavailability, understanding the magnitude and dynamic chemical partitioning of riverine phosphorus fraction loads delivered to a receiving waterbody is necessary to inform management of potential cyanobacteria growth and to reach desired management outcomes (Isles et al. 2017; Stumpf et al. 2012). Long-term continuous monitoring is particularly important to characterize changes as management decisions and land use change influence the amount and composition of phosphorus delivery to receiving waterbodies (Dodd and Sharpley 2016; Jarvie et al. 2017).

TP concentration estimates are often based on correlations of lab measured TP concentration from grab samples with continuously measured discharge, turbidity, or a combination of the two. Although these correlations can be strong (Hyer et al. 2016), this approach has two disadvantages: (1) solute-discharge and solute-turbidity relationships are variable among storm events due to hysteresis effects and threshold behavior changes (Bieroza and Heathwaite 2015; Dhillon and Inamdar 2013), and (2) these methods only estimate TP concentrations and typically do not provide critical information on phosphorus partitioning. Alternatively, SRP concentration can be directly measured in situ at an hourly to sub-hourly frequency with newly available wet chemistry instruments (e.g., Cohen et al. 2013).

In situ spectrophotometer sensors offer the potential to concurrently measure multiple phosphorus fraction concentrations (e.g., TP, TDP, SRP) at a high frequency continuously with no reagents or waste products. These sensors measure light absorbance in the UV-Visible spectrum and have been shown to make continuous, concurrent, and accurate measurements of dissolved organic carbon, nitrate (NO_3^-), and total suspended

solids concentrations in surface waters with varying environmental conditions and aqueous matrices (Fichot and Benner 2011; Langergraber et al. 2003; Rieger et al. 2006; Sakamoto et al. 2009). Because optical sensors can be deployed on a long-term basis and operate continuously, researchers and watershed managers can better characterize large episodic events when manual sampling may be impractical, expensive, and/or unsafe (Carey et al. 2014; Saraceno et al. 2009). Dynamics that occur on seasonal or diel timescales are also better described by this approach (Heffernan and Cohen 2010; Pellerin et al. 2012). While methods that rely on discrete grab samples may assign a single concentration to an entire storm or day of record, high-frequency measurements capture short timescale hysteresis and threshold behavior changes not documented by discrete samples. In addition, optical sensors have the potential to predict nutrient concentrations and vertical profiles in lakes and reservoirs, where concentration-discharge relationships are not applicable (Birgand et al. 2016; Joung et al. 2017). Continuous and high-frequency monitoring can improve accuracy of load estimates (Guo et al. 2002; Pellerin et al. 2014), though the improvement over concentration-discharge measurement may be limited for some applications (Musolff et al. 2017).

Only a few researchers have attempted to use multi-wavelength UV-Visible spectrophotometers to estimate phosphorus fraction concentrations in a limited number of environmental conditions, and it is unknown how performance may differ among streams draining different land uses and land covers (LULCs). Unlike solutes such as nitrate and dissolved organic carbon, most phosphorus fractions do not directly absorb light in the UV-Visible spectrum, so calibrations with concentrations of different phosphorus fractions rely on proxy correlations alone, similar to correlations relating TP concentration to discharge.

This approach has also been used to predict other non UV-Visible wavelength light absorbing solutes (e.g., Si, Mn, Fe) with promising results (Birgand et al. 2016). Because spectrophotometers measure absorbance throughout the entire UV-Visible spectrum, it is possible that multiple light sensitive proxies co-vary with phosphorus fractions differently by site, season, and/or storm event. Different phosphorus fractions may be tracking light sensitive aqueous components that reflect phosphorus provenance and biogeochemical cycling within a particular catchment and across different temporal scales or flow regimes. UV-Visible spectrophotometer sensors have shown promise to predict phosphorus fractions in some cases (Etheridge et al. 2014), though predictions of TP, TDP, and SRP concentrations from optical sensors have not been evaluated rigorously in a variety of systems. It is not known to what extent site-specific calibrations are necessary as is often the case for other solutes (e.g., Vaughan et al. 2017), or whether multiple different phosphorus fraction concentrations can be predicted accurately from UV-Visible absorbance spectra. If robust proxy correlations were developed, phosphorus fractions could be measured continuously on short timescales that capture rapid changes in hydrologic and biogeochemical processes critical to inform watershed management and nutrient reduction goals.

Generating algorithms to predict nutrient concentrations from absorbance spectra presents a challenge due to the high dimensionality of the independent variables (light absorbance spectra) compared to the single response variable (nutrient concentration). Partial least squares regression (PLSR) can be used to harness the information of a rich collection of independent variables to predict a desired dependent quantity. PLSR is a technique that condenses independent variables into orthogonal, uncorrelated components

and combines them in a multivariate model to predict the parameter of interest. Visible, near-infrared, and far-infrared reflectance spectra have been used extensively in combination with the PLSR approach to describe soil characteristics such as available phosphorus, electrical conductivity, pH, organic carbon, lime requirement, and cation exchange capacity (e.g., McCarty et al. 2002; Viscarra Rossel et al. 2006). In addition, UV-Visible spectra have been used to predict concentrations of various nutrients in fresh and brackish water with encouraging results (Avagyan et al. 2014; Birgand et al. 2016; Vaughan et al. 2017). However, previous studies evaluating this method to predict constituent concentrations in water have not presented model validation results; that is, all of the available laboratory analyses were used to calibrate the model, without verifying predictions using independent observations.

We deployed spectrophotometers in well-characterized watersheds of different LULC (Rosenberg and Schroth 2017; Vaughan et al. 2017) that drive different phosphorus dynamics, concentrations, and partitioning. UV-Visible absorption spectra from spectrophotometers were coupled with grab water samples for conventional laboratory analysis of TP, TDP, and SRP concentrations. Our objectives were to: (1) evaluate in situ UV-Visible spectrophotometer prediction of TP, TDP, and SRP concentrations in riverine waters, (2) compare prediction performance in surface waters draining watersheds of various LULCs, and (3) present statistical validation of these predictions. To our knowledge, this work constitutes the most rigorous assessment to date of the utility of this sensor technology to predict multiple phosphorus fraction concentrations across a range of riverine environments.

Study areas

The study sites were in the Lake Champlain Basin of Vermont in the northeastern US (Table 3.1, Figure 3.1). The study streams were selected because their watershed LULC was dominantly agricultural, urban, or forested, and each watershed met criteria for watershed size, accessibility, and discharge data availability. Hungerford Brook is a primarily agricultural catchment, including dairy production, row crops, hay, and pasture. Potash Brook is situated near the city of Burlington, Vermont's densest population center. Its watershed is primarily characterized by urban and suburban development (54%), and includes some agricultural and forest cover (29% and 11%, respectively). The Wade Brook catchment is primarily forested (95%) and is situated on the western slope of Vermont's Green Mountain chain. Hungerford Brook and Wade Brook drain to the Missisquoi River and Lake Champlain; Potash Brook drains directly to Lake Champlain. Precipitation totals in the Wade Brook catchment are higher than the catchments of Hungerford Brook and Potash Brook due to orographic effects (Table 3.1).

Table 3.1. Summary of study area characteristics.

	Hungerford Brook	Potash Brook	Wade Brook
Primary land cover	Agricultural	Urban / Suburban	Forest
Watershed area (km^2)	48.1	18.4	16.7
Percentage forested	40.5	10.6	95.1
Percentage agricultural	44.8	29.1	0.6
Percentage urban	5.6	53.5	0.8
Percentage impervious area	2.3	23.9	0
Sensor elevation (m)	80	42	320
Maximum watershed elevation (m)	354	143	981
Mean watershed slope (%)	5.6	5.3	26
Mean air temperature (°C)	6.7	7.8	4.2
Mean precipitation ($mm\ yr^{-1}$)	1000	961	1453
Mean annual atmospheric nitrogen deposition ($kg\ N\ km^{-2}$)	450	340	570
Sensor optical path length (mm)	5	5	15
Coordinates (WGS 1984)	44.918403° N, 73.055664° W	44.444331° N, 73.214482° W	44.864468° N, 72.552904° W
Soil and Surficial Geology	Sandy, silty, and stony loams	Sandy and silty loams, clay	Glacial till, sandy loam
Vegetation	Agricultural, mixed northern hardwoods and conifer	Urban / suburban landscaping, mixed northern hardwoods and conifer, agricultural	Mixed northern hardwoods and conifer

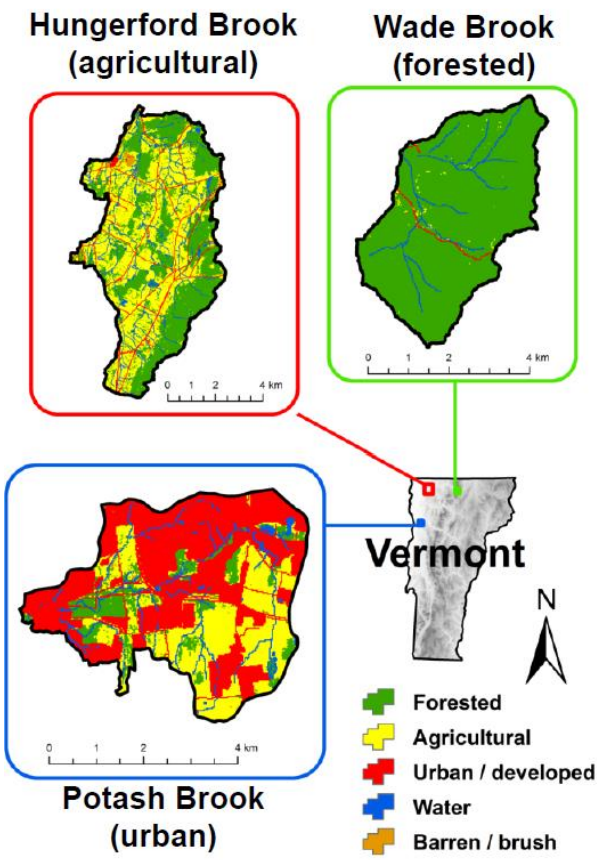

Figure 3.1. Map showing location and land use / land cover of the three study areas.

Methods

In-stream measurements

We used s::can Spectrolyser UV-Visible spectrophotometers (s::can Messtechnik GmbH, Vienna, Austria) in each stream, deployed from June 2014 to December 2016 for spring, summer, and fall seasons. The sensors were housed in PVC tubing for protection during high flows, were solar powered for autonomous operation, and transmitted summary data through a cellular data network. Full UV-Visible spectra measurements were stored on-board the sensor and downloaded manually on site. The spectrophotometers measured light absorbance at wavelengths ranging from 220 to 750 nm at 2.5 nm increments and were programmed to take measurements every 15 minutes. Optical path lengths were either

5 or 15 mm, depending on the typical turbidity of each stream (Table 3.1), and absorbance spectra were normalized by optical path length for comparison. Sensor measurement windows were automatically cleaned before each measurement with a silicone wiper and cleaned manually in the field at least every two weeks using pure ethanol. To focus on dissolved constituents, raw absorbance spectra were corrected for the effects of turbidity by fitting a third-order polynomial in the visible range of the spectrum, extrapolating into the UV portion, and then subtracting the extrapolated absorbance from the raw spectrum (Avagyan et al. 2014; Langergraber et al. 2003).

Laboratory measurements

Manual grab samples were collected at the sensor sites across the monitored seasons during baseflow and storms (peak flow, rising and falling limb), timed to coincide with sensor measurements to calibrate in situ UV-Visible absorbance spectra to laboratory TP, TDP, and SRP concentration measurements (Figure 3.2). Care was taken to collect samples directly adjacent to the sensor measurement window. We analyzed a total of 560 grab samples over the course of the study. Samples taken in 2015 were analyzed for TDP and SRP; samples taken in 2016 were analyzed for TP, TDP, and SRP. We filtered TDP and SRP samples in the field using sample-rinsed glass fiber GF/F filters (nominal pore size of 0.7 µm) into new, triple-rinsed HDPE bottles, and collected TP samples from the stream without filtering. This filter size differs from that of some others studies where 0.45 µm filters are used. This may influence absolute lab value comparability (where values in this study may be slightly higher in comparison), but would not influence the evaluation of model calibration or validation techniques, which is the focus of this work. We stored

samples on ice in the field and in transport, then stored either in a cooler at 2 ºC (for TDP and SRP samples) or in a freezer at -23 ºC (for TP samples) until analysis.

We analyzed for TP concentration by first liberating organic phosphorus as inorganic phosphorus through oxidation by persulfate, followed by the molybdate method (US EPA method 365.1 4500-PJ). We measured TDP concentration the same way as TP after samples had been filtered as described above. SRP concentration was determined colorimetrically by measuring absorbance of 885 nm following sample reaction with molybdate, ascorbic acid, and trivalent antimony, also consistent with US EPA method 365.1 (Parsons et al. 1984). For each analyte, the non-parametric Kruskal-Wallis test (Kruskal and Wallis 1952) was used to determine whether concentrations were significantly different among the three sites.

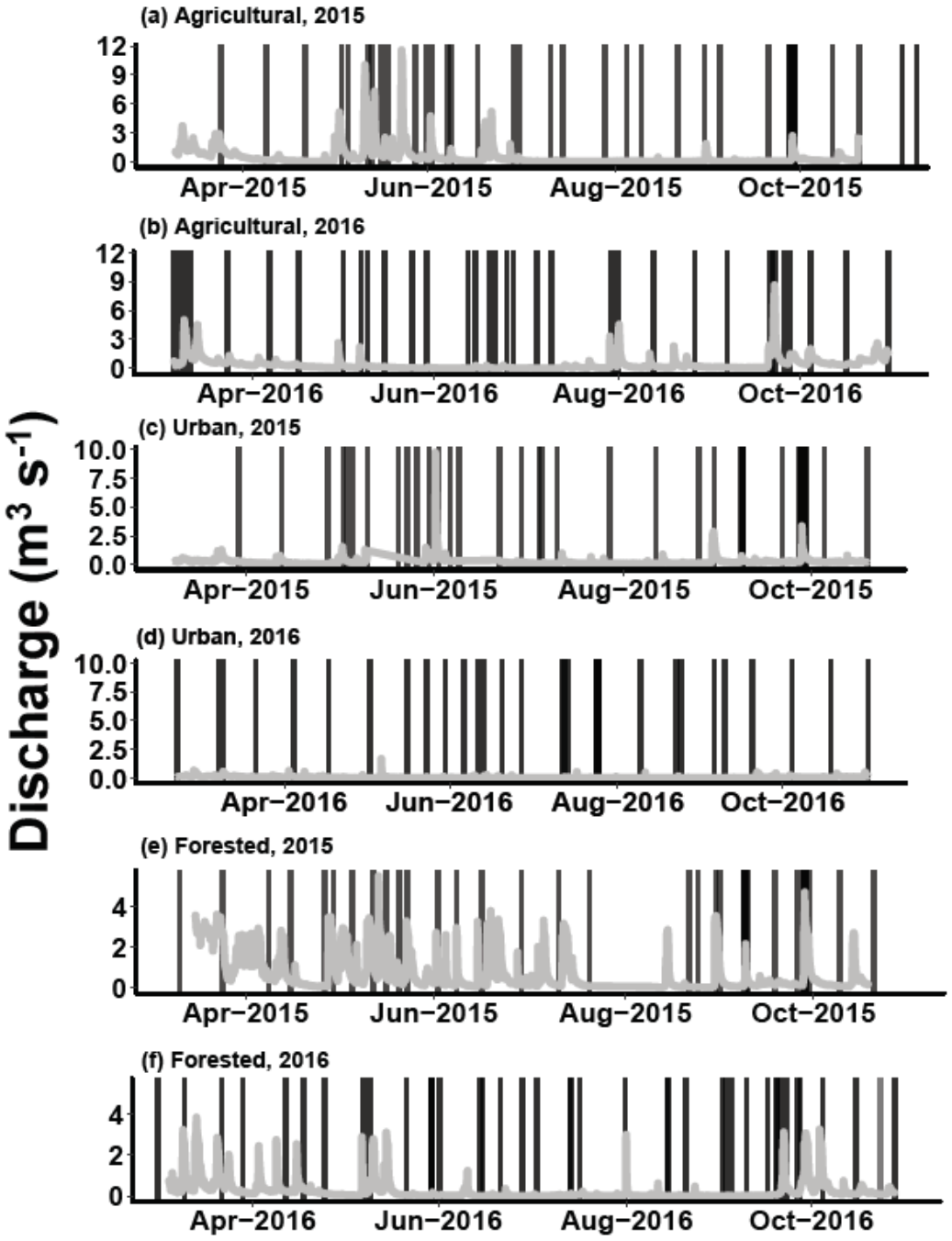

Figure 3.2. Discharge at each site for 2015 and 2016 (grey lines) and timing of manual grab samples (black vertical lines). Samples taken in 2015 were analyzed for TDP and SRP; samples taken in 2016 were analyzed for TP, TDP, and SRP.

Phosphorus fraction concentration prediction: training and validation techniques

When reporting correlations of a particular method to predict lab measurements, it is common to develop a model using all available data and then assume model statistics will apply to future predictions using unknown data. In contrast, we used a bootstrapping technique to validate the accuracy of calibration models built on only a portion of the data to provide a more robust method to assess uncertainty in concentration prediction. Training and validation prediction sets were generated for TP, TDP, and SRP using combined data from all sites for each parameter, and by separating the available data by each site. For each training dataset, 85% of available observations were selected randomly to generate a model. The model was developed by an identical approach to Etheridge et al. (2014), where PLSR was employed with the pls package in R to generate calibration algorithms (Mevik et al. 2015; R Core Team 2015). Each model incorporated a number of components equal to a maximum of approximately 10% of the observations as recommended by Mevik et al. (2015).

The training model was then used to predict a validation set, which was comprised of the remaining 15% of observations that were randomly withheld. This process was repeated 1,000 times with replacement for each parameter, and predictions and statistics for each model were collected and aggregated. We then calculated the means and standard deviations of predicted concentration values for all 1,000 iterations of training and validation sets. Sensor performance was evaluated by performing linear correlations on the mean predicted value for training and validation sets versus the corresponding lab measured values. Throughout the paper, adjusted R^2 values are presented to compare goodness of fit for regressions to remove the bias associated with differing sample sizes

(Ohtani 2000), and root mean square errors (RMSE) are presented as estimates of model accuracy. The result of this process is a quantifiable level of confidence for how accurately UV-Visible absorbance spectra may predict TP, TDP, and SRP concentrations at times when no lab measurement is available for comparison. This type of model validation is common in many disciplines and is more robust than other approaches that develop models using the entire available dataset and therefore provide stronger prediction statistics (Aber 1997).

Logarithmically transformed discharge or turbidity measurements are often used to predict riverine TP concentrations (Hirsch et al. 2010; Stutter et al. 2017). We performed multiple linear regression using these two variables to predict TP concentrations at each site and compared this method with the performance of the UV-Visible spectrophotometers. These models included all available data for each site in order to form comparisons using the most favorable case for this method.

Results

Phosphorus grab samples and UV-Visible absorbance measurements

The non-parametric Kruskal-Wallis test revealed that grab sample concentrations for TP, TDP, and SRP were each significantly different among these three sites ($p < 0.001$; Table 3.2). When UV-Visible absorbance spectra were plotted and colored by corresponding phosphorus fraction concentrations, it is evident that much of the variance in UV-Visible spectra occurs in the wavelength range of 220 – 350 nm (Figure 3.3). Furthermore, while generally higher absorbances correspond with higher phosphorus fraction concentrations, complex relationships exist between spectral data and phosphorus fraction concentrations. The ratio of lab measured TDP to TP concentrations and the ratio

of lab measured SRP to TP concentrations varied considerably at the agricultural and urban sites, and the ratio of SRP to TP was significantly different between these sites as determined by the non-parametric Mann-Whitney U test ($p = 0.001$) (Figure 3.4). The highest observed concentrations of TDP and SRP were higher than the highest TP concentration because relatively large storms in 2015 produced high TDP and SRP concentrations and TP concentrations were not measured at that time.

Table 3.2. Summary statistics for grab samples collected at the study sites (all concentrations are in μg P L^{-1}).

Total phosphorus (2016 only)			
	Agricultural	Urban	Forested
Count	36	27	42
Minimum	13.4	6.50	0.70
Maximum	917	89.6	12.3
Median	79.0	20.6	3.8
Mean	130	24.7	4.5
Variance	31.6	0.40	< 0.10

Total dissolved phosphorus (2015-2016)			
	Agricultural	Urban	Forested
Count	77	80	89
Minimum	8.50	3.5	1.8
Maximum	1413	263	31.6
Median	63.0	32.1	7.6
Mean	133	64.6	10.7
Variance	42.2	5.4	0.10

Soluble reactive phosphorus (2015-2016)			
	Agricultural	Urban	Forested
Count	77	105	89
Minimum	3.0	0.30	0.60
Maximum	1240	231.5	22.8
Median	46.2	17.4	4.2
Mean	110	37.1	6.9
Variance	35.3	2.6	< 0.10

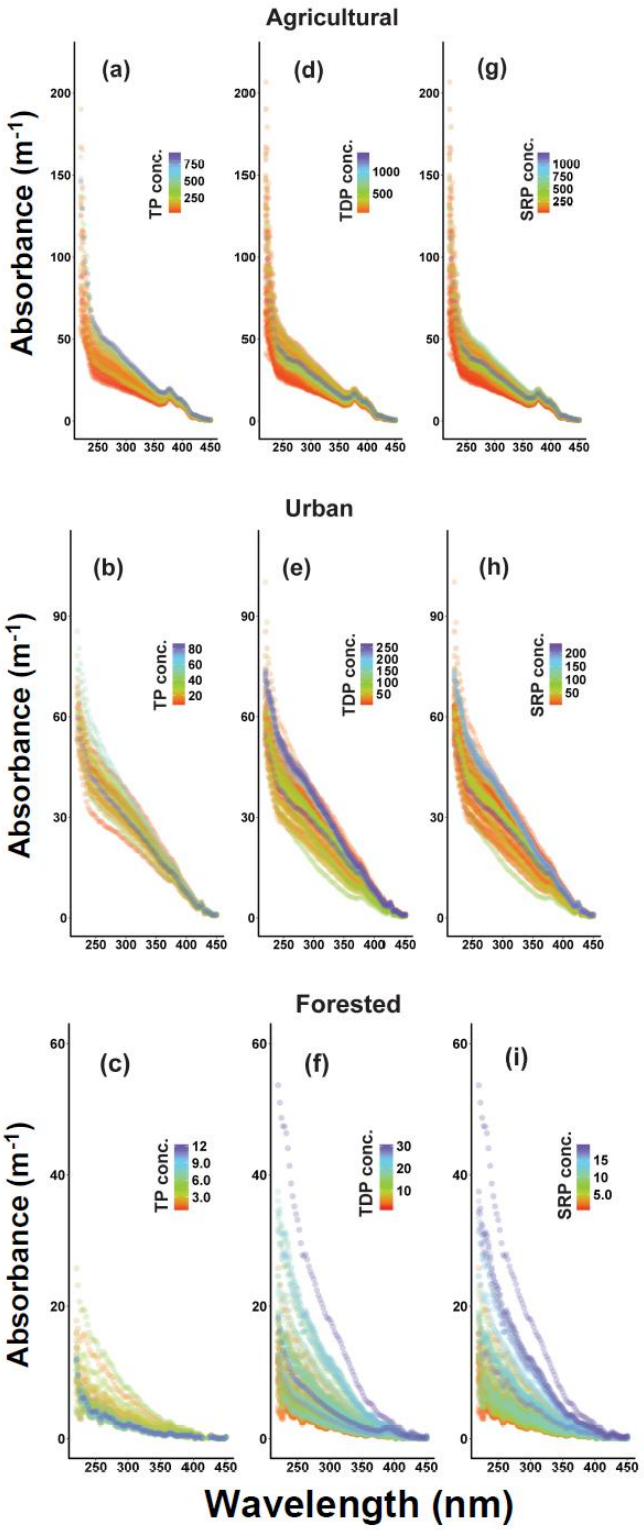

Figure 3.3. Plots of compensated UV-Visible absorbance spectra vs. wavelength of light and corresponding (a-c) TP, (d-f) TDP, and (g-i) SRP concentrations (µg P L^{-1}) in color for agricultural, urban, and forested sites.

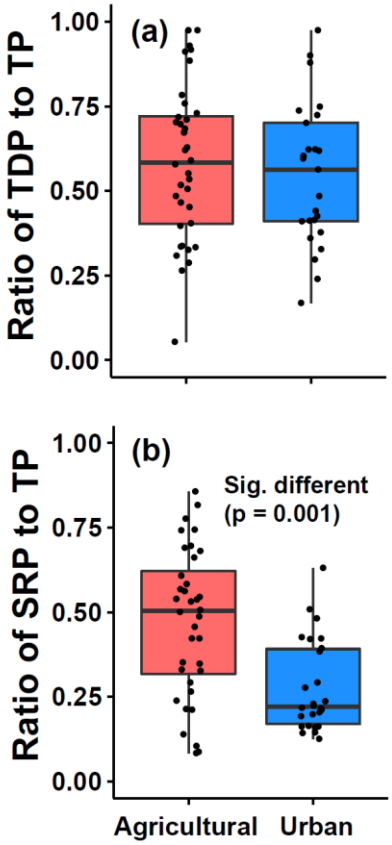

Figure 3.4. Box and whisker plots of the ratios of (a) TDP to TP, and (b) SRP to TP for the agricultural and urban sites in 2016. Data from the forested site is not shown, since concentration differences between different operationally-defined fractions were within the range of analytical error.

Total phosphorus

Predictive models for TP were developed using data for all sites, with ten components (11% of observations). The training sets explained a relatively high proportion of the variance in TP concentration (adj. $R^2 = 0.96$; $p < 0.001$), while correlations from the bootstrap validation method explained approximately three-quarters of the variance in TP concentration (adj. $R^2 = 0.78$; $p < 0.001$) (Figure 3.5). RMSEs were 25 µg P L^{-1} for training sets and 59 µg P L^{-1} for validation sets. The RMSE of the validation set was 75% of the median TP concentration for the agricultural site, and was three and sixteen times greater

than the median TP concentrations at the urban and forested sites, respectively. Separating datasets by site did not improve goodness of fit for predictive models, though it resulted in validation RMSE values that were 74 – 80% of the median TP concentrations at the urban and forested sites (Table 3.3).

When logarithmically transformed discharge and turbidity measurements were used to predict TP concentration using a multiple linear regression model for each site separately, the adjusted coefficients of determination were 0.05, 0.14, and 0.41 for the forested, urban, and agricultural sites, respectively. However, models for the forested and urban sites were not statistically significant and the accuracy for the agricultural site model was lower than for models based on the UV-Visible absorbance spectra (RMSE = 138 µg P L^{-1}).

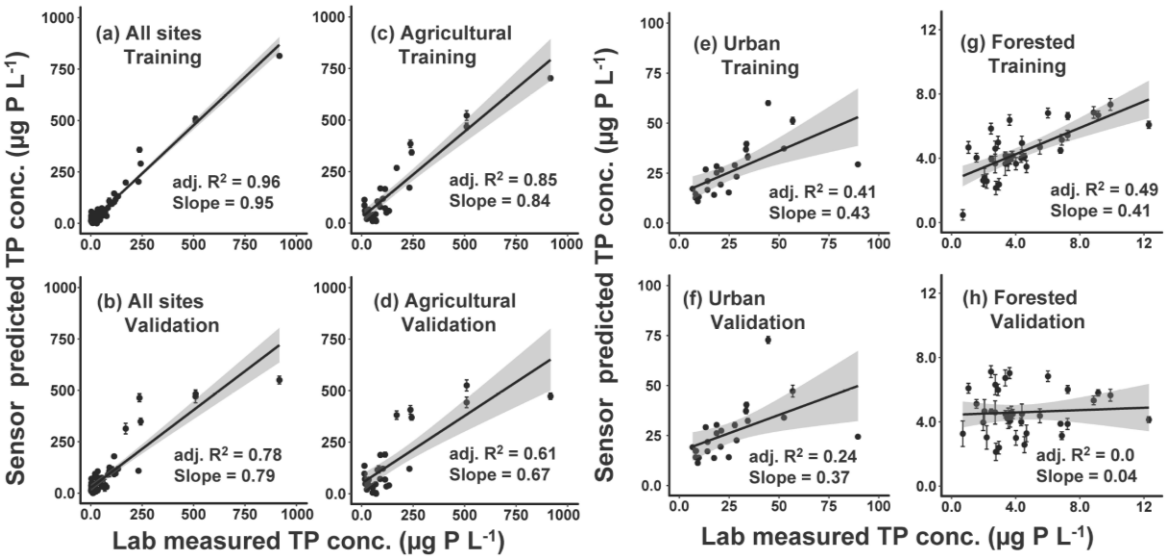

Figure 3.5. Bootstrap TP training and validation plots for (a-b) all combined, (c-d) agricultural, (e-f) urban, and (g-h) forested sites. Correlations were statistically significant ($p < 0.001$) for all but the forested validation sets (h). Shading represents 90% confidence intervals. Error bars represent one standard deviation for the predictions over 1,000 bootstrap iterations. Note that error bars are present for all points but may not be visible and that scales differ among plots.

Table 3.3. Summary of partial least squares regression model results.

Site(s)	Observations	Components	Training adj. R^2	Training RMSE (µg P L^{-1})	Validation adj. R^2	Validation RMSE (µg P L^{-1})
Total phosphorus						
All	90	10	0.96	25	0.78	59
Agricultura	31	4	0.85	70	0.61	115
Urban	24	3	0.41	14	0.24	17
Forested	36	4	0.49	1.9	-0.02	2.8
Total dissolved phosphorus						
All	222	18	0.96	29	0.61	90
Agricultura	70	8	0.88	73	0.56	147
Urban	73	8	0.9	24	0.68	43
Forested	79	9	0.94	1.8	0.72	4.2
Soluble reactive phosphorus						
All	247	18	0.96	23	0.68	68
Agricultura	70	8	0.92	54	0.7	109
Urban	98	10	0.94	13	0.57	36
Forested	79	9	0.95	1.2	0.79	2.4

Total dissolved phosphorus

Predictive models for TDP using data for all sites were developed with 18 components (8% of observations). The training sets explained a relatively high proportion of the variance in TDP concentrations (adj. $R^2 = 0.96$; $p < 0.001$), while correlations from the bootstrap validation method explained nearly two thirds of the variance in TDP concentration (adj. $R^2 = 0.61$; $p < 0.001$) (Table 3.3; Figure 3.6a-b). Separating datasets by site increased accuracy and the proportion of the variance explained in validation sets for the urban site (adj. $R^2 = 0.68$; $p < 0.001$) and the forested site (adj. $R^2 = 0.74$; $p < 0.001$) with eight components, but did not improve validation performance at the agriculture site. Accuracies for these models were limited, however. Validation set RMSEs were greater than the median TDP concentrations for the agricultural and urban sites, and was 55% of the median TDP concentration for the forested site. Plotting residuals in the TDP models by lab measured value, turbidity, and discharge did not reveal discernable patterns in prediction error (Supporting Figure 3.S2).

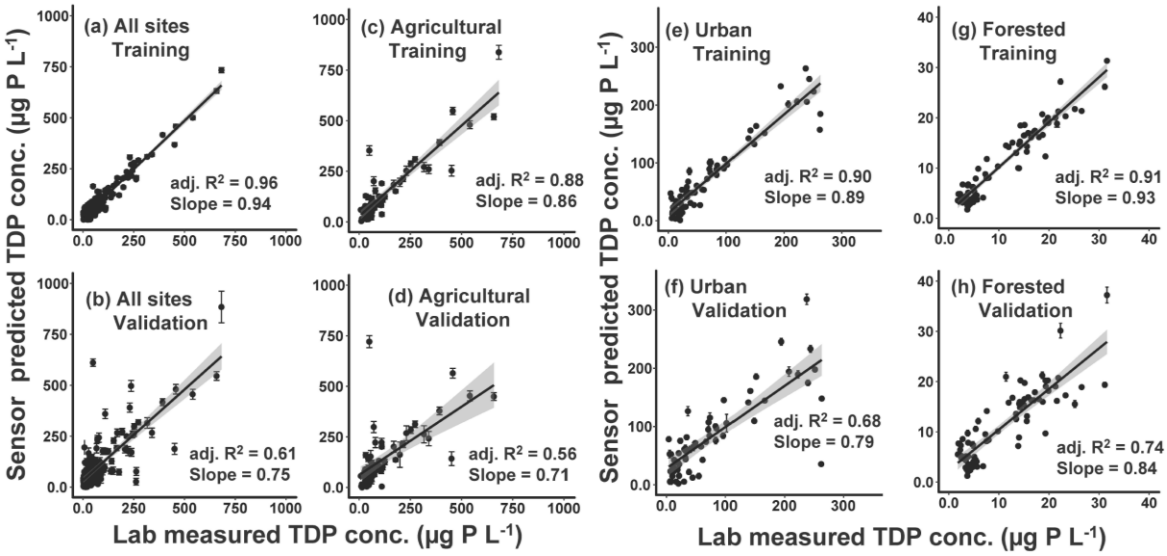

Figure 3.6. Bootstrap TDP training and validation plots for (a-b) all combined, (c-d) agricultural, (e-f) urban, and (g-h) forested sites. All correlations were statistically significant ($p < 0.001$). Shading represents 90% confidence intervals. Error bars represent one standard deviation for the predictions over 1,000 bootstrap iterations. Note that error bars are present for all points but may not be visible and that scales differ among plots.

Soluble reactive phosphorus

Predictive models for SRP using data for all sites were developed with 18 components (7% of observations). The training sets explained a relatively high proportion of the variance in SRP concentration (adj. $R^2 = 0.96$; $p < 0.001$), while correlations from the bootstrap validation method explained approximately two-thirds of the variance in SRP concentration (adj. $R^2 = 0.68$; $p < 0.001$) (Table 3.3; Figure 3.7a-b). Separating datasets by site improved validation accuracy for the urban and forested sites, but did not improve validation accuracy at the agriculture site (Figure 3.7c-h). As with TDP models, no discernable patterns could be found by plotting SRP model residuals by lab measured value, turbidity, and discharge (Supporting Figure 3.S3).

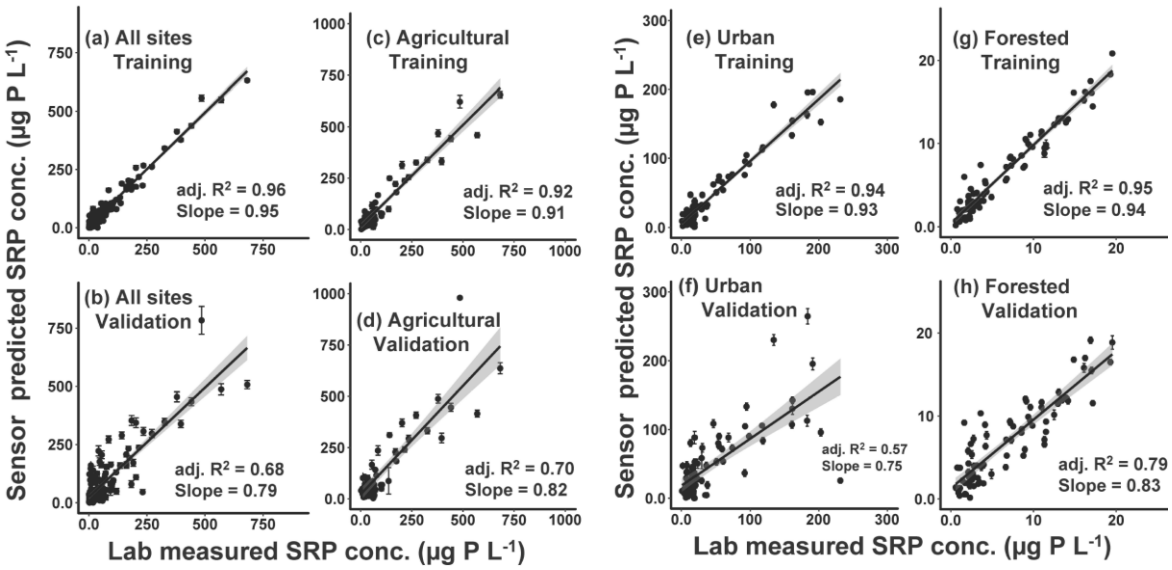

Figure 3.7. Bootstrap SRP training and validation plots for (a-b) all combined, (c-d) agricultural, (e-f) urban, and (g-h) forested sites. All correlations were statistically significant ($p < 0.001$). Shading represents 90% confidence intervals. Error bars represent one standard deviation for the predictions over 1,000 bootstrap iterations. Note that error bars are present for all points but may not be visible and that scales differ among plots.

Discussion

UV-Visible spectra as proxies for phosphorus fraction concentrations

Integrated results from this study suggest that in situ UV-Visible spectrophotometers can concurrently predict the concentration and distribution of the phosphorus fractions (TP, TDP, SRP) at a high frequency and with modest and variable accuracy that may be suitable for some applications (Figure 3.8). Model goodness of fit statistics for these fractions are among the most favorable published for other proxy models. Accuracy limitations remain, however, as RMSE statistics were relatively high compared to median concentration values at our study sites. These analyses indicate that in streams draining watersheds of different primary LULCs and varying seasonal and event conditions, the measured UV-Visible absorbance spectra co-varied with a suite of constituents that varied in proportion with phosphorus fractions of interest. The degree to

which phosphorus fraction concentration correlates with components of the absorbance spectra can be site-specific and may vary by fraction and/or dominant biogeochemical processes and hydrologic pathways within a particular catchment. In the following discussion, we focus on the strengths and limitations of this approach, and make recommendations for how researchers and water resource managers can use this technology for monitoring phosphorus.

Models to predict TP concentrations using all data available explained a relatively high proportion of the variance, but had RMSE values that were higher than the median concentrations at the urban and forested sites (Figure 3.5a-b). Site-specific models had higher accuracy but lower predictive power for the forested site where phosphorus concentrations were lower. We found that models from UV-Visible spectra explained more of the variance in TP concentration than multiple linear regression models using turbidity and logarithmically transformed discharge. The method for TP prediction demonstrated here may be best used in agricultural areas or other sites with elevated TP phosphorus concentrations; these areas may also be where this technology could be most useful for informing management goals.

The UV-Visible spectra were used to predict TDP and SRP concentrations with a greater proportion of variance explained than any other models based on a high-frequency method known to the authors, though RMSE values indicate limited accuracy for low concentrations. The proportion of variance explained suggests that this method is a useful approach to characterize TDP and SRP concentrations, particularly during hot moments for phosphorus transport when concentrations can become elevated (e.g., Underwood et al. 2017). The high bioavailability of dissolved phosphorus fractions makes the unique ability

of this approach to model both the TDP and SRP fractions particularly useful. Furthermore, the necessity of site-specific models suggests that sources and pools of dissolved phosphorus likely differ among sites, and that phosphorus fractions co-vary with different components of the water matrix in contrasting LULCs. In the forested site, organic and inorganic P cycling is primarily from parent material weathering and ecosystem cycling (Likens 2013). While these processes also occur in the urban and agricultural systems, fertilizer amendments and other human activities in urban and agricultural catchments add additional organic and inorganic phosphorus (Daloğlu et al. 2012). Since UV-Visible spectrophotometers have been shown to accurately model dissolved organic carbon concentration (Ruhala and Zarnetske 2017; Vaughan et al. 2017), variance in the phosphorus models may be explained by the presence of organically bound phosphorus. These pools are likely to differ among LULCs, which have very different sources and pools of organic matter (Sickman et al. 2007; Wilson and Xenopoulos 2009). These differences are often more pronounced during storm events, when rapid changes in hydrology cause changes in connectivity of differing source areas (e.g., edge of a row crop field versus a suburban development) to streams.

Site-specific TDP and SRP concentration models performed better than models based on data from all sites for each solute. Therefore, each stream has a distinct relationship between the portion of the aqueous matrix that absorbs UV-Visible light and dissolved phosphorus fraction concentrations (Figure 3.3). The PLSR method tested here relies on the shape of each UV-Visible spectrum curve to determine the phosphorus fraction concentration rather than a narrow wavelength range of absolute absorbance values. This result indicates that the method uses these distinct relationships between

dissolved phosphorus fractions and various aqueous and solid constituents that absorb light across the UV-Visible range that manifest in variable absorbance spectra. While it seems that site-specific calibrations were optimal in this study, it is not yet known whether these relationship differences are due to LULC alone, or whether sites with similar LULCs could have different relationships. Further testing at several agricultural sites, for example, would help determine whether models should be strictly site-specific, or if LULC-specific models could suffice.

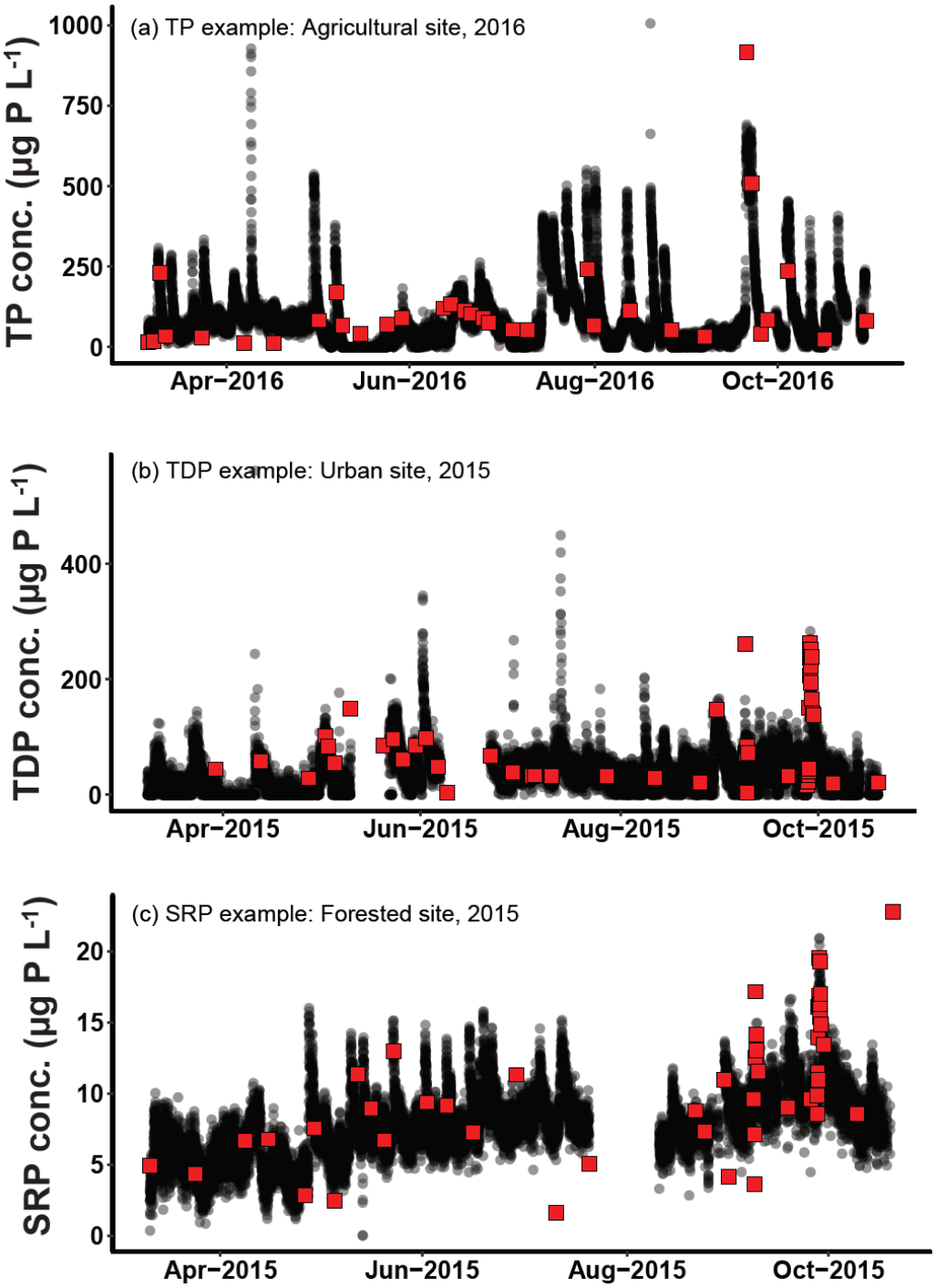

Figure 3.8. Examples of modeled 15-minute phosphorus fraction concentrations using UV-Visible spectra (black dots) and lab-measured values (red squares) for (a) TP at the agricultural site, (b) TDP at the urban site, and (c) SRP at the forested site.

Comparison to other approaches

Several other studies have attempted to relate phosphorus fraction concentrations with parameters that are easier, cheaper, and faster to measure than direct measurement with wet chemistry lab techniques. Other studies showed that roughly 60 – 95% of the variance in TP concentration can be explained by turbidity or discharge, or these variables in combination with other proxy variables (Table 3.4). Results from these studies are derived from models that were based on the predicted data that were used to build the models originally. Thus, their results are most comparable to the training sets reported here, with the difference that 100% of the measurements were commonly used in these other studies, while 85% of the data was used in our training sets. The variance explained in training sets in this study was near or above 90% for all models, exceeding that of most other models reported in the literature. In addition, when we attempted to use logarithmically transformed discharge and turbidity measurements to predict TP concentrations, we found that these models explained a lower proportion of the variance compared with models based on UV-Visible absorbance spectra. Only 55% of the variance in TP concentrations could be explained by a combination of discharge and turbidity, while 96% of the variance in TP concentrations could be explained by the training model derived from the UV-visible spectra. The higher proportion of variance explained by the spectrophotometric proxies compared to the discharge and turbidity proxies may be because our systems are smaller and more susceptible to short-timescale hysteresis-related changes in the relationship between these variables. Other studies that reported a higher proportion of variance in TP concentration explained were in rivers with larger watershed areas than we investigated.

Few studies have investigated the relationship between TDP and SRP concentrations and proxy variables. Underwood et al. (2017) recently used Bayesian linear regression to correlate TDP to discharge and identify operational thresholds where shifts in these relationships occur. More often, TP is predicted using a proxy such as turbidity or discharge, and a percentage of TDP or SRP to TP from a subset of samples is applied uniformly to estimate TDP or SRP loads (e.g., Johnes 2007). We observed that the ratios of lab measured TDP to TP and SRP to TP varied considerably (Figure 3.4), so assuming a constant relationship between these fractions would lead to considerable errors in phosphorus fraction load estimation in the systems studied here. Stubblefield et al. (2007) found no correlation between SRP concentration and turbidity measurements in a subalpine forested stream where the discharge-weighted mean SRP concentration was 8.7% of the TP concentration. Using similar methods to this study, Birgand et al. (2016) found that UV-Visible absorbance explained 89% of the variance in observed SRP concentrations in a eutrophic drinking water reservoir, which is similar to the model results for our SRP model training sets. Besides environmental setting, that study differed from this one in a few notable ways: seven components were used with 36 samples to develop a calibration (~20% rather than ~10% of the number of observations used here), SRP concentrations ranged from 3.5 – 10 µg P L^{-1} (a narrower range than our sites), and no model validation results were reported.

For high-frequency water quality measurements, in situ UV-Visible spectrophotometers have several advantages and some limitations. Advantages include the ability to measure multiple parameters concurrently and rapidly with no reagents, and to deploy sensors for continuous monitoring of baseflow and larger episodic events. There

are field-robust models available that have few moving parts to service. However, limitations include their high cost (currently greater than $15,000 US), which can be prohibitive. As discussed above, UV-Visible spectrophotometer accuracy for phosphorus fraction concentrations and some other analytes may not be acceptable for some applications, particularly at relatively low phosphorus concentrations. For the s::can sensor used here, two further limitations were on-board memory storage and power draw. On-board memory capacity allowed storage of roughly fifteen days of observations at a 15-minute sampling interval. It was a challenge at times to provide necessary power to the sensors when light to our solar panel array was limited by season and/or tree canopy cover.

Instruments that use wet chemistry techniques to measure SRP concentrations directly with the ascorbic acid method in situ have recently become available. For example, the Cycle-PO4 instrument (Wetlabs, Philomath, Oregon, USA) makes direct measurements of SRP concentration with onboard standard checks, which may produce a more accurate estimate of SRP concentration. Results from Cohen et al. (2013) and Sherson et al. (2015) suggest that the Cycle-PO4 measures SRP more accurately than the UV-Visible spectrophotometers tested here at low concentrations. The Systea WIZ probe (Systea, Anagni, Italy) has a similar method to the Cycle-PO4 and also tested relatively well for predicting SRP concentration in recent evaluations (Copetti et al. 2017; Johengen et al. 2017). However, the instruments have several components such as pumps, switches, and filters that are prone to malfunction; they use reagents that generate hazardous waste; and they are more prone to fouling (Pellerin et al. 2016). Both the Cycle-PO4 and the Systea-PO4 have limited capacity to measure elevated SRP concentrations, such as those found in our agricultural and urban sites. The Cycle-PO4 is specified for SRP concentrations of 0 –

300 µg P L^{-1}, and the Systea-PO4 was shown to have limited accuracy for concentrations above 40 µg P L^{-1}. In addition, limited reagent lifetime and sampling frequency precludes the Cycle-PO4 sensor from long-term deployments in remote or rapidly changing environments. The sampling frequency also limits its application for vertical or lateral profiling, where UV-Visible spectrophotometers can be useful. A UV-Visible spectrophotometer is preferable to an in situ wet chemistry instrument if researchers would benefit from concurrent measurements of multiple phosphorus fractions (TP, TDP, and SRP), nitrate (e.g., Rode et al. 2016), dissolved organic carbon (e.g., Ruhala and Zarnetske 2017), and other potential analytes (Birgand et al. 2016) with a single instrument. This concurrent measurement advantage may be the greatest strength of the UV-Visible spectra approach, though building a calibration dataset comes with a considerable cost that will depend on site-specific considerations.

To the authors' knowledge, this study is the first to use a rigorous bootstrap validation technique to investigate how well models predict phosphorus fraction concentrations where lab measured values are not available. Etheridge et al. (2014) and Vaughan et al. (2017) are the only studies we are aware of that test nutrient prediction models by withholding a portion of each calibration dataset (equal to 10% in those studies). This study takes the next step in repeating these validations many times with random observation set selection to reduce sampling error when selecting the 15% to withhold. Our results reflect the expectation that validation models explain less variance than training models (Table 3.3) and demonstrate that method performance may have been inflated by reporting of training sets alone in previous studies. Validation sets are standard for larger-scale models in other scientific disciplines such as global climate general circulation

models (Chervin 1981; Flato et al. 2013), though the exercise is valuable when using a model to predict a dependent variable at any scale. We recommend that future studies using high-frequency water quality sensors perform model validation with bootstrapping to more rigorously estimate uncertainty for new analyte concentration predictions. This approach is particularly useful when developing models that rely on absorbance spectra derived from in situ spectrophotometers to project the concentration of solutes such as dissolved phosphorus fractions that do not directly absorb light in the UV-Visible spectrum.

Table 3.4. Summary of selected studies that related phosphorus fraction concentration to other water quality parameters. (*) indicates that model validation was performed but not reported.

Location	Setting	Watershed Landscape / Characterization	Watershed area or water body size (km^2)	Proxy variable(s)	Statistical method	Observations	R^2	Accuracy	Reference
Total phosphorus									
Chesapeake Bay Watershed, USA	River	Agricultural	136	ln(Discharge), Water temperature	Multiple linear regression	38	0.82	Mallows' Cp = 2.71	Hyer et al. (2016)
Chesapeake Bay Watershed, USA	River	Agricultural	95	ln(Discharge), Dissolved oxygen, ln(Turbidity)	Multiple linear regression	32	0.96	Mallows' Cp = 2.09	Hyer et al. (2016)
North Carolina, USA	Brackish marsh	Constructed brackish marsh, agricultural	NA	UV-Visible absorbance	Partial least squares regression	NA	0.73*	Root mean square error = 23 µg P L^{-1}	Etheridge et al. (2014)
Vermont USA and Quebec, CA	River	Agricultural	92	Acoustic doppler profiler backscatter	Linear regression with log-transformed data and Duan correction	317	0.67	NA	Schuett and Bowden (2014)
Lake Tahoe Basin, California USA	River	Subalpine forest	25	Turbidity	Linear regression	117	0.62	NA	Stubblefield et al. (2007)
Lake Tahoe Basin, California USA	River	Subalpine forest	29.5	Turbidity	Linear regression	51	0.83	NA	Stubblefield et al. (2007)
Australia	River	Mixed landscape	5000	Turbidity	Linear regression	NA	0.9	NA	Grayson et al. (1996)
Soluble reactive phosphorus (PO_4^3)									
West Virginia, USA	Reservoir	Eutrophic drinking water reservoir	0.12	UV-Visible absorbance	Partial least squares regression	36	0.89	2X Residual St Error = 1.08 µg P L^{-1}	Birgand et al. (2016)
North Carolina, USA	Brackish marsh	Constructed brackish marsh, agricultural	NA	UV-Visible absorbance	Partial least squares regression	NA	0.66*	Root mean square error = 10 µg p L^{-1}	Etheridge et al. (2014)
Lake Tahoe basin, California USA	River	Subalpine forest	25	Turbidity	Linear regression	NA	No correlation	NA	Stubblefield et al. (2007)

Implications for application in watershed monitoring

The advantage of high-frequency water quality data is generally two-fold: it can reveal short-timescale effects previously invisible to researchers, and it can aid in more accurate load estimation. Because our results indicate that UV-Visible absorbance is generally sensitive to changes in phosphorus fraction concentrations (models had acceptable coefficients of determination), but had relatively low accuracy (models had relatively high RMSE values), we suggest that in situ spectrophotometers are best applied to understanding short-timescale phosphorus dynamics, especially in systems with relatively high phosphorus fraction concentrations. Depending on site-specific model performance, this technology may be suited to provide valuable, yet possibly semi-quantitative information about phosphorus fraction dynamics during storms or diel cycles, illuminating potential nutrient sources and biological processes. This technique could be especially informative when developed in combination with models for other useful parameters (e.g., nitrate, dissolved organic carbon).

The relatively high RMSE value to median concentrations ratios found here suggest that phosphorus load estimates calculated with this method may have substantial uncertainty, unless site-specific models elsewhere show improved accuracy. Optimal models to predict TP concentration had RMSE values that were 75 – 80% of median TP concentrations. This ratio is an indication of the level of uncertainty a load estimate may have, though actual uncertainty would depend on annual hydrologic conditions and site-specific factors.

Conclusions and recommendations

We have shown that UV-Visible spectra collected by in situ spectrophotometric sensors can be used to simultaneously predict TP, TDP and SRP concentrations in many situations. For our sites, the ratios of TDP to TP and SRP to TP varied notably, so that if high-frequency measurements of TDP and SRP were of main interest in a study or management decision, the use of in situ spectrophotometers is clearly warranted. Since these sensors also measure turbidity, and nitrate and DOC concentrations, there is the capability to measure diverse chemical constituents concurrently. If estimates for these other parameters are a primary monitoring goal, phosphorus fractions model development could be a relatively low-risk, low-cost addition.

This technology is best suited to sites with elevated TP concentrations if TP concentrations are the primary fraction of interest. We recommend that all models be checked to determine if separating data by site improves or weakens model performance. When using the PLSR method, we recommend following Mevik et al. (2015) to use the number of components equal to ~10% of observations, as a higher percentage of components can lead to over-parameterization. Over-parameterization may lead to more favorable training model statistics, but also to weaker validation model performance statistics, and noisier and less accurate time series prediction. The success of this method may be influenced by the number and variety of grab samples that can be attained, analyzed, and incorporated into prediction models. We recommend that users of this technology take care to obtain grab samples as close in time and space to the sensor measurement as possible to obtain a reliable calibration.

There has been significant effort to create "global calibrations" or calibration "libraries" for various predictive proxies and predicted constituents (e.g., Shepherd and Walsh 2002). Although this type of effort is beyond the scope of this study, our results indicate that that common models for phosphorus fraction concentrations were not preferable to site-specific models for three sites with variable LULC. Future work is necessary to rule out the possibility of a more extensive library to explain a greater amount of variance across multiple types of sites and water matrices.

The number of samples needed to develop useful models to predict phosphorus fraction concentrations using UV-Visible spectra will be dependent on many factors that will likely be site-specific. For example, the greater the variability in the concentration at the monitoring location, the more samples will be needed to form an adequate predictive model. Although evaluating these criteria will depend on subjective expert opinion, researcher geochemical/hydrologic intuition, and available observational data prior to sensor deployment, we suggest that an adequate PLSR model must meet the following conditions:

1. The PLSR model has a validated accuracy and goodness of fit that is acceptable for the application
2. The number of observations is equal to or greater than 10 times the number of components in the PLSR model
3. The range of the sampled concentrations is approximately equal to the range of concentrations likely to occur at the site

4. Samples were collected during times representative of the various conditions at the site (e.g., baseflow, rising and falling limbs of storms, seasonal conditions, nutrient amendment schedules, biological hot moments, see Figure 3.2)

As use of in situ optical spectrophotometers increases, researchers and managers will gain a better picture of their performance to measure several water quality parameters. In the foreseeable future, this type of instrumentation may extend our ability to monitor critical nutrients at times and places that would be difficult to sample in any other way. Results presented in this work also indicate that with further study in a more diverse set of environments, phosphorus fractions may be monitored with increasing reliability to inform watershed management goals.

Acknowledgements

This material is based upon work supported by the National Science Foundation under VTEPSCoR Grant No. EPS-1101317, EPS-IIA1330446, and OIA 1556770, the Vermont Water Resources and Lakes Studies Center (project 2016VT80B) which is part of the National Institutes for Water Resources, and NSF EAR Grant No. 1561014 to AWS. We thank Ryan Sleeper, Saul Blocher, Joshua Benes, JohnFranco Saraceno, François Birgand, and two anonymous reviewers for their helpful contributions to this work. Any opinions, findings, and conclusions, or recommendations expressed in this material are those of the authors and do not necessarily reflect the views of the National Science Foundation, Vermont EPSCoR, or any other supporting organization. Any use of trade, firm, or product names is for descriptive purposes only and does not imply endorsement by the U.S. Government.

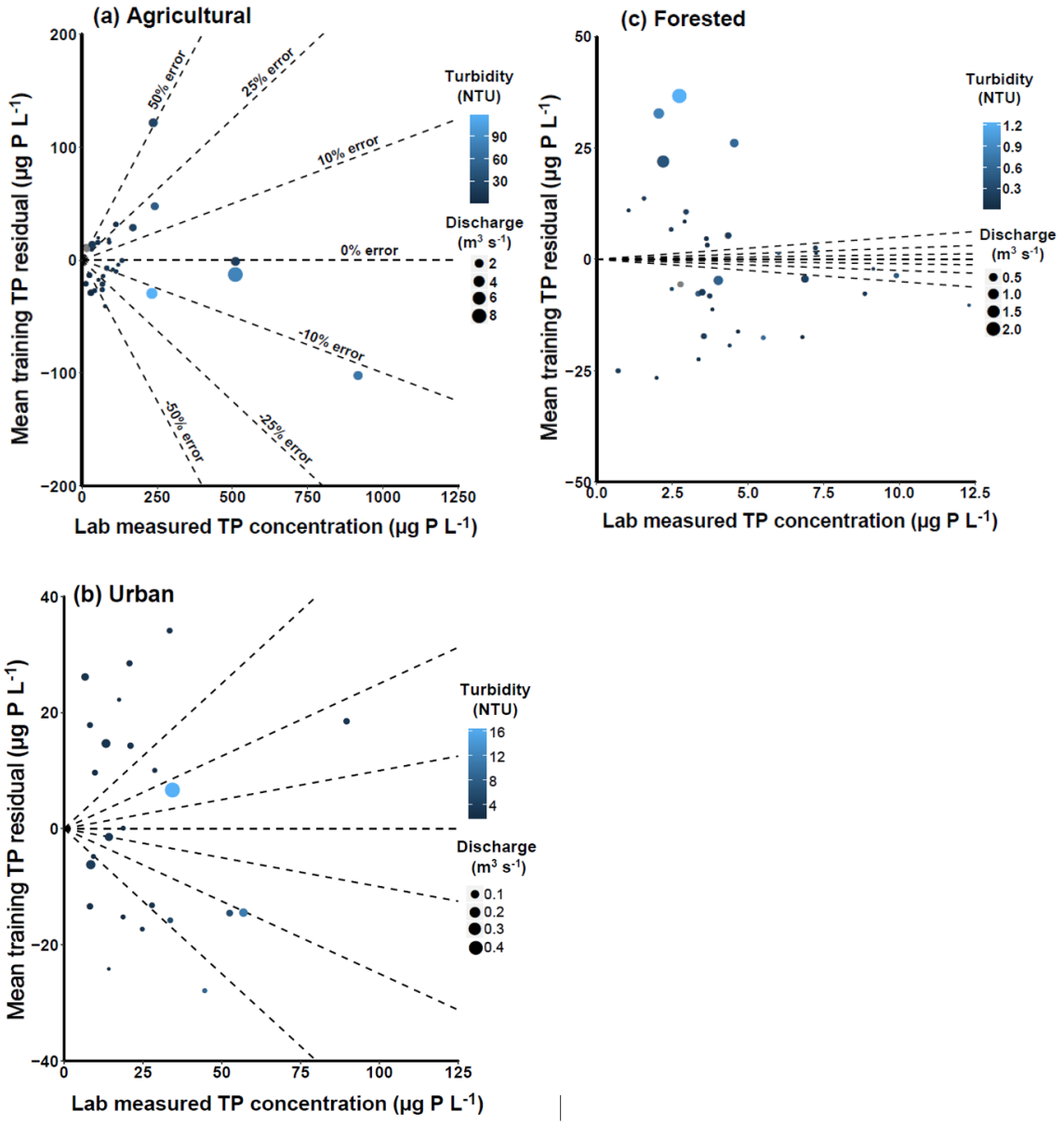

Supporting Figure 3.S1. Plots of mean training TP residual versus lab measured TP concentration using validation sets for (a) agricultural, (b) urban, and (c) forested sites. Points are colored by turbidity values and sized by discharge value. Dotted lines represent ± 50, 25, 10, and 0% prediction error. Grey points are used where turbidity values are not available.

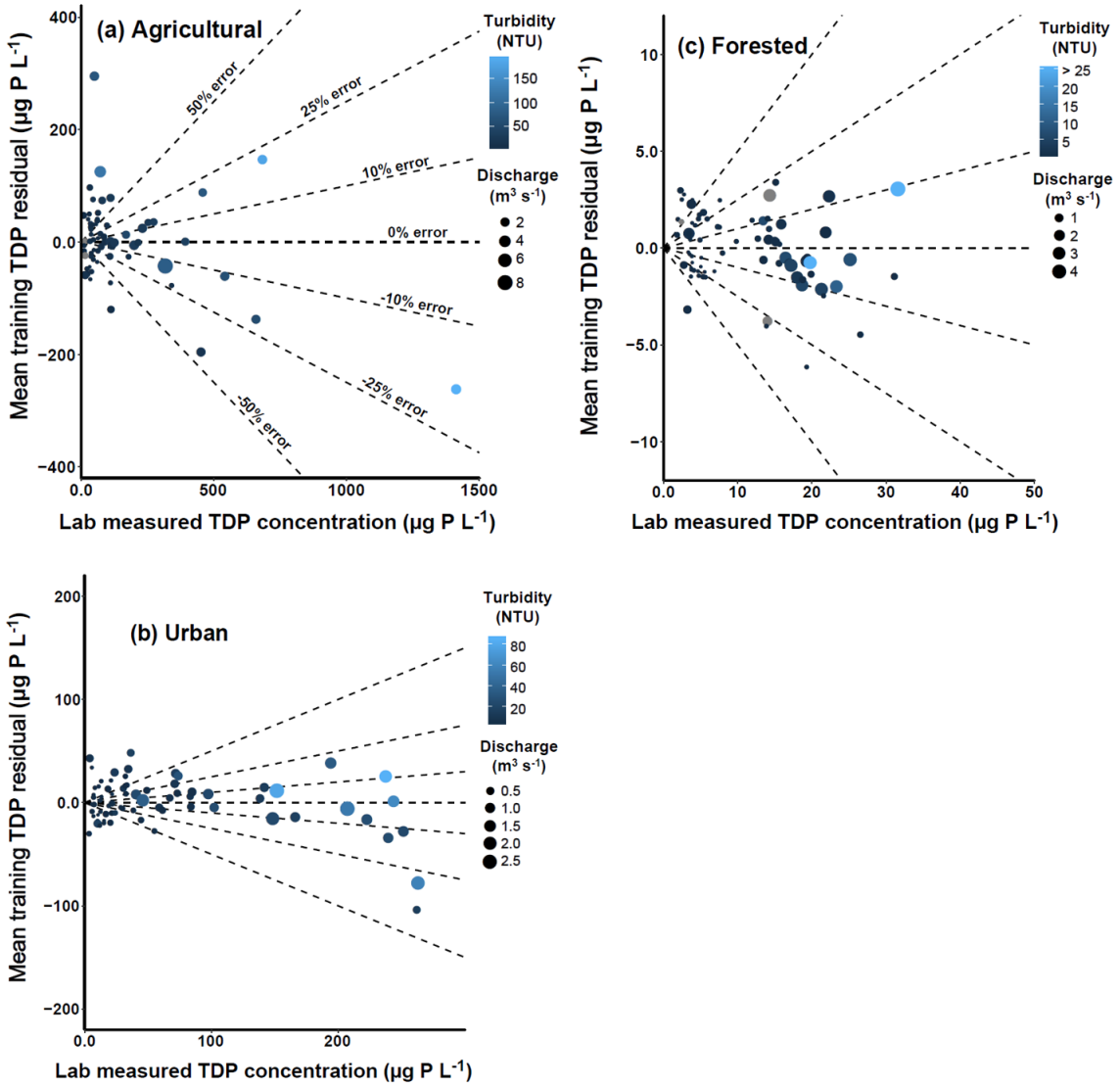

Supporting Figure 3.S2. Plots of mean training TDP residual versus lab measured TDP concentration using validation sets for (a) agricultural, (b) urban, and (c) forested sites. Points are colored by turbidity values and sized by discharge value. Dotted lines represent ± 50, 25, 10, and 0% prediction error. Grey points are used where turbidity values are not available.

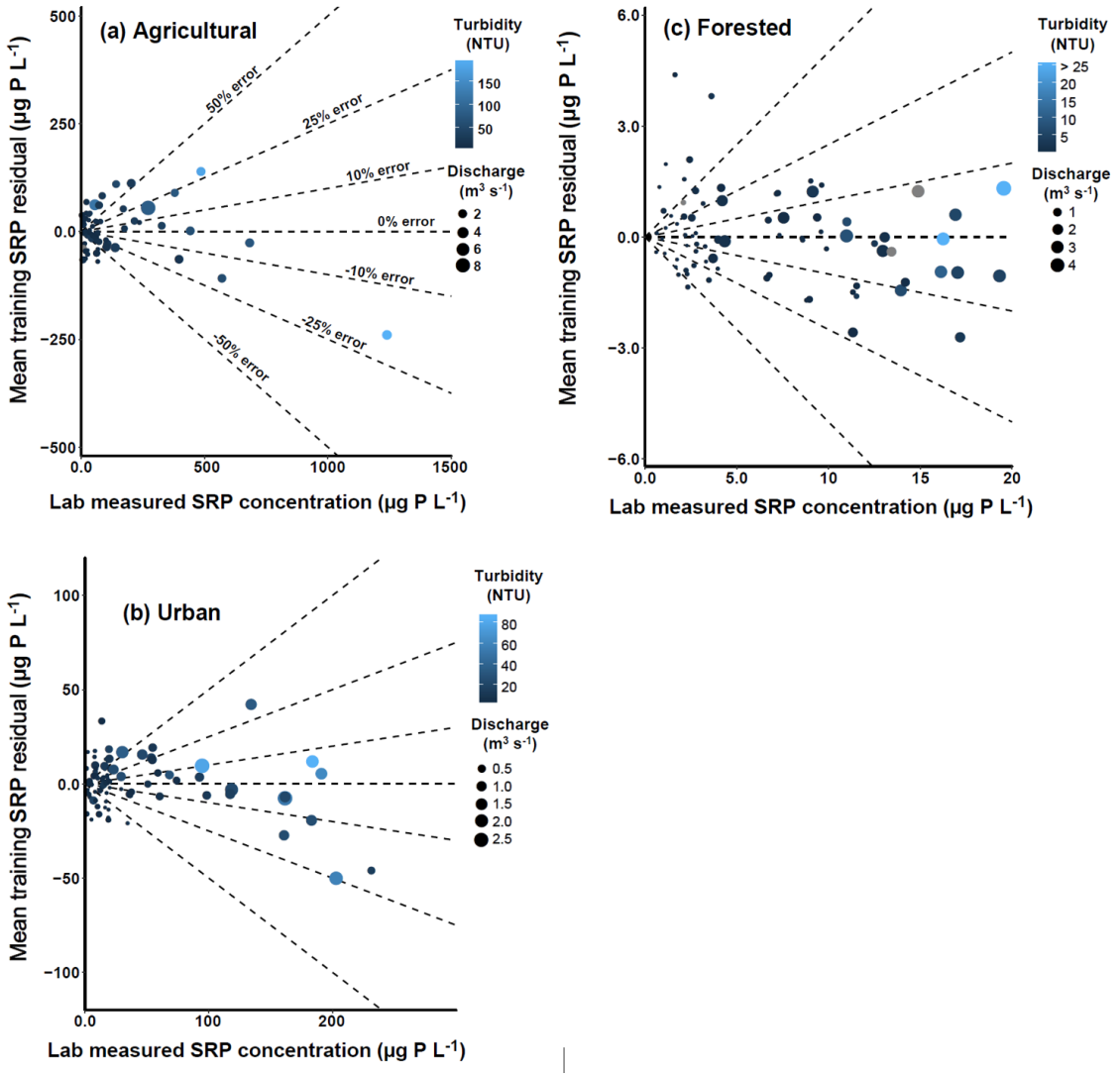

Supporting Figure 3.S3. Plots of mean training SRP residual versus lab measured SRP concentration using validation sets for (a) agricultural, (b) urban, and (c) forested sites. Points are colored by turbidity values and sized by discharge value. Dotted lines represent ± 50, 25, 10, and 0% prediction error. Grey points are shown where turbidity values are not available.

References

Aber, J. D., 1997, Why Don't We Believe the Models?: Bulletin of the Ecological Society of America, v. 78, no. 3, p. 232-233.

Avagyan, A., Runkle, B. R. K., and Kutzbach, L., 2014, Application of high-resolution spectral absorbance measurements to determine dissolved organic carbon concentration in remote areas: Journal of Hydrology, v. 517, p. 435-446.

Bieroza, M. Z., and Heathwaite, A. L., 2015, Seasonal variation in phosphorus concentration–discharge hysteresis inferred from high-frequency in situ monitoring: Journal of Hydrology, v. 524, p. 333-347.

Birgand, F., Aveni-Deforge, K., Smith, B., Maxwell, B., Horstman, M., Gerling, A. B., and Carey, C. C., 2016, First report of a novel multiplexer pumping system coupled to a water quality probe to collect high temporal frequency in situ water chemistry measurements at multiple sites: Limnology and Oceanography: Methods, v. 14, no. 12, p. 767-783.

Carey, R. O., Wollheim, W. M., Mulukutla, G. K., and Mineau, M. M., 2014, Characterizing storm-event nitrate fluxes in a fifth order suburbanizing watershed using in situ sensors: Environmental Science & Technology, v. 48, no. 14, p. 7756-7765.

Carpenter, S. R., Caraco, N. F., Correll, D. L., Howarth, R. W., Sharpley, A. N., and Smith, V. H., 1998, Nonpoint pollution of surface waters with phosphorus and nitrogen: Ecological Applications, v. 8, no. 3, p. 559-568.

Chervin, R. M., 1981, On the Comparison of Observed and GCM Simulated Climate Ensembles: Journal of the Atmospheric Sciences, v. 38, no. 5, p. 885-901.

Cohen, M. J., Kurz, M. J., Heffernan, J. B., Martin, J. B., Douglass, R. L., Foster, C. R., and Thomas, R. G., 2013, Diel phosphorus variation and the stoichiometry of ecosystem metabolism in a large spring-fed river: Ecological Monographs, v. 83, no. 2, p. 155-176.

Conley, D. J., Paerl, H. W., Howarth, R. W., Boesch, D. F., Seitzinger, S. P., Havens, K. E., Lancelot, C., and Likens, G. E., 2009, Controlling Eutrophication: Nitrogen and Phosphorus: Science, v. 323, no. 5917, p. 1014-1015.

Copetti, D., Valsecchi, L., Capodaglio, A. G., and Tartari, G., 2017, Direct measurement of nutrient concentrations in freshwaters with a miniaturized analytical probe: evaluation and validation: Environmental Monitoring and Assessment, v. 189, no. 4, p. 144.

Correll, D. L., 1998, The Role of Phosphorus in the Eutrophication of Receiving Waters: A Review: Journal of Environmental Quality, v. 27, p. 261-266.

Correll, D. L., Jordan, T. E., and Weller, D. E., 1999, Transport of nitrogen and phosphorus from rhode river watersheds during storm events: Water Resources Research, v. 35, no. 8, p. 2513-2521.

Daloğlu, I., Cho, K. H., and Scavia, D., 2012, Evaluating Causes of Trends in Long-Term Dissolved Reactive Phosphorus Loads to Lake Erie: Environmental Science & Technology, v. 46, no. 19, p. 10660-10666.

Dhillon, G. S., and Inamdar, S., 2013, Extreme storms and changes in particulate and dissolved organic carbon in runoff: Entering uncharted waters?: Geophysical Research Letters, v. 40, no. 7.

Djodjic, F., Montas, H., Shirmohammadi, A., Bergström, L., and Ulén, B., 2002, A Decision Support System for Phosphorus Management at a Watershed Scale: Journal of Environmental Quality, v. 31, no. 3, p. 937-945.

Dodd, R. J., and Sharpley, A. N., 2016, Conservation practice effectiveness and adoption: unintended consequences and implications for sustainable phosphorus management: Nutrient Cycling in Agroecosystems, v. 104, no. 3, p. 373-392.

Etheridge, J. R., Birgand, F., Osborne, J. A., Osburn, C. L., Burchell, M. R., II, and Irving, J., 2014, Using in situ ultraviolet-visual spectroscopy to measure nitrogen, carbon, phosphorus, and suspended solids concentrations at a high frequency in a brackish tidal marsh: Limnology and Oceanography-Methods, v. 12, p. 10-22.

Fichot, C. G., and Benner, R., 2011, A novel method to estimate DOC concentrations from CDOM absorption coefficients in coastal waters: Geophysical Research Letters, v. 38.

Flato, G., Marotzke, J., Abiodun, B., Braconnot, P., Chou, S. C., Collins, W., Cox, P., Driouech, F., Emori, S., Eyring, V., Forest, C., Gleckler, P., Guilyardi, E., Jakob, C., Kattsov, V., Reason, C., and Rummukainen, M., 2013, Evaluation of Climate Models, *in* Stocker, T. F., Qin, D., Plattner, G.-K., Tignor, M., Allen, S. K., Boschung, J., Nauels, A., Xia, Y., Bex, V., and Midgley, P. M., eds., Climate Change 2013: The Physical Science Basis. Contribution of Working Group I to the Fifth Assessment Report of the Intergovernmental Panel on Climate Change: Cambridge, United Kingdom and New York, NY, USA, Cambridge University Press, p. 741–866.

Giles, C. D., Lee, L. G., Cade-Menun, B. J., Hill, J. E., Isles, P. D. F., Schroth, A. W., and Druschel, G. K., 2015, Characterization of Organic Phosphorus Form and Bioavailability in Lake Sediments using 31P Nuclear Magnetic Resonance and Enzymatic Hydrolysis: Journal of Environmental Quality, v. 44, p. 882-894.

Grayson, R. B., Finlayson, B. L., Gippel, C. J., and Hart, B. T., 1996, The Potential of Field Turbidity Measurements for the Computation of Total Phosphorus and Suspended Solids Loads: Journal of Environmental Management, v. 47, no. 3, p. 257-267.

Guo, Y., Markus, M., and Demissie, M., 2002, Uncertainty of nitrate-N load computations for agricultural watersheds: Water Resources Research, v. 38, no. 10, p. 3-1-3-12.

Heffernan, J. B., and Cohen, M. J., 2010, Direct and indirect coupling of primary production and diel nitrate dynamics in a subtropical spring-fed river: Limnology and Oceanography, v. 55, no. 2, p. 677-688.

Hirsch, R. M., Moyer, D. L., and Archfield, S. A., 2010, Weighted Regressions on Time, Discharge, and Season (WRTDS), with an Application to Chesapeake Bay River Inputs1: JAWRA Journal of the American Water Resources Association, v. 46, no. 5, p. 857-880.

Hyer, K. E., Denver, J. M., Langland, M. J., Webber, J. S., Böhlke, J. K., Hively, W. D., and Clune, J. W., 2016, Spatial and temporal variation of stream chemistry associated with contrasting geology and land-use patterns in the Chesapeake Bay watershed—Summary of results from Smith Creek, Virginia; Upper Chester River, Maryland; Conewago Creek, Pennsylvania; and Difficult Run, Virginia, 2010–2013, 2016-5093.

Isles, P. D. F., Xu, Y., Stockwell, J. D., and Schroth, A. W., 2017, Climate-driven changes in energy and mass inputs systematically alter nutrient concentration and stoichiometry in deep and shallow regions of Lake Champlain: Biogeochemistry, v. 133, no. 2, p. 201-217.

Jarvie, H. P., Johnson, L. T., Sharpley, A. N., Smith, D. R., Baker, D. B., Bruulsema, T. W., and Confesor, R., 2017, Increased Soluble Phosphorus Loads to Lake Erie: Unintended Consequences of Conservation Practices?: J Environ Qual, v. 46, no. 1, p. 123-132.

Johengen, T., Purcell, H., Tamburri, M., Loewensteiner, D., Smith, G. J., Schar, D., McManus, M., Walker, G., and Stauffer, B., 2017, Performance verification statment for Systea WIZ Probe phosphoate analyzer: Alliance for Coastal Technologies.

Johnes, P. J., 2007, Uncertainties in annual riverine phosphorus load estimation: Impact of load estimation methodology, sampling frequency, baseflow index and catchment population density: Journal of Hydrology, v. 332, no. 1, p. 241-258.

Jordan, P., Arnscheidt, A., Mcgrogan, H., and Mccormick, S., 2007, Characterising phosphorus transfers in rural catchments using a continuous bank-side analyser: Hydrology and Earth System Sciences Discussions, v. 11, no. 1, p. 372-381.

Joung, D., Leduc, M., Ramcharitar, B., Xu, Y., Isles, P. D. F., Stockwell, J. D., Druschel, G. K., Manley, T., and Schroth, A. W., 2017, Winter weather and lake-watershed physical configuration drive phosphorus, iron, and manganese dynamics in water and sediment of ice-covered lakes: Limnology and Oceanography, v. 62, no. 4, p. 1620-1635.

Kane, D. D., Conroy, J. D., Peter Richards, R., Baker, D. B., and Culver, D. A., 2014, Re-eutrophication of Lake Erie: Correlations between tributary nutrient loads and phytoplankton biomass: Journal of Great Lakes Research, v. 40, no. 3, p. 496-501.

Kruskal, W. H., and Wallis, W. A., 1952, Use of ranks in one-criterion variance analysis: Journal of the American Statistical Association, v. 47, no. 260, p. 583-621.

Langergraber, G., Fleischmann, N., and Hofstadter, F., 2003, A multivariate calibration procedure for UV/VIS spectrometric quantification of organic matter and nitrate in wastewater: Water Science and Technology, v. 47, no. 2, p. 63-71.

Likens, G. E., 2013, Biogeochemistry of a forested ecosystem, New York, NY, Springer, 208 p.:

McCarty, G. W., Reeves, J. B., Reeves, V. B., Follett, R. F., and Kimble, J. M., 2002, Mid-Infrared and Near-Infrared Diffuse Reflectance Spectroscopy for Soil Carbon Measurement: Soil Science Society of America Journal, v. 66, no. 2, p. 640-646.

Medalie, L., 2016, Concentration, flux, and trend estimates with uncertainty for nutrients, chloride, and total suspended solids in tributaries of Lake Champlain, 1990–2014, 2016-1200.

Mevik, B., Wehrens, R., and Liland, K. H., 2015, pls: Partial Least Squares and Principal Component Regression.

Musolff, A., Fleckenstein, J. H., Rao, P. S. C., and Jawitz, J. W., 2017, Emergent archetype patterns of coupled hydrologic and biogeochemical responses in catchments: Geophysical Research Letters, v. 44, no. 9, p. 4143-4151.

Ohtani, K., 2000, Bootstrapping R2 and adjusted R2 in regression analysis: Economic Modelling, v. 17, no. 4, p. 473-483.

Parsons, T. R., Maita, Y., and Lalli, C. M., 1984, 1.6 - Determination of Phosphate, A Manual of Chemical & Biological Methods for Seawater Analysis: Amsterdam, Pergamon, p. 22-25.

Pellerin, B. A., Bergamaschi, B. A., Gilliom, R. J., Crawford, C. G., Saraceno, J., Frederick, C. P., Downing, B. D., and Murphy, J. C., 2014, Mississippi River Nitrate Loads from High Frequency Sensor Measurements and Regression-Based Load Estimation: Environmental Science & Technology, v. 48, no. 21, p. 12612-12619.

Pellerin, B. A., Saraceno, J. F., Shanley, J. B., Sebestyen, S. D., Aiken, G. R., Wollheim, W. M., and Bergamaschi, B. A., 2012, Taking the pulse of snowmelt: in situ sensors reveal seasonal, event and diurnal patterns of nitrate and dissolved organic matter variability in an upland forest stream: Biogeochemistry, v. 108, no. 1, p. 183-198.

Pellerin, B. A., Stauffer, B. A., Young, D. A., Sullivan, D. J., Bricker, S. B., Walbridge, M. R., Clyde, G. A., and Shaw, D. M., 2016, Emerging Tools for Continuous Nutrient Monitoring Networks: Sensors Advancing Science and Water Resources Protection: JAWRA Journal of the American Water Resources Association, v. 52, no. 4, p. 993-1008.

R Core Team, 2015, R: A language and environment for statistical computing.: Vienna, Austria, R Foundation for Statistical Computing.

Rieger, L., Langergraber, G., and Siegrist, H., 2006, Uncertainties of spectral in situ measurements in wastewater using different calibration approaches: Water Science and Technology, v. 53, no. 12, p. 187-197.

Rode, M., Wade, A. J., Cohen, M. J., Hensley, R. T., Bowes, M. J., Kirchner, J. W., Arhonditsis, G. B., Jordan, P., Kronvang, B., Halliday, S. J., Skeffington, R. A., Rozemeijer, J. C., Aubert, A. H., Rinke, K., and Jomaa, S., 2016, Sensors in the

Stream: The High-Frequency Wave of the Present: Environmental Science & Technology, v. 50, no. 19, p. 10297-10307.

Rosenberg, B. D., and Schroth, A. W., 2017, Coupling of reactive riverine phosphorus and iron species during hot transport moments: impacts of land cover and seasonality: Biogeochemistry, v. 132, no. 1, p. 103-122.

Ruhala, S. S., and Zarnetske, J. P., 2017, Using in-situ optical sensors to study dissolved organic carbon dynamics of streams and watersheds: A review: Science of The Total Environment, v. 575, p. 713-723.

Sakamoto, C. M., Johnson, K. S., and Coletti, L. J., 2009, Improved algorithm for the computation of nitrate concentrations in seawater using an in situ ultraviolet spectrophotometer: Limnology and Oceanography-Methods, v. 7, p. 132-143.

Saraceno, J. F., Pellerin, B. A., Downing, B. D., Boss, E., Bachand, P. A. M., and Bergamaschi, B. A., 2009, High-frequency in situ optical measurements during a storm event: Assessing relationships between dissolved organic matter, sediment concentrations, and hydrologic processes: Journal of Geophysical Research-Biogeosciences, v. 114.

Schroth, A. W., Giles, C. D., Isles, P. D. F., Xu, Y., Perzan, Z., and Druschel, G. K., 2015, Dynamic Coupling of Iron, Manganese, and Phosphorus Behavior in Water and Sediment of Shallow Ice-Covered Eutrophic Lakes: Environmental Science & Technology, v. 49, no. 16, p. 9758-9767.

Schuett, E., and Bowden, W. B., 2014, Use of Acoustic Doppler Current Profiler Data to Estimate Sediment and Total Phosphorus Loads to Lake Champlain from the Rock River: Final Report to the Vermont Agency of Natural Resources.

Sharpley, A. N., Chapra, S. C., Wedepohl, R., Sims, J. T., Daniel, T. C., and Reddy, K. R., 1994, Managing Agricultural Phosphorus for Protection of Surface Waters: Issues and Options: Journal of Environmental Quality, v. 23, no. 3, p. 437-451.

Sharpley, A. N., Kleinman, P. J. A., Heathwaite, A. L., Gburek, W. J., Folmar, G. J., and Schmidt, J. P., 2008, Phosphorus Loss from an Agricultural Watershed as a Function of Storm Size All rights reserved. No part of this periodical may be reproduced or transmitted in any form or by any means, electronic or mechanical, including photocopying, recording, or any information storage and retrieval system, without permission in writing from the publisher: Journal of Environmental Quality, v. 37, no. 2, p. 362-368.

Shepherd, K. D., and Walsh, M. G., 2002, Development of Reflectance Spectral Libraries for Characterization of Soil Properties: Soil Science Society of America Journal, v. 66, no. 3, p. 988-998.

Sherson, L. R., Van Horn, D. J., Gomez-Velez, J. D., Crossey, L. J., and Dahm, C. N., 2015, Nutrient dynamics in an alpine headwater stream: use of continuous water quality sensors to examine responses to wildfire and precipitation events: Hydrological Processes, v. 29, no. 14, p. 3193-3207.

Sickman, J. O., Zanoli, M. J., and Mann, H. L., 2007, Effects of urbanization on organic carbon loads in the Sacramento River, California: Water Resources Research, v. 43, no. 11, p. W11422.

Stubblefield, A. P., Reuter, J. E., Dahlgren, R. A., and Goldman, C. R., 2007, Use of turbidometry to characterize suspended sediment and phosphorus fluxes in the Lake Tahoe basin, California, USA: Hydrological Processes, v. 21, no. 3, p. 281-291.

Stumpf, R. P., Wynne, T. T., Baker, D. B., and Fahnenstiel, G. L., 2012, Interannual Variability of Cyanobacterial Blooms in Lake Erie: PLoS ONE, v. 7, no. 8, p. e42444.

Stutter, M., Dawson, J. J. C., Glendell, M., Napier, F., Potts, J. M., Sample, J., Vinten, A., and Watson, H., 2017, Evaluating the use of in-situ turbidity measurements to quantify fluvial sediment and phosphorus concentrations and fluxes in agricultural streams: Science of The Total Environment, v. 607-608, p. 391-402.

Underwood, K. L., Rizzo, D. M., Schroth, A. W., and Dewoolkar, M. M., 2017, Evaluating Spatial Variability in Sediment and Phosphorus Concentration-Discharge Relationships Using Bayesian Inference and Self-Organizing Maps: Water Resources Research, v. 53, no. 12, p. 10293-10316.

Vaughan, M. C. H., Bowden, W. B., Shanley, J. B., Vermilyea, A., Sleeper, R., Gold, A. J., Pradhanang, S. M., Inamdar, S. P., Levia, D. F., Andres, A. S., Birgand, F., and Schroth, A. W., 2017, High-frequency dissolved organic carbon and nitrate measurements reveal differences in storm hysteresis and loading in relation to land cover and seasonality: Water Resources Research, v. 53, no. 7, p. 5345-5363.

Viscarra Rossel, R. A., Walvoort, D. J. J., McBratney, A. B., Janik, L. J., and Skjemstad, J. O., 2006, Visible, near infrared, mid infrared or combined diffuse reflectance spectroscopy for simultaneous assessment of various soil properties: Geoderma, v. 131, no. 1, p. 59-75.

Wilson, H. F., and Xenopoulos, M. A., 2009, Effects of agricultural land use on the composition of fluvial dissolved organic matter: Nature Geosci, v. 2, no. 1, p. 37-41.

CHAPTER 4. SHINING LIGHT ON THE STORM: IN-STREAM OPTICS REVEAL HYSTERESIS OF DISSOLVED ORGANIC MATTER CHARACTER

Abstract

The quantity and character of dissolved organic matter (DOM) can change rapidly during storm events, affecting key biogeochemical processes, carbon bioavailability, metal pollutant transport, and disinfectant byproduct formation during drinking water treatment. We used in situ ultraviolet-visible spectrophotometers to concurrently measure dissolved organic carbon (DOC) concentration and spectral slope ratio, a proxy for DOM molecular weight. Measurements were made at 15-minute intervals over three years in three streams draining primarily agricultural, urban, and forested watersheds. We describe storm event dynamics by calculating hysteresis indices for DOC concentration and spectral slope ratio for 220 storms and present a novel analytical framework that compares and interprets these metrics together. DOC concentration and spectral slope ratio differed significantly among sites, and storm DOM dynamics were remarkably variable at each site and among the three sites. Distinct patterns emerged for storm DOM dynamics depending on land use / land cover (LULC) of each watershed. In agricultural and forested streams, DOC concentration increased later in the storm cycle, and spectral slope ratio dynamics indicate that this delayed flux was of relatively higher molecular weight material compared to the beginning of each storm. In contrast, DOM character during storms at the urban stream generally shifted to lower molecular weight while DOC concentration increased on the falling limb, indicating either the introduction of lower molecular weight DOM, the exhaustion of a higher molecular weight DOM sources, or a combination of these factors. We show that the combination of high-frequency DOM character and quantity metrics have the potential

to provide new insight into short-timescale DOM dynamics and can reveal previously unknown effects of LULC on the chemical nature, source, and timing of DOM export during storms.

Introduction

Dissolved organic matter (DOM) is an important component of a river's load that is central to many biogeochemical cycles and pressing water quality issues. DOM is a major source of terrestrial carbon to receiving waterbodies (Prairie 2008), attenuates ultraviolet radiation that is harmful to microorganisms (Bukaveckas and Robbins-Forbes 2000; Morris et al. 1995), and affects metal pollutant transport and bioavailability (Driscoll et al. 1988; Ravichandran 2004). DOM plays a key role in stream metabolism in temperate forests (Roberts et al. 2007), and its availability can limit denitrification, a microbial process that is central to maintaining water quality standards (Sobczak et al. 2003). DOM also has been identified as the primary cause of harmful trihalomethane disinfectant byproduct formation during drinking water treatment (Chow et al. 2007; Kraus et al. 2008; Nguyen et al. 2013; Reckhow and Singer 1990). Globally, DOM is a significant source of CO_2 emissions into the atmosphere (Battin et al. 2009; Cole et al. 2007; Weyhenmeyer et al. 2012), and is a link between upland carbon sources and the ocean carbon budgets (Ludwig et al. 1996; Raymond and Bauer 2001). Determining the composition of DOM has been an active area of research and is critical to understanding the role of DOM in these cycles and processes (Hedges et al. 2000; Jaffé et al. 2012; Sleighter et al. 2010).

The natural and anthropogenically influenced pool of DOM in surface waters can contain thousands of compounds (Kim et al. 2006; Sleighter and Hatcher 2007; Stubbins et al. 2014). The "character" of DOM refers to the specific composition of this pool, which

can differ over several temporal and spatial scales and among various ecosystem types (e.g., Jaffé et al. 2008). Human influences and land use / land cover (LULC) can strongly influence DOM character during times of both baseflow and storm events (e.g., Dalzell et al. 2005; Wilson and Xenopoulos 2008). A "size-reactivity continuum" has been shown to exist between molecular weight of the DOM pool and bioreactivity, where bioreactivity increases from small to large size, and from old to fresh diagenetic state in oceans (Amon and Benner 1996) and lakes (Kellerman 2015). Bioreactivity has been shown to vary according to other intrinsic factors of the DOM pool, such as aromaticity, oxidation state, and elemental ratios (Kellerman et al. 2015). DOM character can also have important implications for water quality management, since waters with elevated dissolved organic carbon (DOC) concentrations and high aromatic content have higher formation potential of disinfectant byproducts (Kitis et al. 2001; Reckhow and Singer 1990). Optical metrics have been used to characterize DOM pools for decades, and recent advances in optical metrics have led to improved quantitative metric-based understanding of DOM character.

DOM can be characterized and classified into groups or types, depending on structural, ultraviolet-visible absorbance, and fluorescent properties. Fluorescent properties of aquatic DOM have been used to classify DOM as protein-like, humic-like, soil fulvic acid content, and by potential watershed sources (e.g., Stedmon et al. 2003). Similarly, absorbance properties of DOM in ultraviolet-visible spectrum can indicate the humic and aromatic content of the DOM pool (Del Vecchio and Blough 2004; Weishaar et al. 2003). Some of these properties can be semi-quantitatively described using one or more calculated proxy variables or indices such as the spectral slope and spectral slope ratio (Helms et al. 2008), fluorescence index (Stubbins et al. 2014), and specific ultra-violet absorbance

(Weishaar et al. 2003). The spectral slope can vary independently from DOC concentration (Brown 1977), and has been used to characterize the relative abundance of fulvic acids and humic acids in marine waters (Carder et al. 1989; Hayase and Tsubota 1985). Spectral slope and spectral slope ratio are generally inversely proportional to the molecular weight of the DOM pool, and increase following photodegradation (Helms et al. 2008; Kellerman et al. 2015). In addition, the spectral slope has been shown to correlate with the percentage of terrigenous DOM in river-influenced coastal areas in the Gulf of Mexico (Fichot and Benner 2012). While there has been significant effort to characterize DOM from different sources, less is known about the role that storms play in the transport of organic material of variable character, and how LULC and DOM provenance affect these intra- and inter-storm dynamics.

In situ optical water quality sensors can provide rapid and accurate measurements of DOC concentration, which has led to a greater understanding of the important role that storms play in biogeochemical cycles (e.g., Rode et al. 2016; Ruhala and Zarnetske 2017). These instruments have been used to better quantify relationships between solute concentration and stream discharge, which can change over multiple timescales from storm-event (e.g., Saraceno et al. 2009) to decadal (Kuk-Hyun and Scott 2018). Quantifying a change in the solute-discharge relationship, or "hysteresis," can improve understanding of solute transport pathways and active source areas (e.g. Chanat et al. 2002; Evans and Davies 1998; House and Warwick 1998). To date, in situ optical sensors have been used to characterize hysteresis for DOC concentration (e.g., Buffam et al. 2001; Hood et al. 2006; Vaughan et al. 2017), but there is also the potential to characterize hysteresis in DOM character using proxies derived from ultraviolet-visible absorbance spectra. While

solute or particulate concentration hysteresis indicates the proximity of that constituent to the point of measurement in space and/or time, measuring hysteresis of the spectral slope ratio would quantify the relative shift(s) in DOM character in a stream during a storm event. Furthermore, combining this information with hysteresis of DOC concentration would show how the DOM quantity and character change during storms, which may provide insight regarding potential DOM sources, hydrologic pathways, and better characterization of DOM pools entering receiving waters.

Here, we explore the utility of combining DOM quantity and character hysteresis metrics to better understand the dynamic nature of DOM pools exported from different LULCs during storm events, and how this relates to changing hydrologic flow paths and DOM source and supply. To do this, we measured spectral slope ratio and DOC concentration at 15-minute intervals in three well-characterized streams draining watersheds with different LULCs over three years. We developed a novel analytical framework representing storm event-based hysteresis dynamics for both DOM quantity and character. We then used this framework to demonstrate insights regarding the relationship between DOM quantity and character during and among storms, how this is influenced by LULC, and what this may reveal about variability in DOM provenance and potential bioavailability and reactivity following storms.

Study areas

Study sites are located in the Lake Champlain Basin, Vermont in the northeastern US (Figure 4.1). Watershed characteristics and dynamics of carbon and nutrients at these sites have been well-characterized in previous work (Rosenberg and Schroth 2017; Vaughan et al. 2017). LULC in the Hungerford Brook watershed is primarily agricultural,

including dairy, row crops, hay, and pasture. Potash Brook is situated near the city of Burlington, Vermont's densest population center. Its watershed is primarily characterized by urban and suburban development (54%), though there is some agricultural (29%) and forest cover (11%). The Wade Brook watershed is primarily forested (95%) and is situated on the western slope of Vermont's Green Mountain chain. Hungerford Brook and Wade Brook drain to the Missisquoi River and Lake Champlain; Potash Brook drains directly to Lake Champlain.

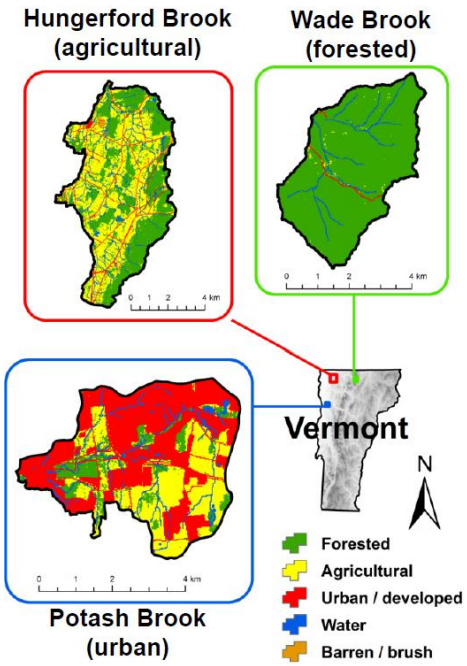

Figure 4.1. Map showing location and land use / land cover of the three study areas.

Methods

In situ measurements

We used s::can Spectrolyser ultraviolet-visible spectrophotometers (s::can Messtechnik GmbH, Vienna, Austria) in each stream, deployed from June 2014 through December 2016 for spring, summer, and fall seasons and removed them each winter season

due to stream ice cover. The sensors were housed in PVC tubing for protection during high flows, were solar powered for autonomous operation, and transmitted data in real time through a cellular data network. The spectrophotometers measured light absorbance at wavelengths ranging from 220 to 750 nm at 2.5 nm increments and were programmed to take measurements every 15 minutes. Sensor measurement windows were automatically cleaned before each measurement with a silicone wiper and cleaned manually in the field at least every two weeks using pure ethanol. Raw absorbance spectra were corrected for turbidity by fitting a third-order polynomial in the visible range of the spectrum, extrapolating into the UV portion, and then subtracting the extrapolated absorbance from the raw spectrum (Avagyan et al. 2014; Langergraber et al. 2003).

Discharge data were acquired from a U.S. Geological Survey gaging station where available (Hungerford Brook Station 04293900), or calculated from stage-discharge rating curves developed with velocity-area calculations (Turnipseed and Sauer 2010) and/or salt dilution (Moore 2005). Stage was measured at a 15-minute timestep using atmospherically compensated pressure transducers.

Dissolved organic carbon concentration calibration

Manual grab samples were collected during baseflow and storms to calibrate in situ absorbance spectrophotometer measurements to laboratory measurements. Collection occurred on at least a bi-weekly schedule, with additional samples taken during times of sensor maintenance and during storm events when possible in order to characterize the full range of hydrologic and chemical stream conditions. A total of 326 grab samples were analyzed for DOC concentration over the duration of this study. Each sample was filtered using rinsed glass fiber GF/F filters (nominal pore size of 0.7 μm) into new HDPE bottles.

Samples were stored on ice in the field, then stored in a cooler at 2 ºC until analysis. Laboratory DOC concentration measurements were made using a Shimadzu TOC-L analyzer using the combustion catalytic oxidation method.

The ultraviolet-visible spectra were used to develop site-specific partial least squares regression models to predict DOC concentration. Models were created with the pls package in R (Mevik et al. 2015; R Core Team 2015), and were used to generate time series predictions of DOC concentration at 15-minute intervals for all available ultraviolet-visible spectra measurements. Each model incorporated a number of components equal to a maximum of approximately 10% of the observations as recommended by Mevik et al. (2015). A more detailed account of this method can be found in Vaughan et al. (2017). For each site, the models predicted at least 95% of the variance in laboratory-measured DOC concentration, and standard errors ranged from ±0.025 mg C L^{-1} at the forested site to ±0.045 mg L^{-1} at the agricultural site. We compared differences in DOC concentration among the three sites using the non-parametric Kruskal-Wallis test (Kruskal and Wallis 1952), and compared differences in the variance in DOC concentration among sites using Levene's test (Levene 1960).

Spectral slope ratio calculation

Spectral slope was calculated using turbidity-corrected ultraviolet-visible spectra, following the equation

$$a_\lambda = a_{\lambda_{ref}} e^{-S(\lambda - \lambda_{ref})}, \quad (1)$$

where a is the Naperian absorption coefficient (m^{-1}) (Aiken 2014), λ is wavelength (nm), λ_{ref} is the reference wavelength (285 nm), and S is the best fit spectral slope (nm^{-1}). The spectral slope ratio (Sr; Helms et al. 2008) was then found by dividing the spectral slope

of absorbance between 275 – 295 nm by the spectral slope of absorbance between 350 – 400 nm. This method was applied to all turbidity-corrected ultraviolet-visible absorbance spectra, collected at 15-minute intervals over the three years of monitoring. As with DOC concentration, differences in the medians and variances of spectral slope ratio among sites were compared with the Kruskal-Wallis and Levene's tests, respectively.

Calculation of flushing and hysteresis indices

A detailed description for the storm flushing index and hysteresis index calculation used here is provided in Vaughan et al. (2017). These methods are adapted from Butturini et al. (2008) and Lloyd et al. (2016), respectively. We calculated these indices for both DOC concentration and spectral slope ratio for all storms. The application of these indices to spectral slope ratio is a new approach that adds valuable information. Both indices are based on normalized discharge and parameter values (DOC concentration or spectral slope ratio):

$$Q_{i,norm} = \frac{Q_i - Q_{min}}{Q_{max} - Q_{min}} \quad (2)$$

$$C_{i,norm} = \frac{C_i - C_{min}}{C_{max} - C_{min}}, \quad (3)$$

where Q_i and C_i are the discharge and parameter values at timestep i, Q_{max} and Q_{min} are the maximum and minimum discharge values in the storm, and C_{max} and C_{min} are the maximum and minimum parameter values in the storm. This normalization method transforms discharge and parameter values from 0 to 1, where 0 indicates the lowest value during the storm, and 1 represents the highest value during the storm.

The storm flushing index is equal to the normalized parameter value at peak storm discharge minus the normalized parameter value at the initial storm discharge. Values of

this index range from -1 to 1, where negative values indicate a decrease in parameter value on the rising limb, positive values indicate an increase in parameter value on the rising limb, and the distance from zero indicates the magnitude of this difference.

The hysteresis index at each discharge interval HI_j was determined by the equation:

$$HI_j = C_{j,rising} - C_{j,falling}\ , \tag{4}$$

where C_j is found by linear regression of $C_{i,norm}$ at 1% intervals of $Q_{i,norm}$ on both the rising and falling limbs at interval *j* using two adjacent measurements. An overall hysteresis index for each storm event was determined by calculating the mean of all HI_j values for the storm. Values of this index also range from of -1 to 1, where negative values indicate anti-clockwise hysteresis, positive values indicate clockwise hysteresis, and the magnitude of *HI* indicates the normalized difference between the rising and falling limbs.

Novel analytical framework

The storm DOC concentration flushing index characterizes the relative change in DOM quantity on the rising limb, whereas the DOC concentration storm hysteresis index describes the difference in DOM quantity on the falling limb relative to the rising limb. We also calculated these indices for a proxy of DOM character (spectral slope ratio). To the knowledge of the authors, hysteresis of spectral slope ratio has not yet been calculated with high-frequency data. Plots of both spectral slope ratio flushing index versus DOC concentration flushing index and spectral slope ratio hysteresis index versus DOC concentration hysteresis index create four-quadrant Cartesian spaces where the domain of all values is -1 to 1. This framework offers a novel, concise, and information-rich view of storm DOM dynamics. The interpretations herein are predicated on the assumption and demonstrated result that spectral slope ratio is inversely proportional to the molecular

weight of the sampled DOM pool (Fichot and Benner 2012; Helms et al. 2008). We did not have the opportunity to characterize DOM pool using other tools such as excitation-emission matrix spectroscopy or high-resolution liquid chromatographic separation and tandem mass spectrometry (e.g., Petras et al. 2017).

Plotting storm flushing index of spectral slope ratio versus storm flushing index of DOC concentration creates four quadrants that represent distinct storm DOM quantity and character dynamics at times before the peak discharge (rising limb) (Figure 4.2a). Storms that fall in quadrant (I) of this space have positive flushing indices for both spectral slope ratio and DOC concentration, indicating rising limbs where DOM molecular weight decreases and DOC concentration increases. Because concentration increases while DOM character changes, this indicates increased mobilization of lower molecular weight DOM on the rising limb. Storms situated in quadrant (II) demonstrate a decrease in DOM molecular weight and DOC concentration on rising limbs. Because concentration is decreasing, this may indicate an exhaustion of proximal DOM sources with relatively higher molecular weight. Storms in quadrant (III) have negative flushing index values for both spectral slope ratio and DOC concentration, suggesting an exhaustion of proximal, relatively lower molecular weight DOM sources while discharge increases. Finally, for storm events plotting in quadrant (IV), both DOM molecular weight and DOC concentration increase on the rising limbs, suggesting the mobilization of relatively high molecular weight DOM to the stream as discharge increases. The coordinate location for each storm indicates the magnitude of the dynamic described in each quadrant.

Plots of storm hysteresis index of spectral slope ratio versus storm hysteresis index of DOC concentration provides further context to interpret potential sources of DOM based

on shifts in quantity and character metrics from rising limb to falling limb during a storm (Figure 4.2b). Storms that fall in quadrant (I) may reflect a source of proximal, relatively low molecular weight DOM that was depleted later in the storm, since the falling limb is relatively lower than the rising limb in DOC concentration, but higher in DOM molecular weight. Quadrant (II) storms may be characterized by increased mobilization of relatively higher molecular weight DOM from more distal DOM sources delivered later in the storm cycle. In quadrant (III), storms may deliver more distal sources of relatively lower molecular weight DOM that passes the point of measurement later in the storm cycle, as storm hysteresis indices for both spectral slope ratio and DOC concentration are negative. Finally, storms that fall in quadrant (IV) may deliver proximal sources of relatively higher molecular weight DOM that is depleted during the storm, since the DOM character shifts to lower molecular weight while the DOC concentration is lower on the falling limb.

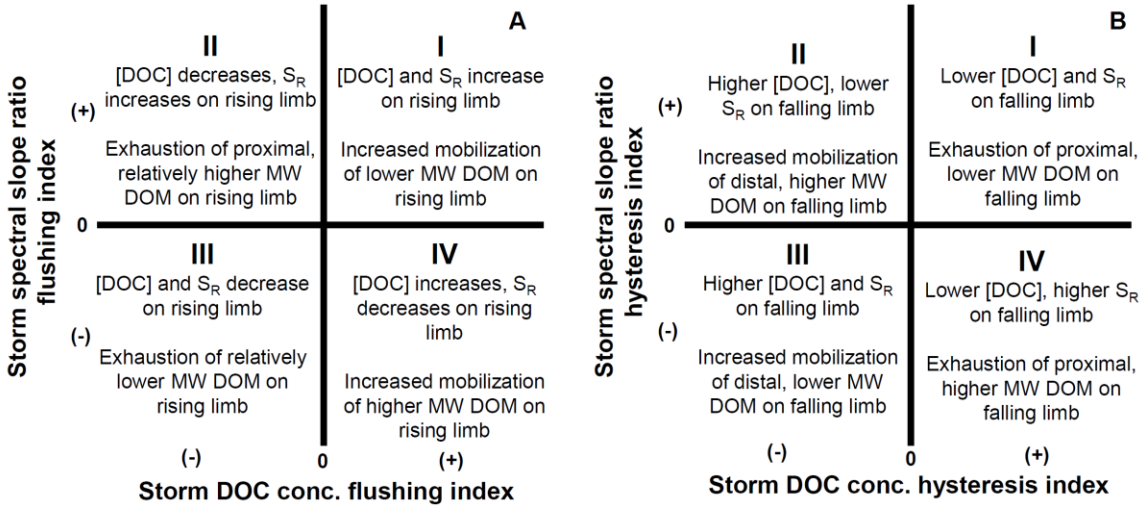

Figure 4.2. Interpretations for each quadrant in the Cartesian plotting spaces of (a) storm spectral slope ratio (SR) flushing index versus storm DOC concentration ([DOC]) flushing index and (b) storm spectral slope ratio hysteresis index versus storm DOC concentration hysteresis index.

Results

DOC concentration and spectral slope ratio

Over the three years of monitoring, approximately 160,000 concurrent measurements were made of DOC concentration and spectral slope ratio at the three study sites (Figure 4.3). DOC concentrations were significantly different among sites, as determined by the Kruskal-Wallis test ($p < 0.001$), and the variance in DOC concentration was also significantly different among sites, as determined by Levene's test ($p < 0.001$) (Figure 4.4a). DOC concentrations were generally higher and had highest variance at the agricultural site (median = 6.8 mg C L^{-1}; variance = 3.5 [mg C L^{-1}]^2), followed by the urban site (median = 4.6 mg C L^{-1}; variance = 1.2 [mg C L^{-1}]^2). DOC concentrations were generally lowest and had the lowest variance at the forested site (median = 1.8 mg C L^{-1}; variance = 0.6 [mg C L^{-1}]^2).

Spectral slope ratio values were significantly different among sites ($p < 0.001$), and the variance in spectral slope ratio values was also significantly different among sites ($p < 0.001$) (Figure 4.4b). Spectral slope ratios were generally lowest at the urban site (median = 0.60), indicating the presence of relatively higher molecular weight DOM relative to the other two sites. Variance in spectral slope ratio was also lowest at the urban site (variance = 0.0045). The agricultural site had generally higher spectral slope ratios than the urban site, and a variance in spectral slope ratios that was an order of magnitude greater than the urban site (median = 1.0; variance = 0.033). The spectral slope ratios were generally highest at the forested site, where variance in spectral slope ratio was also highest by an order of magnitude over the agricultural site, and two orders of magnitude over the urban site

(median = 1.2; variance = 0.15). The relationship between spectral slope ratio and DOC concentration varied for each site, and among the three sites (Figure 4.4c).

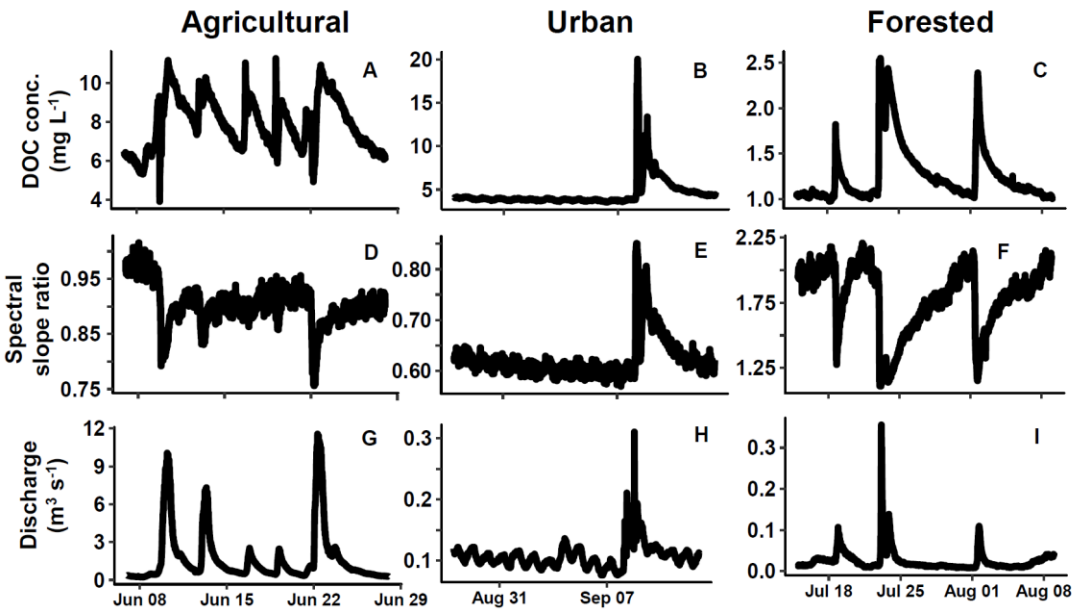

Figure 4.3. Example time series plots of (a-c) DOC concentration, (d-f) spectral slope ratio, and (g-i) discharge at the agricultural (left), urban (center), and forested (right) sites.

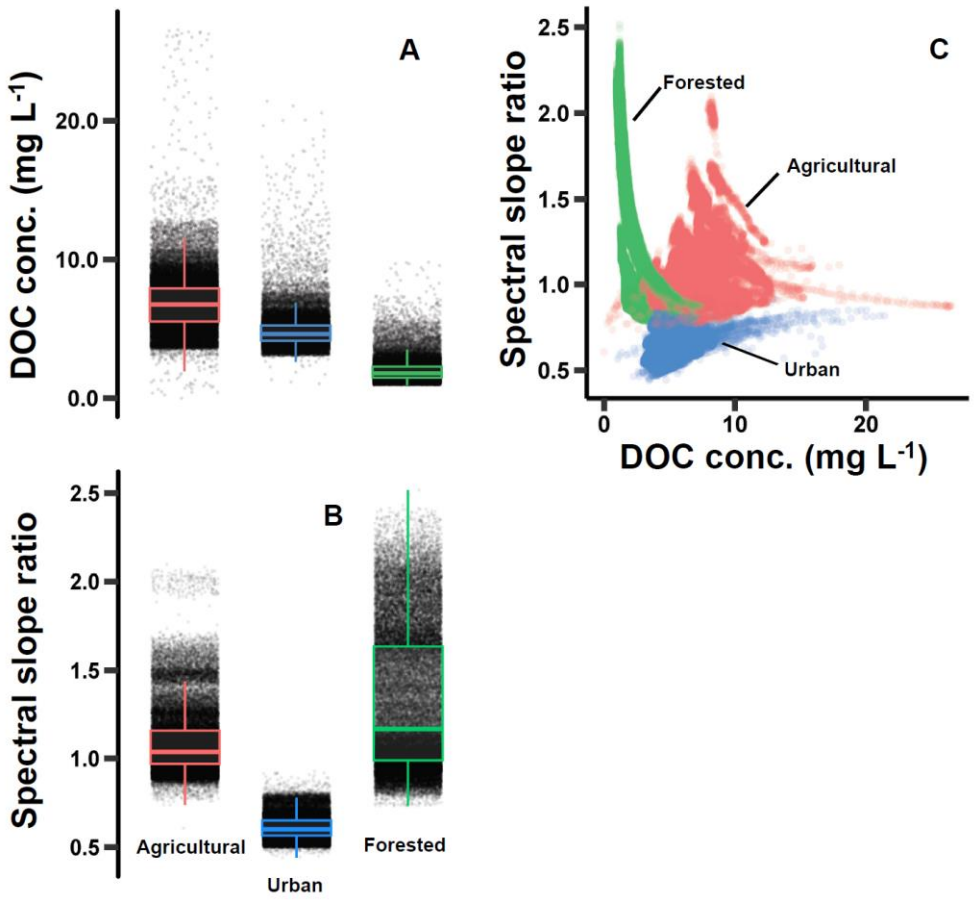

Figure 4.4. Values and box and whisker plots of sensor-measured (a) DOC concentration and (b) spectral slope ratio at the three sites; (c) sensor-measured spectral slope ratio vs. sensor-predicted DOC concentration at the three sites. For all plots, each point represents a single measurement and all measurements taken over the three-year monitoring period are included.

Storm dynamics of dissolved organic matter

We measured DOC concentration and spectral slope ratio at 15-minute intervals for a total of 220 storms at the three sites during the three years of monitoring, comprising a total of approximately 38,000 concurrent measurements during storm events. Plots of the mean and range of spectral slope ratio for each storm versus the storm volume-weighted DOC concentration (calculated as the ratio of DOC mass flux to water flux) illustrate the differences in these relationships among sites (Figure 4.5). There was a remarkable amount of variability and short-timescale changes in storm hysteresis dynamics for each site, and

among the three sites (Figure 4.6). However, plots of storm spectral slope ratio flushing index versus storm DOC concentration flushing index reveal site-specific patterns at each of the three sites (Figure 4.7a-c). Similarly, plots of storm spectral slope ratio hysteresis index versus storm DOC concentration hysteresis index were variable within and among sites, but formed distinct patterns in the four-quadrant Cartesian space (Figure 4.7d-f).

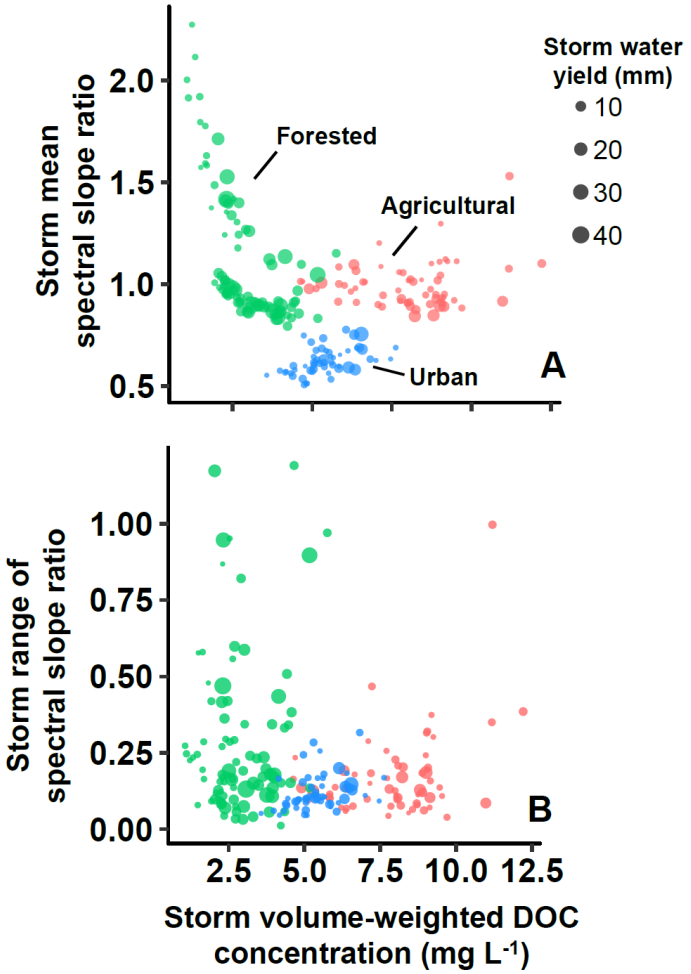

Figure 4.5. Plots of (a) storm mean spectral slope ratio and (b) storm range of spectral slope ratios vs. the storm ratio of DOC flux and water flux (equal to the storm volume-weighted DOC concentration). Each point represents one of the 220 observed storms, and the size of each point is scaled to the storm water yield (equal to the water flux divided by watershed area) of the storm.

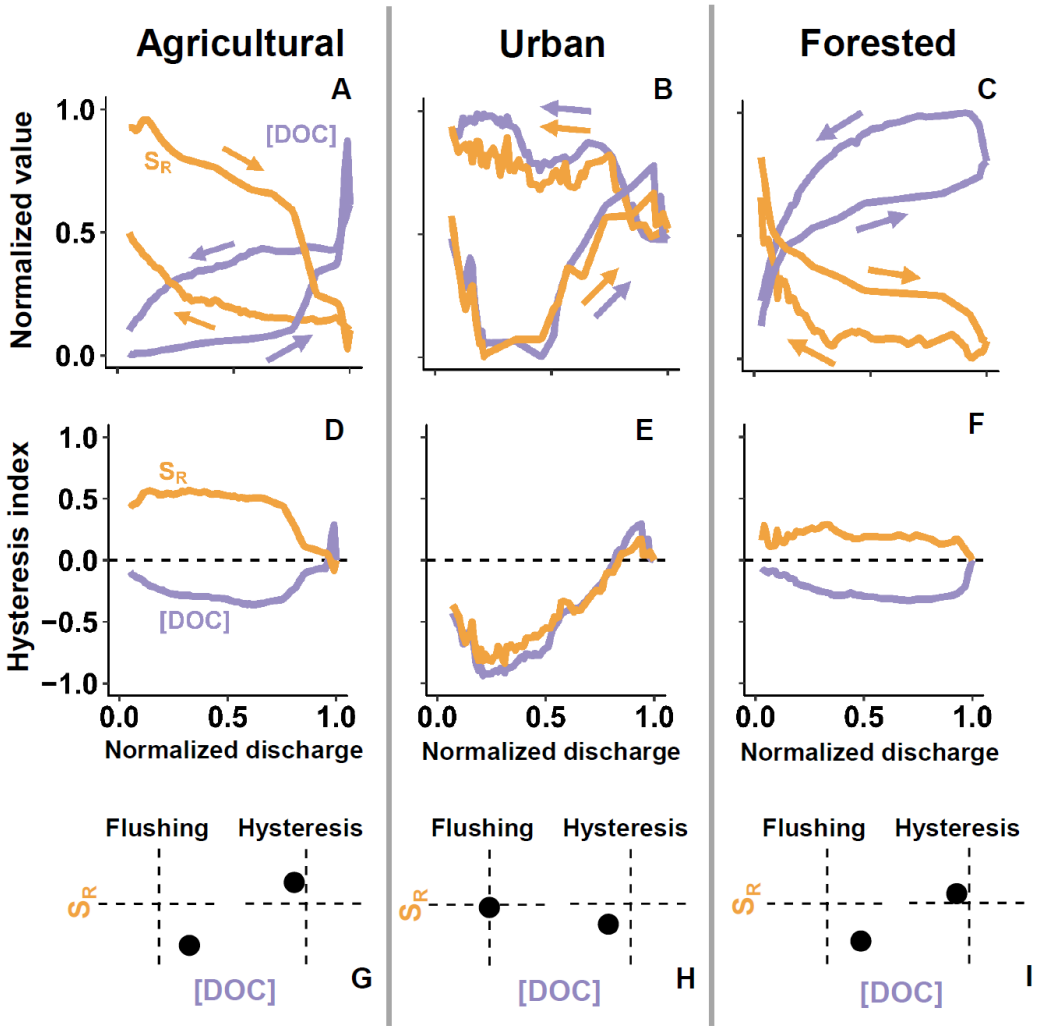

Figure 4.6. Plots of three example storms out of the 220 observed, demonstrating (a-c) storm-normalized spectral slope ratio (S_R; orange) and DOC concentration ([DOC]; purple) vs. storm-normalized discharge, (d-f) spectral slope ratio and DOC concentration hysteresis indices at 1% intervals of discharge vs. storm-normalized discharge, and (g-i) storm spectral slope ratio flushing index vs. storm DOC concentration flushing index, and storm spectral slope ratio hysteresis index vs. storm DOC hysteresis index (as in Figure 4.2). Each column represents one storm at the agricultural (left), urban (center), and forested (right) sites. The arrows indicate the direction of time.

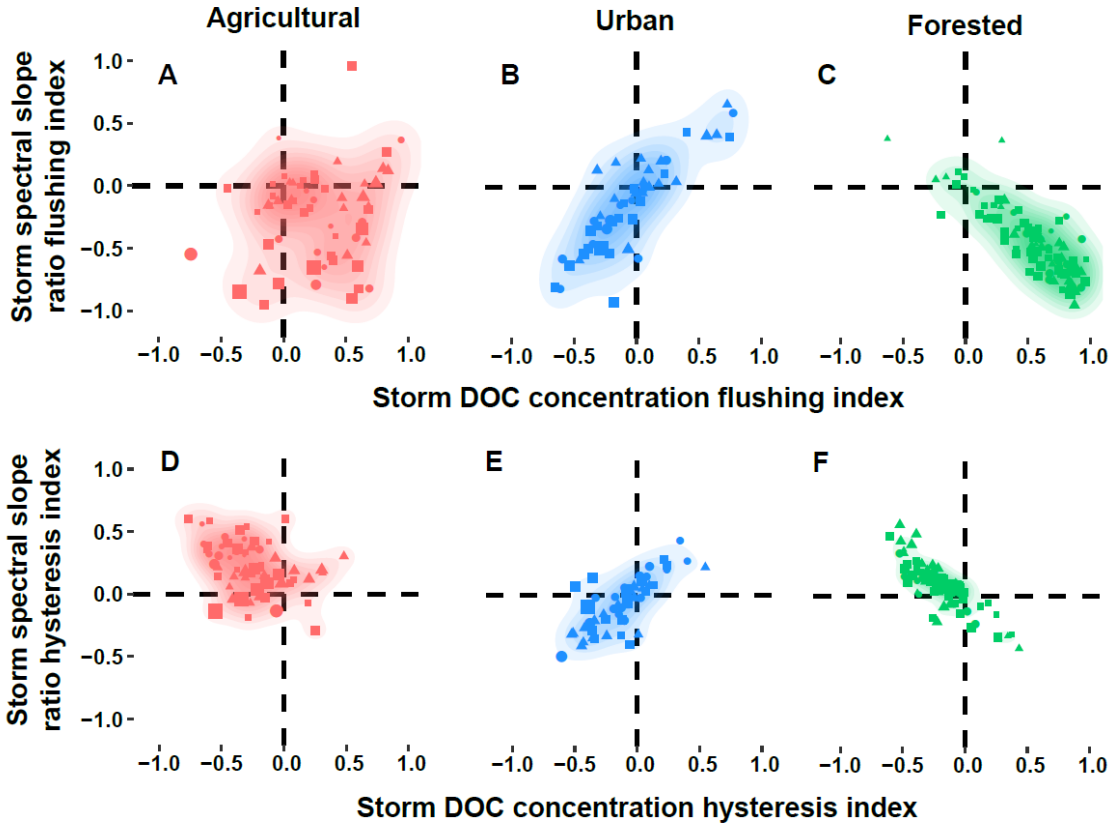

Figure 4.7. Plots of storm spectral slope ratio flushing index vs. storm DOC concentration flushing index for all storms at (a) agricultural, (b) urban, and (c) forested sites. Plots of (a-c) storm spectral slope flushing index vs. storm DOC concentration flushing index, and (d-f) storm spectral slope ratio hysteresis index vs. storm DOC concentration hysteresis index at agricultural (left), urban (center), and forested (right) sites. Each point represents a storm and point sizes are proportional to storm discharge peak. Points are shaped by storm season where triangles are spring, squares are summer, and circles are fall. Shading is provided as a visual aid to highlight patterns.

Discussion

The results presented here provide a unique view of storm event DOM quantity and character dynamics among various LULCs for a relatively large number of storms. To the authors' knowledge, these are the first comprehensive high-frequency time series of riverine DOM quantity and character among different LULCs. In the discussion below, we employ our novel quantitative and qualitative framework to provide valuable insight regarding reactivity and timing of release of DOM fractions during storm events among

LULCs that would be logistically impossible to capture by conventional grab sampling approaches. Subsequent discussion demonstrates that our analytical framework is a powerful tool for harnessing high-frequency DOM data to understand LULC and intra-storm controls on DOM dynamics.

DOM differences among sites

Land use / land cover not only influences the quantity and character of DOM transported from a watershed, but also influences the degree to which these parameters vary at baseflow and during storms. The high degree of heterogeneity in the concentrations, potential sources, and DOM character among the sites was indicated by significant differences in the median and variances of DOC concentration and spectral slope ratio (Figure 4.4). This finding also was reflected in the relationship between spectral slope ratio and DOC concentration, as there were distinct differences in these relationships among sites (Figure 4.4c). Interestingly, our results indicate that despite pronounced differences in water matrices due to LULC, the spectral slope ratio seems to converge to a similar value at relatively high DOC concentrations at each site. This pattern may reflect similar DOM pool composition at high DOC concentrations due to the contribution of distal sources of DOM from upland terrestrial landscapes, though more analyses will be necessary to characterize DOM under these conditions. Together, these results demonstrate the value of continuous measurements throughout the range of hydrologic and seasonal conditions to show the notable influence that LULC has on DOM quantity and character, and in capturing the substantial variability of riverine DOM character among these LULCs.

The relatively elevated DOC concentrations found in the agricultural stream are consistent with others' results. Agricultural watersheds have been shown to have elevated

baseflow DOC concentrations relative to other non-agricultural streams in the same region, and DOC concentration often increases during storm events (Dalzell et al. 2005; Royer and David 2005; Saraceno et al. 2009; Vidon et al. 2008). In addition, agricultural activities influence sources of stream water DOM and lead to greater in-stream DOM production because of increased stream fertility (Stanley et al. 2012; Wilson and Xenopoulos 2008). When spectral slope ratio is plotted against DOC concentration (Figure 4.4c), it is clear that the agricultural site represents a highly heterogeneous mixture of DOM, likely stemming from several watershed sources. High molecular weight DOM sources may include organic soil layer leachates, dissolved vascular plant tissue, and leachates from manure amendments. These sources may influence the autochthonous in-stream production of lower molecular weight bacterial communities, further influencing the heterogeneity in DOM character at the point of measurement.

DOC concentrations at the urban site were significantly higher than those found in the forested system, which leads to increased storm loading of DOM as reported and discussed in Vaughan et al. (2017). The urban site also had significantly higher molecular weight DOM, and significantly less heterogeneity in DOM molecular weight than the other sites (Figure 4.4a-b). This was a surprising result, given the multitude of potential DOM sources in an urban-suburban environment. Our interpretation is that the DOM sources are either relatively consistent in proportional supply among storm events and/or some component of urban modification to catchment hydrology promotes a more homogeneous but distinct character of urban stream DOM. McElmurry et al. (2014) surveyed DOM sources from watersheds of different LULC in Michigan, USA, and found that the average DOM molecular weight ranked in descending order from primarily forested, agricultural,

and urban and suburban watersheds, with only urban and suburban LULC not being different from one another. This result contrasts with our results, since significantly lower spectral slope ratios at our urban site indicate higher molecular weight DOM compared to the other sites. While that study differed in general sampling approach, scope, and analytical methods, the contrasting results may be an indication of regional variability among LULC classes.

The relatively lower DOC concentrations observed at the forested site may reflect the lack of additional DOM sources that likely contribute to DOC concentrations and loads at the agricultural and urban sites. The forested site also had the highest median spectral slope ratio, indicating the lowest molecular weight DOM. The variance in this quantity was the highest among the three sites, indicating notable variability on annual and event-based timescales. It is unclear whether this variability is due to the heterogeneity of DOM sources, or due to variability in its delivery to streams due to hydrologic conductivity during baseflow and storm events. DOM sourced from forested watersheds often have higher molecular weight DOM stemming from plant exudates that is freshly bioavailable (McElmurry et al. 2014; McKnight et al. 2001). The higher spectral slope ratios and indication of lower molecular weight DOM at our forested site may be the result of in-stream processing of these fresh DOM sources, and/or the signal of in-stream primary production and bacterial and algal exudates (Reche et al. 1998; Williams et al. 2010).

Land use / land cover influences on DOM storm dynamics

Our analytical framework provides a rich view of short time-scale DOM dynamics, which are hypothetically interpreted in Figure 4.2. Incorporating spectral slope ratio into this framework provides novel insights for storm DOM dynamics at the urban site, where

DOM character dynamics differ from the other sites markedly in ways that could not have been observed with more traditional methods. This method also provides new evidence to support patterns that others have observed at agricultural and forested sites, and adds richer context to reveal the heterogeneity of DOM sources and processing in an agricultural system.

Our framework reveals new evidence to support general patterns of DOM behavior observed by others in streams draining agricultural and forested catchments, where DOM character shifts from relatively lower molecular weight DOM during baseflow toward aromatic, higher molecular weight DOM during stormflow (Figures 4.7a and 4.7c; quadrant IV). At agricultural sites, this shift has been attributed to the mobilization of leachates from vascular crop tissue and organic-rich soil (Dalzell et al. 2005; Hernes et al. 2008; Saraceno et al. 2009; Vidon et al. 2008). In forested systems, DOC concentration and aromatic and humic content has also been shown to increase markedly during storms due to rising water table and changing water flowpaths through the organic layers of soil, and the additions of throughfall and litter leachate to stream runoff (Inamdar et al. 2011; Yoon and Raymond 2012). As discharge decreased on the falling limb, most storms showed higher molecular weight DOM and higher DOC concentrations, representing a different and possibly terrestrial source of DOM later in the storm (Figures 4.7d and 4.7f; quadrant II).

Plotting flushing and hysteresis indices for both quantity and character metrics showed that there was a much greater amount of variability in the magnitude of these dynamics at the agricultural site than the forested site. Watershed heterogeneity and variability in potential DOM sources at the agricultural site may have led to this greater

variability in storm dynamics. Many factors in the agricultural landscape can influence the production, processing, and resulting molecular weight of DOM molecules that may have contributed to this heterogeneity. For example, practices such as tillage can increase soil aeration, leading to increased microbial processing of plant material and increased production of lower molecular weight compounds (Dalzell et al. 2005; Kiem and Kögel-Knabner 2003). The variability in storm dynamics could in part be due to the hydrologic connection of subsurface tile drainage systems, which are commonly used in our agricultural watershed to increase crop yield (Moore 2016). This type of drainage increases the amount of generated runoff, and delivers this runoff in less time than in undrained fields (Blann et al. 2009). Subsurface tile drainage water can carry relatively low molecular weight DOM with little evidence of terrestrially derived material (Dalzell et al. 2011), and provide a direct link for crop residuals on fields to bypass soil microbe degradation and travel to stream networks through surface inlets. The variability in hydrologic flowpaths through a combination of subsurface tile drainage, surface tile inlets, and less altered shallow subsurface flowpaths could contribute to the higher degree of variability observed in storm DOM dynamics at agricultural streams compared to forested watersheds.

DOM storm dynamics at the urban site were markedly different from the agricultural and forested sites, as revealed by distinct patterns of coordinate locations in our framework (Figures 4.7b and 4.7e). As reported in Vaughan et al. (2017), DOC concentration hysteresis at our urban site was similar to the other sites, though distinct differences in DOM sources were not discoverable without the added DOM character information. This shows that during a typical storm at the urban site, DOC concentration decreased on the rising limb of the storm, while changes in the spectral slope ratio indicated

that the DOM character shifted to higher molecular weight as storm flow increased (Figure 4.7b; quadrant III). On a typical falling limb, the DOC concentration was higher than on the rising limb, while the character of the DOM shifted to relatively lower molecular weight than on the rising limb (Figure 4.7e; quadrant III). This shift may be due to the introduction of distal, lower molecular weight DOM that was not present during the rising limb. The anthropogenic influence of the developed landscape leads to greatly increased lateral hydrologic connectivity (Walsh et al. 2005) and increased in-stream transformations of DOM (Stanley et al. 2012). Human-made replacements for headwater streams, such as storm drains and gutters, become the sources and storage pools of DOM sources, assuming the analogous ecological role of headwater riparian zones. Organic matter is processed in these areas before delivery to stream network through fragmentation, wetting-drying facilitated leaching, and hydraulic abrasion (Kaushal and Belt 2012). Other developed watershed sources, such as impervious road surfaces and parking lots, may not have this stored pool of higher molecular DOM, nor a mechanism for processing (McElmurry et al. 2014). The dynamics we observed may be due to the mobilization and exhaustion of DOM from storm drains and other pools of relatively higher molecular weight DOM that act as an analog to riparian wetlands early in the storm, then sources may shift to more distal, lower molecular weight DOM sources that had accumulated on impervious surfaces in the watershed. Targeted end-member watershed sampling in developed areas in conjunction with the framework we have presented would aid in further understanding these processes.

Our approach also showed that although DOM character was highly dynamic during storm events, the bulk DOM character did not co-vary with the quantity of exported DOM for any of the sites (Figure 4.5). Some, though not all, of the storms with relatively

low DOC mass per water volume and high mean spectral slope ratio were associated with early season snowmelt at the forested site. This could be the result of snowpack-sourced water that had not dissolved or mobilized more complex terrestrially-derived organic compounds in forest soil. We also see that while many storms had a similar range of spectral slope ratios at all three sites, storms with the greatest intra-storm changes in spectral slope ratio occurred at the forested site (Figure 4.5b). The watershed of the forested site seems to have DOM sources similar to the higher molecular weight (low spectral slope ratio) sources of the agricultural site, but it is unique in the lower molecular weight (higher spectral slope ratio) sources (Figure 4.4a). Together, these results indicate that the activation of different source areas during a storm cause variability in the character of the DOM delivered to waterbodies, though this bulk DOM character is independent of the quantity of DOM exported.

Conclusions

This study demonstrates the value of long-term, high-frequency, continuous monitoring. Because of the high amount of heterogeneity in DOM character and diversity of storm dynamics, the potential for sampling error is high. Emerging sensor technologies makes a near or complete census approach possible, and it may be warranted depending upon management and/or research goals. High-frequency measurements allowed us to observe changes on the timescales at which they occur, and the continuous nature of our monitoring system captured these dynamics no matter the time of day or investigator vacation schedule. Recommendations, considerations, and limitations of using ultraviolet-visible spectrophotometers are discussed at greater length in Vaughan et al. (2017) and Vaughan et al. (2018).

We incorporated high-frequency measurements of DOC concentration and spectral slope ratio into a composite novel analytical framework to aid in interpretation of short-timescale storm DOM dynamics. This data-rich framework revealed remarkable variability in storm dynamics at each of three sites with contrasting LULC, and revealed distinct and informative patterns among the sites due to LULC impact on DOM supply and provenance during storm events. Analysis of 220 events provides new evidence that relatively high molecular weight, potentially terrestrially-derived DOM sources contribute to the DOM pool later in storm cycles at agricultural and forested sites. Furthermore, our framework clearly demonstrates that landscape heterogeneity exerts a strong influence on storm DOM character dynamics at our forested and agricultural catchments. In addition, our framework revealed the surprising result that DOM molecular weight tends to decrease later in storm cycles at our urban site, even as DOC concentration increases. Harnessing high-frequency data using our approach provides new insight to characterize the changing sources of DOM during storm events, and adds reason for caution when determining DOM provenance through DOC concentration hysteresis alone.

References

Aiken GR (2014) Fluorescence and dissolved organic matter: A chemist's perspective. Cambridge University Press, New York, NY. doi:10.1017/cbo9781139045452.005

Amon RMW, Benner R (1996) Bacterial utilization of different size classes of dissolved organic matter Limnol Oceanogr 41:41-51

Avagyan A, Runkle BRK, Kutzbach L (2014) Application of high-resolution spectral absorbance measurements to determine dissolved organic carbon concentration in remote areas Journal of Hydrology 517:435-446 doi:10.1016/j.jhydrol.2014.05.060

Battin TJ, Luyssaert S, Kaplan LA, Aufdenkampe AK, Richter A, Tranvik LJ (2009) The boundless carbon cycle Nature Geosci 2:598-600

Blann KL, Anderson JL, Sands GR, Vondracek B (2009) Effects of Agricultural Drainage on Aquatic Ecosystems: A Review Critical Reviews in Environmental Science and Technology 39:909-1001 doi:10.1080/10643380801977966

Brown M (1977) Transmission spectroscopy examinations of natural waters: C. Ultraviolet spectral characteristics of the transition from terrestrial humus to marine yellow substance Estuarine and Coastal Marine Science 5:309-317 doi:https://doi.org/10.1016/0302-3524(77)90058-5

Buffam I, Galloway JN, Blum LK, McGlathery KJ (2001) A stormflow/baseflow comparison of dissolved organic matter concentrations and bioavailability in an Appalachian stream Biogeochemistry 53:269-306 doi:10.1023/A:1010643432253

Bukaveckas PA, Robbins-Forbes M (2000) Role of dissolved organic carbon in the attenuation of photosynthetically active and ultraviolet radiation in Adirondack lakes Freshwater Biology 43:339-354 doi:10.1046/j.1365-2427.2000.00518.x

Butturini A, Alvarez M, Bernal S, Vazquez E, Sabater F (2008) Diversity and temporal sequences of forms of DOC and NO3-discharge responses in an intermittent stream: Predictable or random succession? Journal of Geophysical Research: Biogeosciences 113:n/a-n/a doi:10.1029/2008JG000721

Carder KL, Steward RG, Harvey GR, Ortner PB (1989) Marine humic and fulvic acids: Their effects on remote sensing of ocean chlorophyll Limnol Oceanogr 34:68-81 doi:doi:10.4319/lo.1989.34.1.0068

Chanat JG, Rice KC, Hornberger GM (2002) Consistency of patterns in concentration-discharge plots Water Resour Res 38:22-21-22-10 doi:10.1029/2001WR000971

Chow AT, Dahlgren RA, Harrison JA (2007) Watershed sources of disinfection byproduct precursors in the Sacramento and San Joaquin Rivers, California Environmental Science & Technology 41:7645-7652 doi:10.1021/es070621t

Cole JJ et al. (2007) Plumbing the Global Carbon Cycle: Integrating Inland Waters into the Terrestrial Carbon Budget Ecosystems 10:172-185 doi:10.1007/s10021-006-9013-8

Dalzell BJ, Filley TR, Harbor JM (2005) Flood pulse influences on terrestrial organic matter export from an agricultural watershed Journal of Geophysical Research-Biogeosciences 110 doi:10.1029/2005jg000043

Dalzell BJ, King JY, Mulla DJ, Finlay JC, Sands GR (2011) Influence of subsurface drainage on quantity and quality of dissolved organic matter export from agricultural landscapes Journal of Geophysical Research: Biogeosciences 116 doi:doi:10.1029/2010JG001540

Del Vecchio R, Blough NV (2004) On the Origin of the Optical Properties of Humic Substances Environmental Science & Technology 38:3885-3891 doi:10.1021/es049912h

Driscoll CT, Fuller RD, Simone DM (1988) Longitudinal variations in trace-metal concentrations in a northern forested ecosystem J Environ Qual 17:101-107

Evans C, Davies TD (1998) Causes of concentration/discharge hysteresis and its potential as a tool for analysis of episode hydrochemistry Water Resour Res 34:129-137 doi:10.1029/97WR01881

Fichot CG, Benner R (2012) The spectral slope coefficient of chromophoric dissolved organic matter (S275–295) as a tracer of terrigenous dissolved organic carbon in river-influenced ocean margins Limnol Oceanogr 57:1453-1466 doi:doi:10.4319/lo.2012.57.5.1453

Hayase K, Tsubota H (1985) Sedimentary humic acid and fulvic acid as fluorescent organic materials Geochim Cosmochim Ac 49:159-163 doi:https://doi.org/10.1016/0016-7037(85)90200-5

Hedges JI et al. (2000) The molecularly-uncharacterized component of nonliving organic matter in natural environments Organic Geochemistry 31:945-958 doi:https://doi.org/10.1016/S0146-6380(00)00096-6

Helms JR, Stubbins A, Ritchie JD, Minor EC, Kieber DJ, Mopper K (2008) Absorption spectral slopes and slope ratios as indicators of molecular weight, source, and photobleaching of chromophoric dissolved organic matter Limnol Oceanogr 53:955-969 doi:10.4319/lo.2008.53.3.0955

Hernes PJ, Spencer RGM, Dyda RY, Pellerin BA, Bachand PAM, Bergamaschi BA (2008) The role of hydrologic regimes on dissolved organic carbon composition in an agricultural watershed Geochim Cosmochim Ac 72:5266-5277 doi:10.1016/j.gca.2008.07.031

Hood E, Gooseff MN, Johnson SL (2006) Changes in the character of stream water dissolved organic carbon during flushing in three small watersheds, Oregon Journal of Geophysical Research: Biogeosciences 111:n/a-n/a doi:10.1029/2005JG000082

House WA, Warwick MS (1998) Hysteresis of the solute concentration/discharge relationship in rivers during storms Water Research 32:2279-2290 doi:http://dx.doi.org/10.1016/S0043-1354(97)00473-9

Inamdar S et al. (2011) Fluorescence characteristics and sources of dissolved organic matter for stream water during storm events in a forested mid-Atlantic watershed Journal of Geophysical Research-Biogeosciences 116 doi:10.1029/2011jg001735

Jaffé R, McKnight D, Maie N, Cory R, McDowell WH, Campbell JL (2008) Spatial and temporal variations in DOM composition in ecosystems: The importance of long-term monitoring of optical properties Journal of Geophysical Research: Biogeosciences 113:G04032 doi:10.1029/2008JG000683

Jaffé R et al. (2012) Dissolved Organic Matter in Headwater Streams: Compositional Variability across Climatic Regions of North America Geochim Cosmochim Ac 94:95-108 doi:https://doi.org/10.1016/j.gca.2012.06.031

Kaushal SS, Belt KT (2012) The urban watershed continuum: evolving spatial and temporal dimensions Urban Ecosyst 15:409-435 doi:10.1007/s11252-012-0226-7

Kellerman AM (2015) Molecular-level dissolved organic matter dynamics in lakes : Constraints on reactivity and persistence. Doctoral thesis, comprehensive summary, Acta Universitatis Upsaliensis

Kellerman AM, Kothawala DN, Dittmar T, Tranvik LJ (2015) Persistence of dissolved organic matter in lakes related to its molecular characteristics Nature Geoscience 8:454 doi:10.1038/ngeo2440

https://www.nature.com/articles/ngeo2440#supplementary-information

Kiem R, Kögel-Knabner I (2003) Contribution of lignin and polysaccharides to the refractory carbon pool in C-depleted arable soils Soil Biology and Biochemistry 35:101-118 doi:https://doi.org/10.1016/S0038-0717(02)00242-0

Kim S, Kaplan LA, Hatcher PG (2006) Biodegradable dissolved organic matter in a temperate and a tropical stream determined from ultra-high resolution mass spectrometry Limnol Oceanogr 51:1054-1063 doi:10.4319/lo.2006.51.2.1054

Kitis M, Karanfil T, Kilduff JE, Wigton A (2001) The reactivity of natural organic matter to disinfection byproducts formation and its relation to specific ultraviolet absorbance Water Sci Technol 43:9-16

Kraus TEC et al. (2008) Assessing the contribution of wetlands and subsided islands to dissolved organic matter and disinfection byproduct precursors in the Sacramento–San Joaquin River Delta: A geochemical approach Organic Geochemistry 39:1302-1318 doi:http://dx.doi.org/10.1016/j.orggeochem.2008.05.012

Kruskal WH, Wallis WA (1952) Use of ranks in one-criterion variance analysis Journal of the American Statistical Association 47:583-621 doi:10.2307/2280779

Kuk-Hyun A, Scott S (2018) Time-varying suspended sediment-discharge rating curves to estimate climate impacts on fluvial sediment transport Hydrol Process 32:102-117 doi:doi:10.1002/hyp.11402

Langergraber G, Fleischmann N, Hofstadter F (2003) A multivariate calibration procedure for UV/VIS spectrometric quantification of organic matter and nitrate in wastewater Water Sci Technol 47:63-71

Levene H (1960) Robust tests for equality of variances. In: Olkin I (ed) Contributions to Probability and Statistics: Essays in Honor of Harold Hotelling. Stanford University Press, pp 278-292

Lloyd CEM, Freer JE, Johnes PJ, Collins AL (2016) Technical Note: Testing an improved index for analysing storm discharge–concentration hysteresis Hydrol Earth Syst Sci 20:625-632 doi:10.5194/hess-20-625-2016

Ludwig W, Probst J-L, Kempe S (1996) Predicting the oceanic input of organic carbon by continental erosion Global Biogeochemical Cycles 10:23-41 doi:10.1029/95GB02925

McElmurry SP, Long DT, Voice TC (2014) Stormwater Dissolved Organic Matter: Influence of Land Cover and Environmental Factors Environmental Science & Technology 48:45-53 doi:10.1021/es402664t

McKnight DM, Boyer EW, Westerhoff PK, Doran PT, Kulbe T, Andersen DT (2001) Spectrofluorometric characterization of dissolved organic matter for indication of precursor organic material and aromaticity Limnol Oceanogr 46:38-48 doi:doi:10.4319/lo.2001.46.1.0038

Mevik B, Wehrens R, Liland KH (2015) pls: Partial Least Squares and Principal Component Regression.

Moore J (2016) Literature review: tile drainage and phosphorus losses from agricultural land. Lake Champlain Basin Program,

Moore RD (2005) Slug injection using salt in solution Streamline Watershed Management Bulletin 8:1-6

Morris DP et al. (1995) The attentuation of solar UV radiation in lakes and the role of dissolved organic carbon Limnol Oceanogr 40:1381-1391

Nguyen HV-M, Lee M-H, Hur J, Schlautman MA (2013) Variations in spectroscopic characteristics and disinfection byproduct formation potentials of dissolved organic matter for two contrasting storm events Journal of Hydrology 481:132-142 doi:http://dx.doi.org/10.1016/j.jhydrol.2012.12.044

Petras D et al. (2017) High-Resolution Liquid Chromatography Tandem Mass Spectrometry Enables Large Scale Molecular Characterization of Dissolved Organic Matter Frontiers in Marine Science 4 doi:10.3389/fmars.2017.00405

Prairie YT (2008) Carbocentric limnology: looking back, looking forward Can J Fish Aquat Sci 65:543-548 doi:10.1139/F08-011

R Core Team (2015) R: A language and environment for statistical computing. R Foundation for Statistical Computing, Vienna, Austria

Ravichandran M (2004) Interactions between mercury and dissolved organic matter - a review Chemosphere 55:319-331 doi:10.1016/j.chemosphere.2003.11.011

Raymond PA, Bauer JE (2001) Riverine export of aged terrestrial organic matter to the North Atlantic Ocean Nature 409:497-500

Reche II, Pace ML, Cole JJ (1998) Interactions of Photobleaching and Inorganic Nutrients in Determining Bacterial Growth on Colored Dissolved Organic Carbon Microbial ecology 36:270-280

Reckhow DA, Singer PC (1990) Chlorination by-products in drinking waters - from formation potentials to finished water concentrations J Am Water Works Ass 82:173-180

Roberts B, Mulholland P, Hill W (2007) Multiple Scales of Temporal Variability in Ecosystem Metabolism Rates: Results from 2 Years of Continuous Monitoring in a Forested Headwater Stream Ecosystems 10:588-606 doi:10.1007/s10021-007-9059-2

Rode M et al. (2016) Sensors in the Stream: The High-Frequency Wave of the Present Environmental Science & Technology 50:10297-10307 doi:10.1021/acs.est.6b02155

Rosenberg BD, Schroth AW (2017) Coupling of reactive riverine phosphorus and iron species during hot transport moments: impacts of land cover and seasonality Biogeochemistry 132:103-122 doi:10.1007/s10533-016-0290-9

Royer TV, David MB (2005) Export of dissolved organic carbon from agricultural streams in Illinois, USA Aquat Sci 67:465-471 doi:10.1007/s00027-005-0781-6

Ruhala SS, Zarnetske JP (2017) Using in-situ optical sensors to study dissolved organic carbon dynamics of streams and watersheds: A review Science of The Total Environment 575:713-723 doi:https://doi.org/10.1016/j.scitotenv.2016.09.113

Saraceno JF, Pellerin BA, Downing BD, Boss E, Bachand PAM, Bergamaschi BA (2009) High-frequency in situ optical measurements during a storm event: Assessing relationships between dissolved organic matter, sediment concentrations, and hydrologic processes Journal of Geophysical Research-Biogeosciences 114 doi:10.1029/2009jg000989

Sleighter RL, Hatcher PG (2007) The application of electrospray ionization coupled to ultrahigh resolution mass spectrometry for the molecular characterization of natural organic matter J Mass Spectrom 42:559-574 doi:10.1002/jms.1221

Sleighter RL, Liu Z, Xue J, Hatcher PG (2010) Multivariate Statistical Approaches for the Characterization of Dissolved Organic Matter Analyzed by Ultrahigh Resolution Mass Spectrometry Environmental Science & Technology 44:7576-7582 doi:10.1021/es1002204

Sobczak W, Findlay S, Dye S (2003) Relationships between DOC bioavailability and nitrate removal in an upland stream: An experimental approach Biogeochemistry 62:309-327 doi:10.1023/A:1021192631423

Stanley EH, Powers SM, Lottig NR, Buffam I, Crawford JT (2012) Contemporary changes in dissolved organic carbon (DOC) in human-dominated rivers: is there a

role for DOC management? Freshwater Biology 57:26-42 doi:10.1111/j.1365-2427.2011.02613.x

Stedmon CA, Markager S, Bro R (2003) Tracing dissolved organic matter in aquatic environments using a new approach to fluorescence spectroscopy Marine Chemistry 82:239-254 doi:https://doi.org/10.1016/S0304-4203(03)00072-0

Stubbins A, Lapierre JF, Berggren M, Prairie YT, Dittmar T, del Giorgio PA (2014) What's in an EEM? Molecular signatures associated with dissolved organic fluorescence in Boreal Canada Environmental Science & Technology 48:10598-10606 doi:10.1021/es502086e

Turnipseed DP, Sauer VB (2010) Discharge measurements at gaging stations. U.S. Geological Survey,

Vaughan MCH et al. (2017) High-frequency dissolved organic carbon and nitrate measurements reveal differences in storm hysteresis and loading in relation to land cover and seasonality Water Resour Res 53:5345-5363 doi:10.1002/2017WR020491

Vaughan MCH, Bowden WB, Shanley JB, Vermilyea A, Wemple BC, Schroth AW (2018) Using in situ UV-Visible spectrophotometer sensors to quantify riverine phosphorus partitioning and concentration at a high frequency Limnology and Oceanography: Methods doi:10.1002/lom3.10287

Vidon P, Wagner LE, Soyeux E (2008) Changes in the character of DOC in streams during storms in two Midwestern watersheds with contrasting land uses Biogeochemistry 88:257-270 doi:10.1007/s10533-008-9207-6

Walsh CJ, Roy AH, Feminella JW, Cottingham PD, Groffman PM, Morgan RP (2005) The urban stream syndrome: current knowledge and the search for a cure Journal of the North American Benthological Society 24:706-723 doi:10.1899/04-028.1

Weishaar JL, Aiken GR, Bergamaschi BA, Fram MS, Fujii R, Mopper K (2003) Evaluation of Specific Ultraviolet Absorbance as an Indicator of the Chemical Composition and Reactivity of Dissolved Organic Carbon Environmental Science & Technology 37:4702-4708 doi:10.1021/es030360x

Weyhenmeyer GA, Fröberg M, Karltun E, Khalili M, Kothawala D, Temnerud J, Tranvik LJ (2012) Selective decay of terrestrial organic carbon during transport from land to sea Global Change Biol 18:349-355 doi:10.1111/j.1365-2486.2011.02544.x

Williams CJ, Yamashita Y, Wilson HF, Jaffé R, Xenopoulos MA (2010) Unraveling the role of land use and microbial activity in shaping dissolved organic matter characteristics in stream ecosystems Limnol Oceanogr 55:1159-1171 doi:doi:10.4319/lo.2010.55.3.1159

Wilson H, Xenopoulos M (2008) Ecosystem and Seasonal Control of Stream Dissolved Organic Carbon Along a Gradient of Land Use Ecosystems 11:555-568 doi:10.1007/s10021-008-9142-3

Yoon B, Raymond PA (2012) Dissolved organic matter export from a forested watershed during Hurricane Irene Geophysical Research Letters 39 doi:10.1029/2012gl052785

COMPREHENSIVE BIBLIOGRAPHY

Aber JD (1997) Why Don't We Believe the Models? Bulletin of the Ecological Society of America 78:232-233

Aiken GR (2014) Fluorescence and dissolved organic matter: A chemist's perspective. Cambridge University Press, New York, NY. doi:10.1017/cbo9781139045452.005

Aitkenhead-Peterson JA, Steele MK, Nahar N, Santhy K (2009) Dissolved organic carbon and nitrogen in urban and rural watersheds of south-central Texas: land use and land management influences Biogeochemistry 96:119-129 doi:10.1007/s10533-009-9348-2

Amon RMW, Benner R (1996) Bacterial utilization of different size classes of dissolved organic matter Limnol Oceanogr 41:41-51

Andrea B, Francesc G, Jérôme L, Eusebi V, Francesc S (2006) Cross-site comparison of variability of DOC and Nitrate c–q hysteresis during the autumn–winter period in three mediterranean headwater streams: A synthetic approach Biogeochemistry 77:327-349 doi:10.1007/s10533-005-0711-7

Arnold JG, Allen PM, Muttiah R, Bernhardt G (1995) Automated base-flow separation and recession analysis techniques Ground Water 33:1010-1018 doi:10.1111/j.1745-6584.1995.tb00046.x

Aulenbach BT et al. (2016) Approaches to stream solute load estimation for solutes with varying dynamics from five diverse small watersheds Ecosphere 7:n/a-n/a doi:10.1002/ecs2.1298

Avagyan A, Runkle BRK, Kutzbach L (2014) Application of high-resolution spectral absorbance measurements to determine dissolved organic carbon concentration in remote areas Journal of Hydrology 517:435-446 doi:10.1016/j.jhydrol.2014.05.060

Baker JP et al. (1996) Episodic acidification of small streams in the Northeastern United States: Effects on fish populations Ecological Applications 6:422-437 doi:10.2307/2269380

Battin TJ, Luyssaert S, Kaplan LA, Aufdenkampe AK, Richter A, Tranvik LJ (2009) The boundless carbon cycle Nature Geosci 2:598-600

Baumgardner RE, Lavery TF, Rogers CM, Isil SS (2002) Estimates of the atmospheric deposition of sulfur and nitrogen species: Clean Air Status and Trends Network, 1990-2000 Environmental Science & Technology 36:2614-2629 doi:10.1021/Es011146g

Bieroza MZ, Heathwaite AL (2015) Seasonal variation in phosphorus concentration–discharge hysteresis inferred from high-frequency in situ monitoring Journal of Hydrology 524:333-347 doi:http://dx.doi.org/10.1016/j.jhydrol.2015.02.036

Birgand F, Aveni-Deforge K, Smith B, Maxwell B, Horstman M, Gerling AB, Carey CC (2016) First report of a novel multiplexer pumping system coupled to a water quality probe to collect high temporal frequency in situ water chemistry measurements at multiple sites Limnology and Oceanography: Methods 14:767-783 doi:10.1002/lom3.10122

Blann KL, Anderson JL, Sands GR, Vondracek B (2009) Effects of Agricultural Drainage on Aquatic Ecosystems: A Review Critical Reviews in Environmental Science and Technology 39:909-1001 doi:10.1080/10643380801977966

Boesch DF, Brinsfield RB, Magnien RE (2001) Chesapeake Bay eutrophication: Scientific understanding, ecosystem restoration, and challenges for agriculture J Environ Qual 30:303-320

Bowes MJ et al. (2015) Characterising phosphorus and nitrate inputs to a rural river using high-frequency concentration–flow relationships Science of The Total Environment 511:608-620 doi:http://dx.doi.org/10.1016/j.scitotenv.2014.12.086

Bowes MJ, Smith JT, Neal C (2009) The value of high-resolution nutrient monitoring: A case study of the River Frome, Dorset, UK Journal of Hydrology 378:82-96 doi:http://dx.doi.org/10.1016/j.jhydrol.2009.09.015

Boyer E, Goodale C, Jaworski N, Howarth R (2002) Anthropogenic nitrogen sources and relationships to riverine nitrogen export in the northeastern U.S.A Biogeochemistry 57-58:137-169 doi:10.1023/A:1015709302073

Boyer EW, Hornberger GM, Bencala KE, McKnight DM (1997) Response characteristics of DOC flushing in an alpine catchment Hydrol Process 11:1635-1647

Brown M (1977) Transmission spectroscopy examinations of natural waters: C. Ultraviolet spectral characteristics of the transition from terrestrial humus to marine yellow substance Estuarine and Coastal Marine Science 5:309-317 doi:https://doi.org/10.1016/0302-3524(77)90058-5

Brown VA, McDonnell JJ, Burns DA, Kendall C (1999) The role of event water, a rapid shallow flow component, and catchment size in summer stormflow Journal of Hydrology 217:171-190 doi:http://dx.doi.org/10.1016/S0022-1694(98)00247-9

Buda AR, DeWalle DR (2009) Dynamics of stream nitrate sources and flow pathways during stormflows on urban, forest and agricultural watersheds in central Pennsylvania, USA Hydrol Process 23:3292-3305 doi:doi:10.1002/hyp.7423

Buffam I, Galloway JN, Blum LK, McGlathery KJ (2001) A stormflow/baseflow comparison of dissolved organic matter concentrations and bioavailability in an Appalachian stream Biogeochemistry 53:269-306 doi:10.1023/A:1010643432253

Bukaveckas PA, Robbins-Forbes M (2000) Role of dissolved organic carbon in the attenuation of photosynthetically active and ultraviolet radiation in Adirondack lakes Freshwater Biology 43:339-354 doi:10.1046/j.1365-2427.2000.00518.x

Butturini A, Alvarez M, Bernal S, Vazquez E, Sabater F (2008) Diversity and temporal sequences of forms of DOC and NO3-discharge responses in an intermittent stream: Predictable or random succession? Journal of Geophysical Research: Biogeosciences 113:n/a-n/a doi:10.1029/2008JG000721

Camargo JA, Alonso Á (2006) Ecological and toxicological effects of inorganic nitrogen pollution in aquatic ecosystems: A global assessment Environ Int 32:831-849 doi:http://dx.doi.org/10.1016/j.envint.2006.05.002

Carder KL, Steward RG, Harvey GR, Ortner PB (1989) Marine humic and fulvic acids: Their effects on remote sensing of ocean chlorophyll Limnol Oceanogr 34:68-81 doi:doi:10.4319/lo.1989.34.1.0068

Carey RO, Wollheim WM, Mulukutla GK, Mineau MM (2014) Characterizing storm-event nitrate fluxes in a fifth order suburbanizing watershed using in situ sensors Environmental Science & Technology 48:7756-7765 doi:10.1021/es500252j

Carpenter SR, Caraco NF, Correll DL, Howarth RW, Sharpley AN, Smith VH (1998) Nonpoint pollution of surface waters with phosphorus and nitrogen Ecological Applications 8:559-568 doi:10.1890/1051-0761(1998)008[0559:NPOSWW]2.0.CO;2

Caverly E, Kaste JM, Hancock GS, Chambers RM (2013) Dissolved and particulate organic carbon fluxes from an agricultural watershed during consecutive tropical storms Geophysical Research Letters 40:5147-5152 doi:10.1002/grl.50982

Chanat JG, Rice KC, Hornberger GM (2002) Consistency of patterns in concentration-discharge plots Water Resour Res 38:22-21-22-10 doi:10.1029/2001WR000971

Chervin RM (1981) On the Comparison of Observed and GCM Simulated Climate Ensembles Journal of the Atmospheric Sciences 38:885-901 doi:10.1175/1520-0469(1981)038<0885:OTCOOA>2.0.CO;2

Chow AT, Dahlgren RA, Harrison JA (2007) Watershed sources of disinfection byproduct precursors in the Sacramento and San Joaquin Rivers, California Environmental Science & Technology 41:7645-7652 doi:10.1021/es070621t

Cohen MJ, Kurz MJ, Heffernan JB, Martin JB, Douglass RL, Foster CR, Thomas RG (2013) Diel phosphorus variation and the stoichiometry of ecosystem metabolism in a large spring-fed river Ecological Monographs 83:155-176 doi:10.1890/12-1497.1

Cole JJ et al. (2007) Plumbing the Global Carbon Cycle: Integrating Inland Waters into the Terrestrial Carbon Budget Ecosystems 10:172-185 doi:10.1007/s10021-006-9013-8

Conley DJ et al. (2009) Controlling Eutrophication: Nitrogen and Phosphorus Science 323:1014-1015 doi:10.1126/science.1167755

Copetti D, Valsecchi L, Capodaglio AG, Tartari G (2017) Direct measurement of nutrient concentrations in freshwaters with a miniaturized analytical probe: evaluation and validation Environmental Monitoring and Assessment 189:144 doi:10.1007/s10661-017-5847-0

Correll DL (1998) The Role of Phosphorus in the Eutrophication of Receiving Waters: A Review Journal of Environmental Quality 27:261-266 doi:10.2134/jeq1998.00472425002700020004x

Correll DL, Jordan TE, Weller DE (1999) Transport of nitrogen and phosphorus from rhode river watersheds during storm events Water Resour Res 35:2513-2521 doi:10.1029/1999WR900058

Creed IF, Band LE (1998) Export of nitrogen from catchments within a temperate forest: Evidence for a unifying mechanism regulated by variable source area dynamics Water Resour Res 34:3105-3120 doi:10.1029/98WR01924

Daloğlu I, Cho KH, Scavia D (2012) Evaluating Causes of Trends in Long-Term Dissolved Reactive Phosphorus Loads to Lake Erie Environmental Science & Technology 46:10660-10666 doi:10.1021/es302315d

Dalzell BJ, Filley TR, Harbor JM (2005) Flood pulse influences on terrestrial organic matter export from an agricultural watershed Journal of Geophysical Research-Biogeosciences 110 doi:10.1029/2005jg000043

Dalzell BJ, King JY, Mulla DJ, Finlay JC, Sands GR (2011) Influence of subsurface drainage on quantity and quality of dissolved organic matter export from agricultural landscapes Journal of Geophysical Research: Biogeosciences 116 doi:doi:10.1029/2010JG001540

Darwiche-Criado N, Comin FA, Sorando R, Sanchez-Perez JM (2015) Seasonal variability of NO3- mobilization during flood events in a Mediterranean catchment: The influence of intensive agricultural irrigation Agriculture Ecosystems & Environment 200:208-218 doi:10.1016/j.agee.2014.11.002

Davison W (1993) Iron and manganese in lakes Earth-Science Reviews 34:119-163 doi:https://doi.org/10.1016/0012-8252(93)90029-7

Del Vecchio R, Blough NV (2004) On the Origin of the Optical Properties of Humic Substances Environmental Science & Technology 38:3885-3891 doi:10.1021/es049912h

Dhillon GS, Inamdar S (2013) Extreme storms and changes in particulate and dissolved organic carbon in runoff: Entering uncharted waters? Geophysical Research Letters 40 doi:10.1002/Grl.50306

Dinnes DL, Karlen DL, Jaynes DB, Kaspar TC, Hatfield JL, Colvin TS, Cambardella CA (2002) Nitrogen management strategies to reduce nitrate leaching in tile-drained Midwestern soils Agronomy Journal 94:153-171 doi:10.2134/agronj2002.1530

Djodjic F, Montas H, Shirmohammadi A, Bergström L, Ulén B (2002) A Decision Support System for Phosphorus Management at a Watershed Scale J Environ Qual 31:937-945 doi:10.2134/jeq2002.9370

Dodd RJ, Sharpley AN (2016) Conservation practice effectiveness and adoption: unintended consequences and implications for sustainable phosphorus management Nutrient Cycling in Agroecosystems 104:373-392 doi:10.1007/s10705-015-9748-8

Dodds WK, Smith VH (2016) Nitrogen, phosphorus, and eutrophication in streams Inland Waters 6:155-164 doi:10.5268/IW-6.2.909

Donn MJ, Barron OV, Barr AD (2012) Identification of phosphorus export from low-runoff yielding areas using combined application of high frequency water quality data and MODHMS modelling Science of The Total Environment 426:264-271 doi:http://dx.doi.org/10.1016/j.scitotenv.2012.03.021

Driscoll CT, Fuller RD, Simone DM (1988) Longitudinal variations in trace-metal concentrations in a northern forested ecosystem J Environ Qual 17:101-107

Driscoll CT et al. (2001) Acidic deposition in the Northeastern United States: Sources and inputs, ecosystem effects, and management strategies BioScience 51:180-198 doi:10.1641/0006-3568(2001)051[0180:ADITNU]2.0.CO;2

Driscoll CT et al. (2003) Nitrogen pollution in the Northeastern United States: Sources, effects, and management options BioScience 53:357-374 doi:10.1641/0006-3568(2003)053[0357:npitnu]2.0.co;2

Elmore AJ, Kaushal SS (2008) Disappearing headwaters: patterns of stream burial due to urbanization Frontiers in Ecology and the Environment 6:308-312 doi:10.1890/070101

EPA US (2016a) National coastal condition assessment 2010. U.S. Environmental Protection Agency, Office of Water, Office of Research and Development, Washington, DC

EPA US (2016b) National lakes assessment 2012: A collaborative survey of lakes in the United States. Washington, D.C.

EPA US (2016c) National rivers and streams assessment 2008-2009: A collaborative survey. U.S. Environmental Protection Agency, Office of Water, Office of Research and Development, Washington, DC

Etheridge JR, Birgand F, Osborne JA, Osburn CL, Burchell MR, II, Irving J (2014) Using in situ ultraviolet-visual spectroscopy to measure nitrogen, carbon, phosphorus, and suspended solids concentrations at a high frequency in a brackish tidal marsh Limnology and Oceanography-Methods 12:10-22 doi:10.4319/lom.2014.12.10

Evans C, Davies TD (1998) Causes of concentration/discharge hysteresis and its potential as a tool for analysis of episode hydrochemistry Water Resour Res 34:129-137 doi:10.1029/97WR01881

Fellman JB, Hood E, Edwards RT, D'Amore DV (2009) Changes in the concentration, biodegradability, and fluorescent properties of dissolved organic matter during stormflows in coastal temperate watersheds Journal of Geophysical Research: Biogeosciences 114:G01021 doi:10.1029/2008JG000790

Fichot CG, Benner R (2011) A novel method to estimate DOC concentrations from CDOM absorption coefficients in coastal waters Geophysical Research Letters 38 doi:10.1029/2010gl046152

Fichot CG, Benner R (2012) The spectral slope coefficient of chromophoric dissolved organic matter (S275–295) as a tracer of terrigenous dissolved organic carbon in river-influenced ocean margins Limnol Oceanogr 57:1453-1466 doi:doi:10.4319/lo.2012.57.5.1453

Flato G et al. (2013) Evaluation of Climate Models. In: Stocker TF et al. (eds) Climate Change 2013: The Physical Science Basis. Contribution of Working Group I to the Fifth Assessment Report of the Intergovernmental Panel on Climate Change. Cambridge University Press, Cambridge, United Kingdom and New York, NY, USA, pp 741–866. doi:10.1017/CBO9781107415324.020

Galloway JN, Schlesinger WH, Levy H, Michaels A, Schnoor JL (1995) Nitrogen fixation: Anthropogenic enhancement-environmental response Global Biogeochemical Cycles 9:235-252 doi:10.1029/95GB00158

Gerten D, Adrian R (2000) Climate-driven changes in spring plankton dynamics and the sensitivity of shallow polymictic lakes to the North Atlantic Oscillation Limnol Oceanogr 45:1058-1066 doi:10.4319/lo.2000.45.5.1058

Giles CD, Lee LG, Cade-Menun BJ, Hill JE, Isles PDF, Schroth AW, Druschel GK (2015) Characterization of Organic Phosphorus Form and Bioavailability in Lake Sediments using 31P Nuclear Magnetic Resonance and Enzymatic Hydrolysis Journal of Environmental Quality 44:882-894 doi:10.2134/jeq2014.06.0273

Goodale CL, Thomas SA, Fredriksen G, Elliott EM, Flinn KM, Butler TJ, Walter MT (2009) Unusual seasonal patterns and inferred processes of nitrogen retention in forested headwaters of the Upper Susquehanna River Biogeochemistry 93:197-218 doi:10.2307/40647938

Groffman PM, Boulware NJ, Zipperer WC, Pouyat RV, Band LE, Colosimo MF (2002) Soil nitrogen cycle processes in urban riparian zones Environ Sci Technol 36:4547-4552

Guilbert J, Betts AK, Rizzo DM, Beckage B, Bomblies A (2015) Characterization of increased persistence and intensity of precipitation in the northeastern United States Geophysical Research Letters 42:2015GL063124 doi:10.1002/2015GL063124

Guo Y, Markus M, Demissie M (2002) Uncertainty of nitrate-N load computations for agricultural watersheds Water Resour Res 38:3-1-3-12 doi:10.1029/2001WR001149

Hatfield J, Prueger J, Jaynes D Environmental impacts of agricultural drainage in the Midwest. In: Proceedings of the 7th Annual Drainage Symposium, Orlando, FL. American Society of Agricultural Engineers, St. Joseph, MI. pp. 28ñ35, 1998.

Hayase K, Tsubota H (1985) Sedimentary humic acid and fulvic acid as fluorescent organic materials Geochim Cosmochim Ac 49:159-163 doi:https://doi.org/10.1016/0016-7037(85)90200-5

Hedges JI et al. (2000) The molecularly-uncharacterized component of nonliving organic matter in natural environments Organic Geochemistry 31:945-958 doi:https://doi.org/10.1016/S0146-6380(00)00096-6

Heffernan JB, Cohen MJ (2010) Direct and indirect coupling of primary production and diel nitrate dynamics in a subtropical spring-fed river Limnol Oceanogr 55:677-688 doi:10.4319/lo.2010.55.2.0677

Helms JR, Stubbins A, Ritchie JD, Minor EC, Kieber DJ, Mopper K (2008) Absorption spectral slopes and slope ratios as indicators of molecular weight, source, and photobleaching of chromophoric dissolved organic matter Limnol Oceanogr 53:955-969 doi:10.4319/lo.2008.53.3.0955

Hernes PJ, Spencer RGM, Dyda RY, Pellerin BA, Bachand PAM, Bergamaschi BA (2008) The role of hydrologic regimes on dissolved organic carbon composition in an agricultural watershed Geochim Cosmochim Ac 72:5266-5277 doi:10.1016/j.gca.2008.07.031

Hinton MJ, Schiff SL, English MC (1997) The significance of storms for the concentration and export of dissolved organic carbon from two Precambrian Shield catchments Biogeochemistry 36:67-88 doi:10.1023/A:1005779711821

Hirsch RM, Moyer DL, Archfield SA (2010) Weighted Regressions on Time, Discharge, and Season (WRTDS), with an Application to Chesapeake Bay River Inputs1 JAWRA Journal of the American Water Resources Association 46:857-880 doi:10.1111/j.1752-1688.2010.00482.x

Hood E, Gooseff MN, Johnson SL (2006) Changes in the character of stream water dissolved organic carbon during flushing in three small watersheds, Oregon Journal of Geophysical Research: Biogeosciences 111:n/a-n/a doi:10.1029/2005JG000082

House WA, Warwick MS (1998) Hysteresis of the solute concentration/discharge relationship in rivers during storms Water Research 32:2279-2290 doi:http://dx.doi.org/10.1016/S0043-1354(97)00473-9

Howarth RW (2008) Coastal nitrogen pollution: A review of sources and trends globally and regionally Harmful Algae 8:14-20 doi:http://dx.doi.org/10.1016/j.hal.2008.08.015

Howarth RW, Marino R (2006) Nitrogen as the limiting nutrient for eutrophication in coastal marine ecosystems: Evolving views over three decades Limnol Oceanogr 51:364-376 doi:10.4319/lo.2006.51.1_part_2.0364

Hyer KE, Denver JM, Langland MJ, Webber JS, Böhlke JK, Hively WD, Clune JW (2016) Spatial and temporal variation of stream chemistry associated with contrasting geology and land-use patterns in the Chesapeake Bay watershed—Summary of results from Smith Creek, Virginia; Upper Chester River, Maryland; Conewago Creek, Pennsylvania; and Difficult Run, Virginia, 2010–2013. Reston, VA. doi:10.3133/sir20165093

Inamdar S et al. (2011) Fluorescence characteristics and sources of dissolved organic matter for stream water during storm events in a forested mid-Atlantic watershed Journal of Geophysical Research-Biogeosciences 116 doi:10.1029/2011jg001735

Inamdar SP, O'Leary N, Mitchell MJ, Riley JT (2006) The impact of storm events on solute exports from a glaciated forested watershed in western New York, USA Hydrol Process 20:3423-3439 doi:10.1002/hyp.6141

Isles PDF, Xu Y, Stockwell JD, Schroth AW (2017) Climate-driven changes in energy and mass inputs systematically alter nutrient concentration and stoichiometry in deep and shallow regions of Lake Champlain Biogeochemistry 133:201-217 doi:10.1007/s10533-017-0327-8

Jaffé R, McKnight D, Maie N, Cory R, McDowell WH, Campbell JL (2008) Spatial and temporal variations in DOM composition in ecosystems: The importance of long-term monitoring of optical properties Journal of Geophysical Research: Biogeosciences 113:G04032 doi:10.1029/2008JG000683

Jaffé R et al. (2012) Dissolved Organic Matter in Headwater Streams: Compositional Variability across Climatic Regions of North America Geochim Cosmochim Ac 94:95-108 doi:https://doi.org/10.1016/j.gca.2012.06.031

Jarvie HP, Johnson LT, Sharpley AN, Smith DR, Baker DB, Bruulsema TW, Confesor R (2017) Increased Soluble Phosphorus Loads to Lake Erie: Unintended Consequences of Conservation Practices? J Environ Qual 46:123-132 doi:10.2134/jeq2016.07.0248

Jarvie HP, Sharpley AN, Spears B, Buda AR, May L, Kleinman PJA (2013) Water Quality Remediation Faces Unprecedented Challenges from "Legacy Phosphorus" Environmental Science & Technology 47:8997-8998 doi:10.1021/es403160a

Johengen T et al. (2017) Performance verification statment for Systea WIZ Probe phosphoate analyzer. Alliance for Coastal Technologies,

Johnes PJ (2007) Uncertainties in annual riverine phosphorus load estimation: Impact of load estimation methodology, sampling frequency, baseflow index and catchment population density Journal of Hydrology 332:241-258 doi:https://doi.org/10.1016/j.jhydrol.2006.07.006

Johnson FA, East JW (1982) Cyclical relationships between river discharge and chemical concentration during flood events Journal of Hydrology 57:93-106 doi:http://dx.doi.org/10.1016/0022-1694(82)90105-6

Johnson KS, Coletti LJ (2002) In situ ultraviolet spectrophotometry for high resolution and long-term monitoring of nitrate, bromide and bisulfide in the ocean Deep Sea Research Part I: Oceanographic Research Papers 49:1291-1305 doi:http://dx.doi.org/10.1016/S0967-0637(02)00020-1

Jordan P, Arnscheidt A, Mcgrogan H, Mccormick S (2007) Characterising phosphorus transfers in rural catchments using a continuous bank-side analyser Hydrology and Earth System Sciences Discussions 11:372-381

Joung D et al. (2017) Winter weather and lake-watershed physical configuration drive phosphorus, iron, and manganese dynamics in water and sediment of ice-covered lakes Limnol Oceanogr 62:1620-1635 doi:doi:10.1002/lno.10521

Kane DD, Conroy JD, Peter Richards R, Baker DB, Culver DA (2014) Re-eutrophication of Lake Erie: Correlations between tributary nutrient loads and phytoplankton biomass Journal of Great Lakes Research 40:496-501 doi:https://doi.org/10.1016/j.jglr.2014.04.004

Kaushal SS, Belt KT (2012) The urban watershed continuum: evolving spatial and temporal dimensions Urban Ecosyst 15:409-435 doi:10.1007/s11252-012-0226-7

Kaushal SS et al. (2008) Interaction between urbanization and climate variability amplifies watershed nitrate export in Maryland Environmental Science & Technology 42:5872-5878 doi:10.1021/es800264f

Kellerman AM (2015) Molecular-level dissolved organic matter dynamics in lakes : Constraints on reactivity and persistence. Doctoral thesis, comprehensive summary, Acta Universitatis Upsaliensis

Kellerman AM, Kothawala DN, Dittmar T, Tranvik LJ (2015) Persistence of dissolved organic matter in lakes related to its molecular characteristics Nature Geoscience 8:454 doi:10.1038/ngeo2440

https://www.nature.com/articles/ngeo2440#supplementary-information

Kiem R, Kögel-Knabner I (2003) Contribution of lignin and polysaccharides to the refractory carbon pool in C-depleted arable soils Soil Biology and Biochemistry 35:101-118 doi:https://doi.org/10.1016/S0038-0717(02)00242-0

Kim S, Kaplan LA, Hatcher PG (2006) Biodegradable dissolved organic matter in a temperate and a tropical stream determined from ultra-high resolution mass spectrometry Limnol Oceanogr 51:1054-1063 doi:10.4319/lo.2006.51.2.1054

Kirchner JW, Feng XH, Neal C, Robson AJ (2004) The fine structure of water-quality dynamics: the (high-frequency) wave of the future Hydrol Process 18:1353-1359 doi:10.1002/Hyp.5537

Kitis M, Karanfil T, Kilduff JE, Wigton A (2001) The reactivity of natural organic matter to disinfection byproducts formation and its relation to specific ultraviolet absorbance Water Sci Technol 43:9-16

Kominoski JS, Rosemond AD (2011) Conservation from the bottom up: forecasting effects of global change on dynamics of organic matter and management needs for river networks Freshwater Science 31:51-68 doi:10.1899/10-160.1

Kraus TEC et al. (2008) Assessing the contribution of wetlands and subsided islands to dissolved organic matter and disinfection byproduct precursors in the Sacramento–San Joaquin River Delta: A geochemical approach Organic Geochemistry 39:1302-1318 doi:http://dx.doi.org/10.1016/j.orggeochem.2008.05.012

Kruskal WH, Wallis WA (1952) Use of ranks in one-criterion variance analysis Journal of the American Statistical Association 47:583-621 doi:10.2307/2280779

Kuk-Hyun A, Scott S (2018) Time-varying suspended sediment-discharge rating curves to estimate climate impacts on fluvial sediment transport Hydrol Process 32:102-117 doi:doi:10.1002/hyp.11402

Langergraber G, Fleischmann N, Hofstadter F (2003) A multivariate calibration procedure for UV/VIS spectrometric quantification of organic matter and nitrate in wastewater Water Sci Technol 47:63-71

Lawler JJ et al. (2014) Projected land-use change impacts on ecosystem services in the United States Proceedings of the National Academy of Sciences doi:10.1073/pnas.1405557111

Levene H (1960) Robust tests for equality of variances. In: Olkin I (ed) Contributions to Probability and Statistics: Essays in Honor of Harold Hotelling. Stanford University Press, pp 278-292

Likens GE (2013) Biogeochemistry of a forested ecosystem. Third edn. Springer, New York, NY. doi:10.1007/978-1-4614-7810-2

Lloyd CEM, Freer JE, Johnes PJ, Collins AL (2016) Technical Note: Testing an improved index for analysing storm discharge–concentration hysteresis Hydrol Earth Syst Sci 20:625-632 doi:10.5194/hess-20-625-2016

Ludwig W, Probst J-L, Kempe S (1996) Predicting the oceanic input of organic carbon by continental erosion Global Biogeochemical Cycles 10:23-41 doi:10.1029/95GB02925

McCarty GW, Reeves JB, Reeves VB, Follett RF, Kimble JM (2002) Mid-Infrared and Near-Infrared Diffuse Reflectance Spectroscopy for Soil Carbon Measurement Soil Science Society of America Journal 66:640-646 doi:10.2136/sssaj2002.6400

McClain ME et al. (2003) Biogeochemical Hot Spots and Hot Moments at the Interface of Terrestrial and Aquatic Ecosystems Ecosystems 6:301-312 doi:10.1007/s10021-003-0161-9

McElmurry SP, Long DT, Voice TC (2014) Stormwater Dissolved Organic Matter: Influence of Land Cover and Environmental Factors Environmental Science & Technology 48:45-53 doi:10.1021/es402664t

McGlynn BL, McDonnell JJ (2003) Quantifying the relative contributions of riparian and hillslope zones to catchment runoff Water Resour Res 39:1310 doi:10.1029/2003WR002091

McKnight DM, Boyer EW, Westerhoff PK, Doran PT, Kulbe T, Andersen DT (2001) Spectrofluorometric characterization of dissolved organic matter for indication of precursor organic material and aromaticity Limnol Oceanogr 46:38-48 doi:doi:10.4319/lo.2001.46.1.0038

Medalie L (2016) Concentration, flux, and trend estimates with uncertainty for nutrients, chloride, and total suspended solids in tributaries of Lake Champlain, 1990–2014. Reston, VA. doi:10.3133/ofr20161200

Mevik B, Wehrens R, Liland KH (2015) pls: Partial Least Squares and Principal Component Regression.

Michalak AM et al. (2013) Record-setting algal bloom in Lake Erie caused by agricultural and meteorological trends consistent with expected future conditions Proceedings of the National Academy of Sciences 110:6448-6452 doi:10.1073/pnas.1216006110

Monteith DT et al. (2007) Dissolved organic carbon trends resulting from changes in atmospheric deposition chemistry Nature 450:537-U539 doi:10.1038/Nature06316

Moore J (2016) Literature review: tile drainage and phosphorus losses from agricultural land. Lake Champlain Basin Program,

Moore RD (2005) Slug injection using salt in solution Streamline Watershed Management Bulletin 8:1-6

Moore TR, Jackson RJ (1989) Dynamics of dissolved organic carbon in forested and disturbed catchments, Westland, New Zealand: 2. Larry River Water Resour Res 25:1331-1339 doi:10.1029/WR025i006p01331

Morel B, Durand P, Jaffrezic A, Gruau G, Molenat J (2009) Sources of dissolved organic carbon during stormflow in a headwater agricultural catchment Hydrol Process 23:2888-2901 doi:10.1002/hyp.7379

Morris DP et al. (1995) The attentuation of solar UV radiation in lakes and the role of dissolved organic carbon Limnol Oceanogr 40:1381-1391

Musolff A, Fleckenstein JH, Rao PSC, Jawitz JW (2017) Emergent archetype patterns of coupled hydrologic and biogeochemical responses in catchments Geophysical Research Letters 44:4143-4151 doi:doi:10.1002/2017GL072630

Newcomer TA, Kaushal SS, Mayer PM, Shields AR, Canuel EA, Groffman PM, Gold AJ (2012) Influence of natural and novel organic carbon sources on denitrification in forest, degraded urban, and restored streams Ecological Monographs 82:449-466 doi:10.1890/12-0458.1

Nguyen HV-M, Lee M-H, Hur J, Schlautman MA (2013) Variations in spectroscopic characteristics and disinfection byproduct formation potentials of dissolved organic matter for two contrasting storm events Journal of Hydrology 481:132-142 doi:http://dx.doi.org/10.1016/j.jhydrol.2012.12.044

O'Neil JM, Davis TW, Burford MA, Gobler CJ (2012) The rise of harmful cyanobacteria blooms: The potential roles of eutrophication and climate change Harmful Algae 14:313-334 doi:https://doi.org/10.1016/j.hal.2011.10.027

Oeurng C, Sauvage S, Coynel A, Maneux E, Etcheber H, Sánchez-Pérez J-M (2011) Fluvial transport of suspended sediment and organic carbon during flood events in a large agricultural catchment in southwest France Hydrol Process 25:2365-2378 doi:doi:10.1002/hyp.7999

Oeurng C, Sauvage S, Sánchez-Pérez J-M (2010) Temporal variability of nitrate transport through hydrological response during flood events within a large agricultural catchment in south-west France Science of The Total Environment 409:140-149 doi:http://dx.doi.org/10.1016/j.scitotenv.2010.09.006

Ohtani K (2000) Bootstrapping R2 and adjusted R2 in regression analysis Economic Modelling 17:473-483 doi:https://doi.org/10.1016/S0264-9993(99)00034-6

Outram FN et al. (2014) High-frequency monitoring of nitrogen and phosphorus response in three rural catchments to the end of the 2011–2012 drought in England Hydrol Earth Syst Sci 18:3429-3448 doi:10.5194/hess-18-3429-2014

Pardo LH et al. (2011) Effects of nitrogen deposition and empirical nitrogen critical loads for ecoregions of the United States Ecological Applications 21:3049-3082 doi:10.1890/10-2341.1

Parr TB, Cronan CS, Ohno T, Findlay SEG, Smith SMC, Simon KS (2015) Urbanization changes the composition and bioavailability of dissolved organic matter in headwater streams Limnol Oceanogr:n/a-n/a doi:10.1002/lno.10060

Parsons TR, Maita Y, Lalli CM (1984) 1.6 - Determination of Phosphate. In: A Manual of Chemical & Biological Methods for Seawater Analysis. Pergamon, Amsterdam, pp 22-25. doi:https://doi.org/10.1016/B978-0-08-030287-4.50015-3

Paternoster R, Brame R, Mazerolle P, Piquero A (1998) Using the correct statistical test for the equality of regression coefficients Criminology 36:859-866 doi:10.1111/j.1745-9125.1998.tb01268.x

Pellerin BA, Bergamaschi BA, Downing BD, Saraceno JF, Garrett JA, Olsen LD (2013) Optical techniques for the determination of nitrate in environmental waters: Guidelines for instrument selection, operation, deployment, maintenance, quality assurance, and data reporting. U.S. Geological Survey Techniques and Methods 1-D5,

Pellerin BA et al. (2014) Mississippi River Nitrate Loads from High Frequency Sensor Measurements and Regression-Based Load Estimation Environmental Science & Technology 48:12612-12619 doi:10.1021/es504029c

Pellerin BA, Saraceno JF, Shanley JB, Sebestyen SD, Aiken GR, Wollheim WM, Bergamaschi BA (2012) Taking the pulse of snowmelt: in situ sensors reveal seasonal, event and diurnal patterns of nitrate and dissolved organic matter variability in an upland forest stream Biogeochemistry 108:183-198 doi:10.1007/s10533-011-9589-8

Pellerin BA et al. (2016) Emerging Tools for Continuous Nutrient Monitoring Networks: Sensors Advancing Science and Water Resources Protection JAWRA Journal of the American Water Resources Association 52:993-1008 doi:doi:10.1111/1752-1688.12386

Petras D et al. (2017) High-Resolution Liquid Chromatography Tandem Mass Spectrometry Enables Large Scale Molecular Characterization of Dissolved Organic Matter Frontiers in Marine Science 4 doi:10.3389/fmars.2017.00405

Pierson DC, Samal NR, Owens EM, Schneiderman EM, Zion MS (2013) Changes in the timing of snowmelt and the seasonality of nutrient loading: can models simulate the impacts on freshwater trophic status? Hydrol Process 27:3083-3093 doi:10.1002/hyp.9894

Porter JH, Hanson PC, Lin C-C (2012) Staying afloat in the sensor data deluge Trends in Ecology & Evolution 27:121-129 doi:10.1016/j.tree.2011.11.009

Prairie YT (2008) Carbocentric limnology: looking back, looking forward Can J Fish Aquat Sci 65:543-548 doi:10.1139/F08-011

R Core Team (2015) R: A language and environment for statistical computing. R Foundation for Statistical Computing, Vienna, Austria

Ravichandran M (2004) Interactions between mercury and dissolved organic matter - a review Chemosphere 55:319-331 doi:10.1016/j.chemosphere.2003.11.011

Raymond P, Saiers J (2010) Event controlled DOC export from forested watersheds Biogeochemistry 100:197-209 doi:10.1007/s10533-010-9416-7

Raymond PA, Bauer JE (2001) Riverine export of aged terrestrial organic matter to the North Atlantic Ocean Nature 409:497-500

Reche II, Pace ML, Cole JJ (1998) Interactions of Photobleaching and Inorganic Nutrients in Determining Bacterial Growth on Colored Dissolved Organic Carbon Microbial ecology 36:270-280

Reckhow DA, Singer PC (1990) Chlorination by-products in drinking waters - from formation potentials to finished water concentrations J Am Water Works Ass 82:173-180

Rieger L, Langergraber G, Siegrist H (2006) Uncertainties of spectral in situ measurements in wastewater using different calibration approaches Water Sci Technol 53:187-197 doi:10.2166/wst.2006.421

Roberts B, Mulholland P, Hill W (2007) Multiple Scales of Temporal Variability in Ecosystem Metabolism Rates: Results from 2 Years of Continuous Monitoring in a Forested Headwater Stream Ecosystems 10:588-606 doi:10.1007/s10021-007-9059-2

Rode M et al. (2016) Sensors in the Stream: The High-Frequency Wave of the Present Environmental Science & Technology 50:10297-10307 doi:10.1021/acs.est.6b02155

Rosenberg BD, Schroth AW (2017) Coupling of reactive riverine phosphorus and iron species during hot transport moments: impacts of land cover and seasonality Biogeochemistry 132:103-122 doi:10.1007/s10533-016-0290-9

Rosenzweig BR, Moon HS, Smith JA, Baeck ML, Jaffe PR (2008) Variation in the instream dissolved inorganic nitrogen response between and within rainstorm events in an urban watershed Journal of Environmental Science and Health, Part A 43:1223-1233 doi:10.1080/10934520802225190

Royer TV, David MB (2005) Export of dissolved organic carbon from agricultural streams in Illinois, USA Aquat Sci 67:465-471 doi:10.1007/s00027-005-0781-6

Royer TV, David MB, Gentry LE (2006) Timing of riverine export of nitrate and phosphorus from agricultural watersheds in Illinois: Implications for reducing nutrient loading to the Mississippi River Environmental Science & Technology 40:4126-4131 doi:10.1021/es052573n

Ruhala SS, Zarnetske JP (2017) Using in-situ optical sensors to study dissolved organic carbon dynamics of streams and watersheds: A review Science of The Total Environment 575:713-723 doi:https://doi.org/10.1016/j.scitotenv.2016.09.113

Rusjan S, Brilly M, Mikoš M (2008) Flushing of nitrate from a forested watershed: An insight into hydrological nitrate mobilization mechanisms through seasonal high-frequency stream nitrate dynamics Journal of Hydrology 354:187-202 doi:http://dx.doi.org/10.1016/j.jhydrol.2008.03.009

Sakamoto CM, Johnson KS, Coletti LJ (2009) Improved algorithm for the computation of nitrate concentrations in seawater using an in situ ultraviolet spectrophotometer Limnology and Oceanography-Methods 7:132-143

Sanchez CA, Blackmer AM (1988) Recovery of anhydrous ammonia-derived nitrogen-15 during three years of corn production in Iowa Agronomy Journal 80:102-108 doi:10.2134/agronj1988.00021962008000010023x

SanClements MD, Oelsner GP, McKnight DM, Stoddard JL, Nelson SJ (2012) New Insights into the Source of Decadal Increases of Dissolved Organic Matter in Acid-Sensitive Lakes of the Northeastern United States Environmental Science & Technology 46:3212-3219 doi:10.1021/Es204321x

Saraceno JF, Pellerin BA, Downing BD, Boss E, Bachand PAM, Bergamaschi BA (2009) High-frequency in situ optical measurements during a storm event: Assessing relationships between dissolved organic matter, sediment concentrations, and hydrologic processes Journal of Geophysical Research-Biogeosciences 114 doi:10.1029/2009jg000989

Scavia D et al. (2014) Assessing and addressing the re-eutrophication of Lake Erie: Central basin hypoxia Journal of Great Lakes Research 40:226-246 doi:https://doi.org/10.1016/j.jglr.2014.02.004

Schindler DW, Carpenter SR, Chapra SC, Hecky RE, Orihel DM (2016) Reducing Phosphorus to Curb Lake Eutrophication is a Success Environmental Science & Technology 50:8923-8929 doi:10.1021/acs.est.6b02204

Schroth AW, Giles CD, Isles PDF, Xu Y, Perzan Z, Druschel GK (2015) Dynamic Coupling of Iron, Manganese, and Phosphorus Behavior in Water and Sediment of Shallow Ice-Covered Eutrophic Lakes Environmental Science & Technology 49:9758-9767 doi:10.1021/acs.est.5b02057

Sebestyen SD, Shanley JB, Boyer EW, Kendall C, Doctor DH (2014) Coupled hydrological and biogeochemical processes controlling variability of nitrogen species in streamflow during autumn in an upland forest Water Resour Res 50:1569-1591 doi:10.1002/2013WR013670

Sharpley AN, Chapra SC, Wedepohl R, Sims JT, Daniel TC, Reddy KR (1994) Managing Agricultural Phosphorus for Protection of Surface Waters: Issues and Options J Environ Qual 23:437-451 doi:10.2134/jeq1994.00472425002300030006x

Sharpley AN, Kleinman PJA, Heathwaite AL, Gburek WJ, Folmar GJ, Schmidt JP (2008) Phosphorus Loss from an Agricultural Watershed as a Function of Storm Size All rights reserved. No part of this periodical may be reproduced or transmitted in any form or by any means, electronic or mechanical, including photocopying, recording, or any information storage and retrieval system, without permission in writing from the publisher J Environ Qual 37:362-368 doi:10.2134/jeq2007.0366

Shepherd KD, Walsh MG (2002) Development of Reflectance Spectral Libraries for Characterization of Soil Properties Soil Science Society of America Journal 66:988-998 doi:10.2136/sssaj2002.9880

Sherson LR, Van Horn DJ, Gomez-Velez JD, Crossey LJ, Dahm CN (2015) Nutrient dynamics in an alpine headwater stream: use of continuous water quality sensors

to examine responses to wildfire and precipitation events Hydrol Process 29:3193-3207 doi:10.1002/hyp.10426

Sickman JO, Zanoli MJ, Mann HL (2007) Effects of urbanization on organic carbon loads in the Sacramento River, California Water Resour Res 43:W11422 doi:10.1029/2007WR005954

Sivirichi GM et al. (2011) Longitudinal variability in streamwater chemistry and carbon and nitrogen fluxes in restored and degraded urban stream networks Journal of Environmental Monitoring 13:288-303 doi:10.1039/c0em00055h

Sleighter RL, Hatcher PG (2007) The application of electrospray ionization coupled to ultrahigh resolution mass spectrometry for the molecular characterization of natural organic matter J Mass Spectrom 42:559-574 doi:10.1002/jms.1221

Sleighter RL, Liu Z, Xue J, Hatcher PG (2010) Multivariate Statistical Approaches for the Characterization of Dissolved Organic Matter Analyzed by Ultrahigh Resolution Mass Spectrometry Environmental Science & Technology 44:7576-7582 doi:10.1021/es1002204

Smith VH, Tilman GD, Nekola JC (1999) Eutrophication: impacts of excess nutrient inputs on freshwater, marine, and terrestrial ecosystems Environmental Pollution 100:179-196 doi:http://dx.doi.org/10.1016/S0269-7491(99)00091-3

Sobczak W, Findlay S, Dye S (2003) Relationships between DOC bioavailability and nitrate removal in an upland stream: An experimental approach Biogeochemistry 62:309-327 doi:10.1023/A:1021192631423

Stanley EH, Powers SM, Lottig NR, Buffam I, Crawford JT (2012) Contemporary changes in dissolved organic carbon (DOC) in human-dominated rivers: is there a role for DOC management? Freshwater Biology 57:26-42 doi:10.1111/j.1365-2427.2011.02613.x

Stedmon CA, Markager S, Bro R (2003) Tracing dissolved organic matter in aquatic environments using a new approach to fluorescence spectroscopy Marine Chemistry 82:239-254 doi:https://doi.org/10.1016/S0304-4203(03)00072-0

Stoddard JL et al. (2003) Response of Surface Water Chemistry to the Clean Air Act Amendments of 1990. U.S. Environmental Protection Agency, Research Triangle Park, NC

Stubbins A, Lapierre JF, Berggren M, Prairie YT, Dittmar T, del Giorgio PA (2014) What's in an EEM? Molecular signatures associated with dissolved organic fluorescence in Boreal Canada Environmental Science & Technology 48:10598-10606 doi:10.1021/es502086e

Stubblefield AP, Reuter JE, Dahlgren RA, Goldman CR (2007) Use of turbidometry to characterize suspended sediment and phosphorus fluxes in the Lake Tahoe basin, California, USA Hydrol Process 21:281-291 doi:10.1002/hyp.6234

Stumpf RP, Wynne TT, Baker DB, Fahnenstiel GL (2012) Interannual Variability of Cyanobacterial Blooms in Lake Erie Plos One 7:e42444 doi:10.1371/journal.pone.0042444

Stutter M et al. (2017) Evaluating the use of in-situ turbidity measurements to quantify fluvial sediment and phosphorus concentrations and fluxes in agricultural streams Science of The Total Environment 607-608:391-402 doi:https://doi.org/10.1016/j.scitotenv.2017.07.013

Townsend AR et al. (2003) Human health effects of a changing global nitrogen cycle Frontiers in Ecology and the Environment 1:240-246 doi:10.1890/1540-9295(2003)001[0240:HHEOAC]2.0.CO;2

Turnipseed DP, Sauer VB (2010) Discharge measurements at gaging stations. U.S. Geological Survey,

Underwood KL, Rizzo DM, Schroth AW, Dewoolkar MM (2017) Evaluating Spatial Variability in Sediment and Phosphorus Concentration-Discharge Relationships Using Bayesian Inference and Self-Organizing Maps Water Resour Res 53:10293-10316 doi:10.1002/2017WR021353

Van Herpe Y, Troch PA (2000) Spatial and temporal variations in surface water nitrate concentrations in a mixed land use catchment under humid temperate climatic conditions Hydrol Process 14:2439-2455 doi:10.1002/1099-1085(20001015)14:14<2439::aid-hyp105>3.0.co;2-h

Vaughan MCH et al. (2017) High-frequency dissolved organic carbon and nitrate measurements reveal differences in storm hysteresis and loading in relation to land cover and seasonality Water Resour Res 53:5345-5363 doi:10.1002/2017wr020491

Vaughan MCH, Bowden WB, Shanley JB, Vermilyea A, Wemple BC, Schroth AW (2018) Using in situ UV-Visible spectrophotometer sensors to quantify riverine phosphorus partitioning and concentration at a high frequency Limnology and Oceanography: Methods doi:10.1002/lom3.10287

Vidon P, Wagner LE, Soyeux E (2008) Changes in the character of DOC in streams during storms in two Midwestern watersheds with contrasting land uses Biogeochemistry 88:257-270 doi:10.1007/s10533-008-9207-6

Viscarra Rossel RA, Walvoort DJJ, McBratney AB, Janik LJ, Skjemstad JO (2006) Visible, near infrared, mid infrared or combined diffuse reflectance spectroscopy for simultaneous assessment of various soil properties Geoderma 131:59-75 doi:https://doi.org/10.1016/j.geoderma.2005.03.007

Vitousek PM et al. (1997) Human alteration of the global nitrogen cycle: Sources and consequences Ecological Applications 7:737-750 doi:10.1890/1051-0761(1997)007[0737:HAOTGN]2.0.CO;2

Walford N (2011) Practical statistics for geographers and earth scientists. Wiley-Blackwell, Oxford, UK ; Hoboken, NJ

Walsh CJ, Roy AH, Feminella JW, Cottingham PD, Groffman PM, Morgan RP (2005) The urban stream syndrome: current knowledge and the search for a cure Journal of the North American Benthological Society 24:706-723 doi:10.1899/04-028.1

Walsh J et al. (2014) Climate change impacts in the United States: The third national climate assessment. US Global Change Research Program. doi:10.7930/J0KW5CXT

Webster JR, Newbold JD, Thomas SA, Valett HM, Mulholland PJ (2009) Nutrient uptake and mineralization during leaf decay in streams – a model simulation International Review of Hydrobiology 94:372-390 doi:10.1002/iroh.200811158

Weishaar JL, Aiken GR, Bergamaschi BA, Fram MS, Fujii R, Mopper K (2003) Evaluation of Specific Ultraviolet Absorbance as an Indicator of the Chemical Composition and Reactivity of Dissolved Organic Carbon Environmental Science & Technology 37:4702-4708 doi:10.1021/es030360x

Weyhenmeyer GA, Fröberg M, Karltun E, Khalili M, Kothawala D, Temnerud J, Tranvik LJ (2012) Selective decay of terrestrial organic carbon during transport from land to sea Global Change Biol 18:349-355 doi:10.1111/j.1365-2486.2011.02544.x

Williams CJ, Yamashita Y, Wilson HF, Jaffé R, Xenopoulos MA (2010) Unraveling the role of land use and microbial activity in shaping dissolved organic matter characteristics in stream ecosystems Limnol Oceanogr 55:1159-1171 doi:doi:10.4319/lo.2010.55.3.1159

Wilson H, Xenopoulos M (2008) Ecosystem and Seasonal Control of Stream Dissolved Organic Carbon Along a Gradient of Land Use Ecosystems 11:555-568 doi:10.1007/s10021-008-9142-3

Wilson HF, Xenopoulos MA (2009) Effects of agricultural land use on the composition of fluvial dissolved organic matter Nature Geosci 2:37-41 doi:http://www.nature.com/ngeo/journal/v2/n1/suppinfo/ngeo391_S1.html

Winchell M et al. (2011) Identification of critical source areas of phosphorus within the Vermont sector of the Missisquoi Bay Basin. Lake Champlain Basin Program,

Wironen MB, Bennett EM, Erickson JD (2018) Phosphorus flows and legacy accumulation in an animal-dominated agricultural region from 1925 to 2012 Global Environmental Change 50:88-99 doi:https://doi.org/10.1016/j.gloenvcha.2018.02.017

Yoon B, Raymond PA (2012) Dissolved organic matter export from a forested watershed during Hurricane Irene Geophysical Research Letters 39 doi:10.1029/2012gl052785

Zhang Z et al. (2007) Nutrient runoff from forested watersheds in central Japan during typhoon storms: implications for understanding runoff mechanisms during storm events Hydrol Process 21:1167-1178 doi:10.1002/hyp.6677